January 2008

Preliminary Investigations of a Stochastic Method to solve Electrostatic and Electrodynamic Problems

Sethu Hareesh Kolluru
University of Massachusetts Amherst

PRELIMINARY INVESTIGATIONS OF A STOCHASTIC METHOD TO SOLVE ELECTROSTATIC AND ELECTRODYNAMIC PROBLEMS

A Thesis Presented

by

SETHU HAREESH KOLLURU

Submitted to the Graduate School of the
University of Massachusetts Amherst in partial fulfillment
of the requirements for the degree of

MASTER OF SCIENCE IN ELECTRICAL AND COMPUTER ENGINEERING

September 2008

Electrical and Computer Engineering

PRELIMINARY INVESTIGATIONS OF A STOCHASTIC METHOD TO SOLVE ELECTROSTATIC AND ELECTRODYNAMIC PROBLEMS

A Thesis Presented

by

SETHU HAREESH KOLLURU

Approved as to style and content by:

Ramakrishna Janaswamy, Chair

Marinos Vouvakis, Member

Weibo Gong, Member

C.V. Hollot, Department Head
Electrical and Computer Engineering

This thesis is dedicated to my mother for her love and support.
Mom, you have given me so much, thanks for your faith in me, and for taking my pain during tough times.

ACKNOWLEDGMENTS

Thanks to my advisor, Prof. Ramakrishna Janaswamy for giving me the opportunity to work with him. It has been an honor to work with him and my acknowledgments for his intellectual support and continuous encouragement through my studies. This thesis was made possible by his patience and persistence.I believe that one of the main gains of this 2-years program was working with Prof.Janaswamy and gaining his trust and friendship.

Thanks to Prof.Weibo Gong for agreeing to be on my thesis committee inspite of his busy schedule. Prof.Marinos Vouvakis, thanks for your advice and for motivation you have given me and for acting as a mentor to me.

Thanks to my course advisors, Prof.Dan Schaubert, Prof.Paul Siquera and Prof.Robert Jackson.

Thanks to my colleagues at the Antennas & Propagation Lab, both graduated and current who helped me with guidance, support and advice.

Thanks also to my brother, family and friends, who supported me in the past two years, and for many, much longer than that.

And finally special thanks to my mother, Rajeswari, who suffered through each step along with me, I acknowledge a debt, an appreciation, that extends beyond any words at my command.

This work was funded in part by the US Army Research Office under ARO grant W911NF-04-1-0228 and by the Center for Advanced Sensor and Communication Antennas, University of Massachusetts at Amherst, under the US Air Force Research Laboratory Contract FA8718-04-C-0057.

Thanks to everyone who had a part in this effort.

ABSTRACT

PRELIMINARY INVESTIGATIONS OF A STOCHASTIC METHOD TO SOLVE ELECTROSTATIC AND ELECTRODYNAMIC PROBLEMS

SEPTEMBER 2008

SETHU HAREESH KOLLURU

B.Tech., ACHARYA NAGARJUNA UNIVERSITY

M.S.E.C.E, UNIVERSITY OF MASSACHUSETTS AMHERST

Directed by: Professor Ramakrishna Janaswamy

A stochastic method is developed, implemented and investigated here for solving Laplace, Poisson's, and standard parabolic wave equations. This method is based on the properties of random walk, diffusion process, Ito formula, Dynkin formula and Monte Carlo simulations. The developed method is a local method *i.e.* it gives the value of the solution directly at an arbitrary point rather than extracting its value from complete field solution and thus is inherently parallel. Field computation by this method is demonstrated for electrostatic and electrodynamic propagation problems by considering simple examples and numerical results are presented to validate this method. Numerical investigations are carried out to understand efficacy and limitations of this method and to provide qualitative understanding of various parameters involved in this method.

TABLE OF CONTENTS

Page

LIST OF FIGURES

Figure **Page**

CHAPTER 1

INTRODUCTION

1.1 Background and Motivation

It is rare for real-world electromagnetic problems to admit analytical solutions for the multitude of irregular geometries designed under various constitutive relations of media and boundary conditions. Whenever a problem with such complexity arises, numerical solutions must be employed. Of these numerical methods, methods like finite difference (FDM), finite element (FEM) and boundary element (BEM) have been applied successfully to solve a wide variety of EM problems. However, these methods require extensive preprocessing to cast a particular problem in the required format for computation; the numerical algorithms used for the solution are not always stable. The computer codes used are relatively complex and the only possible output of these methods is the field solution even if the solution is needed at a single point or a small set of points of the solution domain [11]. Therefore all these methods discussed above can be cast under global methods.

An alternative technique to these traditional numerical methods, referred as local method that provides efficient solutions for the relevant problems is investigated in this thesis. The method is local because it delivers the solution at a single point directly rather than extracting it from the field solution. Solutions to the deterministic partial differential equations can be obtained based on probabilistic interpretation to these differential equations. These methods are based on random walk, mean value theorem for differential equations, properties of diffusion processes, Ito formula, Dynkin formula and Monte Carlo simulations. Algorithms designed using this local method have attractive features like [11] :

- *Simple to program:* Unlike traditional numerical methods like FDM, FEM and BEM, computer codes are extremely simple.
- *Always Stable:* The method is stable irrespective of the input parameters chosen to obtain the numerical results.

- *Accurate:* Desired accuracy can be obtained by appropriate choice of parameters involved in this method.
- *Local:* Solution at an arbitrary point can be obtained without having to obtain the complete field solution. Therefore this method is inherently parallel.
- *No meshing:* There is no need to discretize the domain or boundary.

With advantages listed as above, this stochastic method may be good alternative method to the global methods for field computations. However, this method has not been fully explored yet. Initial efforts for successful demonstration of this method are discussed in next section. Field computation by this stochastic method for electrostatic and electrodynamic problems might provide some insight into the efficacy and limitations of this method. Preliminary investigations need to be carried out to identify and understand various parameters involved in this method.

1.2 Brief Literature Survey

The relationship between partial differential equations and Brownian motion was observed a long time ago in 1920′s by Wiener et al [13] and Courant et al [14]. Feynman [16] represented solutions of Schrodinger equation by heuristically introducing path integrals which didn't admit probabilistic interpretation. Kac [10] adapted Feynman's formula to the heat conduction equation which was solved by means of rigorously justified Wiener integration in a functional space with a clear probabilistic sense. Early research on solving Helmholtz equation using Feynman's path integrals centered on the calculation of the classical wedge diffraction coefficients, which were obtained previously using Keller's geometrical theory of diffraction [5]. Following the work by Keller and McLaughlin [6], who were the first to suggest using the path integral to derive diffraction coefficients for the perfectly conducting wedge, there have been a number of variations and improvements on the original wedge diffraction solution scheme. A rigorous discussion of stochastic differential equations, stochastic integrals and Ito formula can be found in the literature on stochastic process [4] and [7]. Lately, [1] has looked at application of random walk methods of wave propagation, where the transport amplitude is obtained stochastically after having found eikonal by some other means. In [11] efforts to solve Helmholtz equation have been successful only at low wavenumbers. A part of the material presented in the following thesis for explanatory purpose is taken from [8], [11] and [15].

1.3 Thesis Objectives

For this thesis, we propose to

- develop, formulate and investigate a stochastic method that is used to obtain local solutions for Laplace, Poisson's and parabolic wave equation.
- implement and demonstrate the stochastic method for simple electrostatic and electrodynamic propagation problems.
- conduct numerical experiments to understand effect of various parameters like time step and number of realizations on the accuracy of the solution.

1.4 Thesis Outline

This thesis is organized as follows. In chapter 2, a stochastic method which involves constructing either random walk or Brownian motion process is introduced. This method is used to solve Laplace equation to obtain potential inside a rectangular region when the potential on its walls is given. Numerical investigations carried out to verify this method and to understand the effect of parameters like time step and number of realizations are documented. Comparisons of the accuracy and time taken by the random walk and Brownian motion approaches are also presented.

In chapter 3, a stochastic method which is very similar to the one used in previous chapter is formulated to solve Poisson's equation in order to find potential inside a parallel plate waveguide with a square cylindrical charge distribution. The theoretical considerations supporting this stochastic method are relatively complex and involve concepts of random process and stochastic integration such as Ito process and properties of Ito diffusion process. Some of the details are discussed in this chapter. Favorable comparisons for potential calculations are followed by the numerical results, that are carried out to understand the effect of parameters like time step and number of realizations on accuracy of the solution.

Chapter 4 discusses the stochastic approach to solve parabolic wave equation with Dirichlet boundary condition and its validation for the problem of computing field inside a parallel plate waveguide with perfectly conducting walls on the top and bottom. Need and the idea of analytic continuation in the context of this problem are also presented here.

In Chapter 5, a stochastic method is developed to obtain local solution of parabolic wave equation with impedance boundary condition. This stochastic approach is used to solve similar problem solved in previous chapter *i.e.* computing field inside a parallel plate waveguide

with impedance walls on the top and bottom. Numerical results with the discussion about the field calculations using this stochastic method are presented. This chapter concludes with the discussion on the effect of parameters like marching step and time step on the accuracy of the stochastic solution.

CHAPTER 2

SOLUTION OF LAPLACE EQUATION

The problem under consideration in this chapter is the solution of Laplace equation in two dimensions, in an area bounded by rectangular grid, given the value of the potential function at all points on the boundary. The equation satisfied by the potential at all interior points is given by Laplace equation

$$\frac{\partial^2 \psi}{\partial^2 x} + \frac{\partial^2 \psi}{\partial^2 y} = 0 \tag{2.1}$$

The standard method is to divide the area into small squares by using a grid system, and transform the partial differential equation into a set of finite difference equations, which can be solved by the Gauss-Siedel iterative method, or some such procedure. This method is suitable when the value of potential is required throughout the area; but when the value of potential is required at only one point, the same amount of computation still has to be done in this method. In the latter case, an alternate approach is to use the method that employs random walk. Investigations on Random Walk method (RW) that can be used to solve Laplace equation is the topic of this chapter.

This chapter is organized as follows. In section 1, an outline of random walk method is presented followed by its proof using mean value theorem. In section 2 algorithm that employs random walk to obtain solution of Laplace equations with Dirichlet boundary conditions is formulated. Numerical experiments conducted to find the potential inside a rectangular box are presented to verify the proposed method and to understand the behavior of various parameters involved in this method.

In section 4, it is demonstrated that random walk behaves as a continuous stochastic process called Brownian motion process if the grid size is reduced to 0. Properties of Brownian motion process including proof that escape probability of a particle exhibiting such process satisfies Laplace equation is presented in section 5. Algorithm employing Brownian motion that provides solution to Laplace equation is discussed in section 6 and numerical results are presented to understand how various parameters behave when we move from discrete space

domain to continuous space domain. this chapter conludes with comparative study between algorithms employing random walk and Brownian motion process to solve Laplace equation.

2.1 The Random Walk Method: Basic Idea

A random walk is the path traced by a particle starting from a fixed point and making constant jumps; however the direction of the jump is decided at random [3].

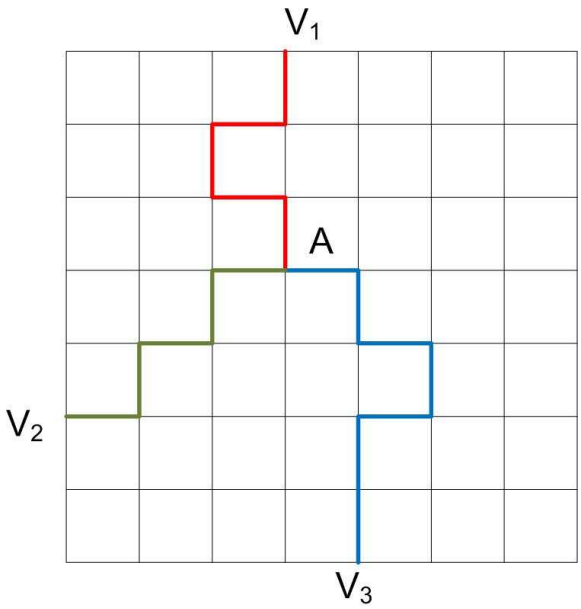

Figure 2.1. Random walk on a 2D grid

Let us suppose that the value of ψ is required at the point A. The method to obtain ψ by random walk operates as follows. Starting from A, the marker is made to move to one of the four adjacent points by moving in one of the four directions up, down, left or right. The direction chosen is random and such that each direction is equally likely. The probability of a move in any one of the directions is therefore 1/4. The choice of direction must be made dependent upon some suitable distribution. This distribution would be simulated by computer which would generate internally a random integer in the range 0 to 3 inclusive.

Having made one such move, the process is repeated until the marker reaches a point on the boundary. At this stage, the value of ψ at this point on the boundary, V_1 say, is noted. The whole random walk process is repeated, starting from A again, terminating at the boundary. The value of ψ at the end-point, V_2, is noted. By this means, a sequence V_i is generated. It will be shown that, if ψ_A denotes the value of ψ at A, then

$$\psi_A = \lim_{n\to\infty}\left[\frac{\sum_{i=1}^{n} V_i}{n}\right] \tag{2.2}$$

This states that the mean value of the end-point potentials V_i tends to ψ_A as the number of random walks tends to infinity. What this means is an approximation to ψ_A can be obtained by repeating the process for sufficiently large number of times.

2.1.1 Proof

Part 1: The Deterministic part Let D represent the region inside rectangular box and B represent the boundary of the box. Let S be the total region consisting of both D and B. In what follows, $(p, q) \in S$ denotes any point, $(i, j) \in D$ any interior point and $(r, s) \in B$ any boundary point. Consider a point (i, j), and let its potential be $\psi_{i,j}$.

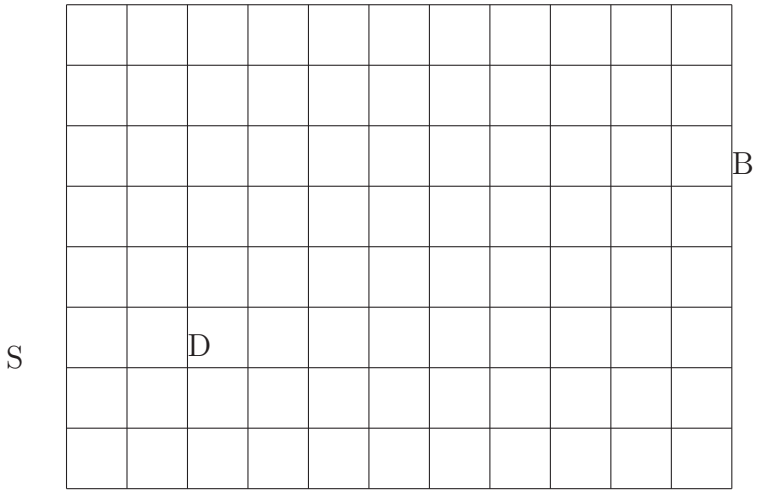

Figure 2.2. 2D Grid inside a rectangular box

As we know inside the box, potential ψ, satisfies Laplace Equation given by:

$$\frac{\partial^2\psi}{\partial^2 x} + \frac{\partial^2\psi}{\partial^2 y} = 0$$

At all interior points, using Taylors series and neglecting higher order terms,

$$\psi_{i,j} = \frac{1}{4}\left(\psi_{i+1,j} + \psi_{i-1,j} + \psi_{i,j+1} + \psi_{i,j-1}\right)$$

At all points on the four walls of the box,

$$\psi_{r,s} = V_{r,s}$$

where $V_{r,s}$ represents the (known) values of ψ at the boundary point (r, s)

It can be seen clearly that the potential at a point is the average of the potential value at the four neighboring points.

Part 2: The Stochastic part Let $P_{i,j}^{r,s}$ be the probability of ultimate absorption at the boundary point (r, s), starting from the interior point (i, j), and executing a random walk of the type already described. Suppose that a reward $V_{r,s}$, is associated with absorption at (r, s), and let $E_{p,q}$ be the expected reward starting from the point (p, q), i.e. the average reward over a large number of trials.

Consider absorption at boundary, starting from (i, j). This can occur in one of four ways,
(i) a first move to $(i + 1, j)$,and then absorption at (r, s) from there,
(ii) a first move to $(i - 1, j)$,and then absorption at (r, s) from there,
(iii) a first move to $(i, j + 1)$,and then absorption at (r, s) from there,
(iv) a first move to $(i, j - 1)$,and then absorption at (r, s) from there.
It follows, by the elementary laws of probability, that

$$P_{i,j}^{r,s} = \frac{1}{4}P_{i+1,j}^{r,s} + \frac{1}{4}P_{i-1,j}^{r,s} + \frac{1}{4}P_{i,j+1}^{r,s} + \frac{1}{4}P_{i,j-1}^{r,s}$$

Multiplying by reward $V_{r,s}$

$$V_{r,s}P_{i,j}^{r,s} = \frac{1}{4}V_{r,s}P_{i+1,j}^{r,s} + \frac{1}{4}V_{r,s}P_{i-1,j}^{r,s} + \frac{1}{4}V_{r,s}P_{i,j+1}^{r,s} + \frac{1}{4}V_{r,s}P_{i,j-1}^{r,s}$$

Finally, summing each term over all possible values of (r,s),

$$\sum_{r,s} V_{r,s}P_{i,j}^{r,s} = \frac{1}{4}\sum_{r,s} V_{r,s}P_{i+1,j}^{r,s} + \frac{1}{4}\sum_{r,s} V_{r,s}P_{i-1,j}^{r,s} + \frac{1}{4}\sum_{r,s} V_{r,s}P_{i,j+1}^{r,s} + \frac{1}{4}\sum_{r,s} V_{r,s}P_{i,j-1}^{r,s}$$

From the definition of expectation, it follows that

$$\sum_{r,s} V_{r,s}P_{i,j}^{r,s} = E_{i,j}$$

with similar expressions for the terms on the right-hand side. Therefore, the equation can be re-written

$$E_{i,j} = \frac{1}{4}E_{i+1,j} + \frac{1}{4}E_{i-1,j} + \frac{1}{4}E_{i,j+1} + \frac{1}{4}E_{i,j-1}$$

This is true for all interior points. As regards boundary points,

$$E_{r,s} = V_{r,s}$$

since the random walk in this case is null.

Relating part 1 and part 2 : Harmonic Function and Uniqueness Principle

A function $f_{i,j}$ defined on S is harmonic if, at all points of D, it satisfies the averaging property

$$f_{i,j} = \frac{1}{4}f_{i+l,j} + \frac{1}{4}f_{i-1,j} + \frac{1}{4}f_{i,j+1} + \frac{1}{4}f_{i,j-1}$$

As we can see, potential $\psi_{i,j}$ and expectation $E_{i,j}$ are harmonic functions on S having same values on boundary. We are going to use the following two principles to show the relation between them [3].

- MAXIMUM PRINCIPLE: A harmonic function $f_{i,j}$ defined on S takes on its maximum value M and its minimum value m only on the boundary.
- UNIQUENESS PRINCIPLE: If $f_{i,j}$ and $g_{i,j}$ are two harmonic functions on S such that $f_{i,j} = g_{i,j}$ on B, then $f_{i,j} = g_{i,j}$ for all points (i, j).

As potential ψ and expectation E are two harmonic functions with same values on boundary, we can conclude that $\psi = E$

Here we have shown how the solution of a deterministic equation (Laplace) is related a stochastic process (Random walk).

2.2 Algorithm

Having understood how the Laplace equation can be solved using random walk method,we proceed further and write the algorithm for this method.

1. Start
2. Set initial point of the random walk (This is the point where the solution is to be obtained)
3. Perform next step in the random walk
4. Is boundary reached?
   If No : Repeat step 3
   If Yes : Proceed to next step
5. Record the potential at the boundary

6. Is N.O of Realizations completed?
   If No : Repeat from Step 2
   If Yes : Proceed to Next step

7. Calculate the mean potential using eqn 2.2

8. Stop

2.3 Numerical Experiments

In this section, we present results from the numerical experiments on the algorithm.

2.3.1 Problem Setup

The problem of interest is to find the potential at any arbitrary point inside a rectangular box of infinite extent in the z-direction with conducting walls and potentials as specified in the Figure 2.3. The square box considered here is of unit dimension. This problem can be classified as electrostatic, interior, elliptic, Dirichlet and deterministic.

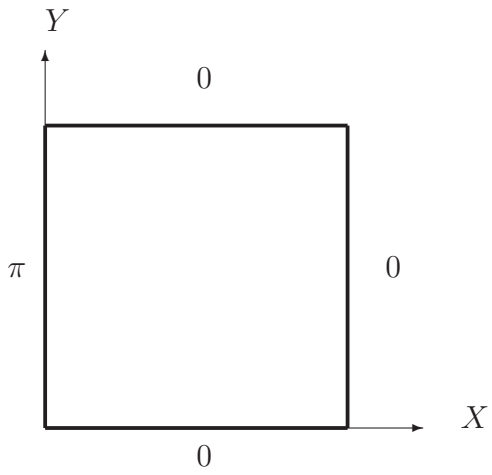

Figure 2.3. Rectangular box with perfectly conducting walls

2.3.2 Analytical Solution

The analytical solution to the problem specified is obtained by solving Laplace equation.The Laplace equation for a homogeneous region is given by

$$\frac{\partial^2 \psi}{\partial^2 x} + \frac{\partial^2 \psi}{\partial^2 y} = 0$$

where ψ -potential.

This Partial Differential Equation(PDE) can be solved by reducing it to a set of Ordinary Differential Equations (ODE).The easiest way to reduce a partial differential equation to a set of ordinary ones is by separating the variables.

$$\begin{aligned} Let \quad \psi(x,y) &= X(x)Y(y) \\ \Rightarrow \frac{\partial^2\psi}{\partial^2 x} + \frac{\partial^2\psi}{\partial^2 y} &= \frac{1}{X}\frac{\partial^2 X}{\partial^2 x} + \frac{1}{Y}\frac{\partial^2 Y}{\partial^2 y} = 0 \end{aligned}$$

Since x and y are independent, and for this to be true each term must be a constant and therefore

$$\frac{\partial^2 X}{\partial^2 x} = +k^2 X$$
$$\frac{\partial^2 Y}{\partial^2 y} = -k^2 Y$$

So the general solutions have the form

$$\begin{aligned} X &= A\cosh(kx) + B\sinh(kx) \\ Y &= C\cos(ky) + D\sin(ky) \end{aligned}$$

with only four of the five constants A, B, C, D, k independent.

The approach is to choose the value of the constants in the general solution above such that the specified boundary conditions are met. Since the principle of superposition applies to solutions of Laplace equation, let ψ_1 be the solution when $V_2 = V_3 = V_4 = 0$ and $V_1 \neq 0$ and ψ_2, ψ_3, ψ_4 be the solutions when only potential $V_2 \neq 0$, $V_3 \neq 0$, $V_4 \neq 0$ respectively. The solution

$$\psi(x,y) = \psi_1(x,y) + \psi_2(x,y) + \psi_3(x,y) + \psi_4(x,y)$$

Finding $\psi_1(x,y)$
Left Boundary

$$\psi_1(0,y) = XY|_{x=0} = A(C\cos(ky) + D\sin(ky))$$
$$\text{As} \quad \psi_1(0,y) \neq 0 \Rightarrow A \neq 0$$

Bottom Boundary

$$\psi_1(x,0) = 0 = XY|_{y=0}$$
$$\Rightarrow C(A\cosh(kx) + B\sinh(kx)) = 0$$
$$\Rightarrow C = 0 \quad \text{or} \quad A = B = 0$$
$$\text{Choose} \quad C = 0$$

Top Boundary

$$\begin{aligned} \psi_1(x,b) = 0 = XY_{y=b} \\ \Rightarrow X(D\sin(ky)) = 0 \\ \Rightarrow k = n\pi/b \quad \text{where} \quad n = 0, \pm 1, \pm 2, \pm 3... \end{aligned}$$

Right Boundary

$$\begin{aligned} \psi(a,y) = 0 = XY_{x=a} \\ \Rightarrow (D\sin(\frac{n\pi}{b}))(A\cosh(\frac{n\pi a}{b}) + B\sinh(n\pi a/b)) = 0 \quad \text{and as} \quad D \neq 0 \\ \Rightarrow \frac{A}{B} = -\tanh(\frac{n\pi a}{b}) \end{aligned}$$

Therefore

$$\begin{aligned} \psi_1(0,y) = V_1 = AD\sin(\frac{n\pi y}{b}) \\ \text{Let} \quad \psi_1(0,y) = \sum_{n=1}^{\infty} A_n \sin(\frac{n\pi y}{b}) \\ \Rightarrow A_n = \frac{2}{a}\int_0^b V_1(y)\sin(\frac{n\pi y}{b})dy \end{aligned}$$

Thus

$$\begin{aligned} \psi_1(x,y) &= \sum_{n=1}^{\infty} A_n \sin(\frac{n\pi y}{b})(\cosh(\frac{n\pi x}{b}) - \coth(\frac{n\pi a}{b})\sinh(\frac{n\pi x}{b})) \\ \psi_2(x,y) &= \sum_{n=1}^{\infty} B_n \sin(\frac{n\pi x}{b})(\cosh(\frac{n\pi x}{a}) - \coth(\frac{n\pi b}{a})\sinh(\frac{n\pi y}{a})) \\ \psi_3(x,y) &= \psi_1(a-x) \\ \psi_4(x,y) &= \psi_2(b-y) \end{aligned}$$

The final solution is

$$\psi(x,y) = \psi_1(x,y) + \psi_2(x,y) + \psi_3(x,y) + \psi_4(x,y) \tag{2.3}$$

2.3.3 Experimental Setup

In order to solve this problem using random walk approach, the first step is to divide the region into a set of parallel and perpendicular lines so as to form a rectangular grid. In

the next step we pick each point on the grid and apply the algorithm. After we are done with a point, we proceed to another point and solve for potential at that point. As we can see, the potential at a point can be determined without the knowledge of the potential at the neighboring points. Therefore, the solution at different points can be obtained using different processors. However, in the discussion below, we obtained the solution serially at one point after one another.

There are two distinct sources of error here,
(i) an error due to grid being too coarse.
(ii) an error due to the limited number of random walks.

The first error comes from approximation made using Taylor's series (it is the same approximation seen in Finite Difference Method). The second error arises from running the simulations with a limited number of simulated random walks. Therefore the parameters influencing the accuracy are
(i)The grid size, h
(ii)The number of simulated random walks (called realizations), N
We expect the accuracy to increase with decrease in grid size and increase in number of realizations.

Our goals in this experiment are
(i) to test whether the error follows the trend discussed above or not.
(ii) what set of parameters is to be chosen to obtain accurate results in small amount of time.

2.3.4 Results and Discussion

The electrostatic potential distribution inside the rectangular region, where the potential on the left wall is specified as π volts and the potential on other walls is specified as 0 volts, is shown in Figures 2.4 and 2.5. A comparision of the analytic solution and solution by random walk method (RW) shows a good agreement between these two.

Figure 2.6 shows the contours of electrostatic potential obtained by analytical solution (red) and random walk method (blue), when grid size $h = 0.5$. Figures 2.7, 2.8, 2.9 and 2.10 show the contours for different grid size $h = 0.4, 0.3, 0.2$ and 0.1 respectively. These set of figures depict how the RW solution approaches analytical solution with increase in number of realizations and decrease in grid size.

For the sake of completeness, time taken by the random walk method to complete, say N number of realizations on a grid size h, for different values of N and h is presented in the

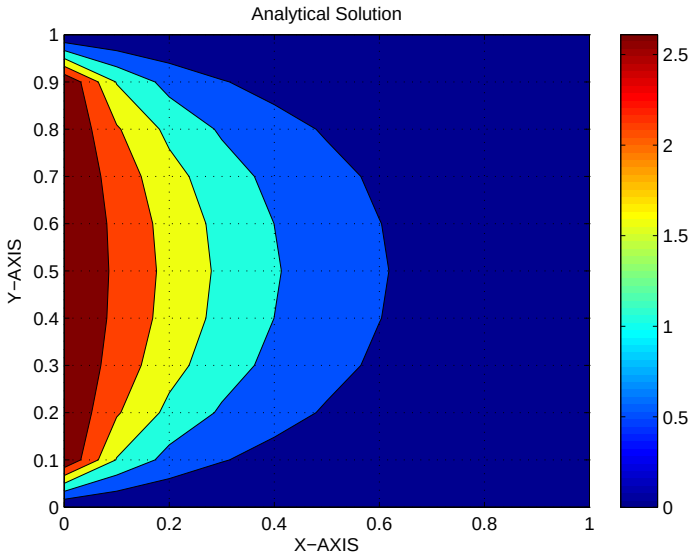

Figure 2.4. Analytical Solution

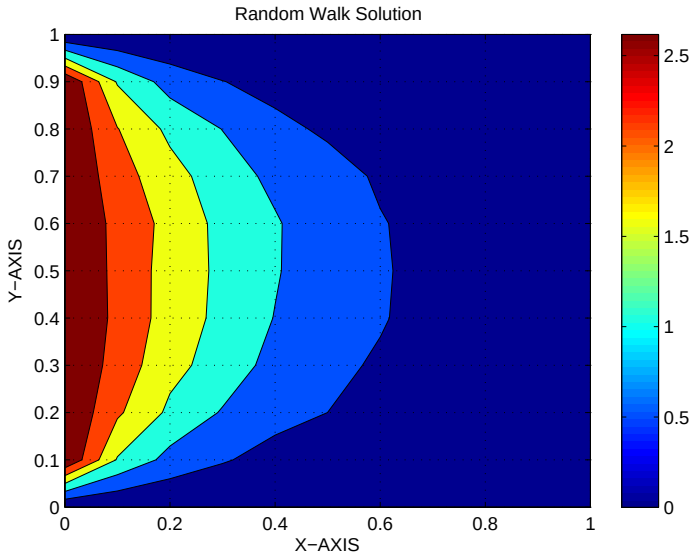

Figure 2.5. RW Solution — $N = 2000$ and $h = 0.1$

Figure 2.11. It can be observed from the figure that time taken by the random walk method increases with increase in number of realizations and decrease in grid size. These results are presented to support our prediction by intuition and give the reader a sense of how fast this algorithm is.

The time taken to complete N realizations on a grid of size $h = 0.1$ is plotted as a function of N. From the Figure 2.12, it can be said that if the number of realizations is doubled, keeping grid size constant, then time taken by RW algorithm also increases by 2.

Figure 2.13 how the time taken to complete $N = 10,000$ realizations on a grid of size h varies as a function of h. The curve tells us that if the grid size is halved, keeping $N = 10,000$ same, the time taken by RW algorithm increases 4 times. For example, for $h = 0.2$ and $N = 10,000$, it takes about 0.75 seconds and for $h = 0.1$ and $N = 10,000$, it takes about 3 seconds.

Experimental Error Analysis: As a measure of the performance of this method, an L_2 error norm is constructed as

$$\epsilon = \frac{100}{|\psi_{max}|}\sqrt{\left(\frac{1}{M}\sum_{i=1}^{M}(\psi_i^n - \psi_i^e)^2\right)}$$

where ψ_i^e is the exact analytical solution, ψ_i^n is the RW solution and M is the number of randomly choosen points in the domain where the unknown ψ is evaluated.

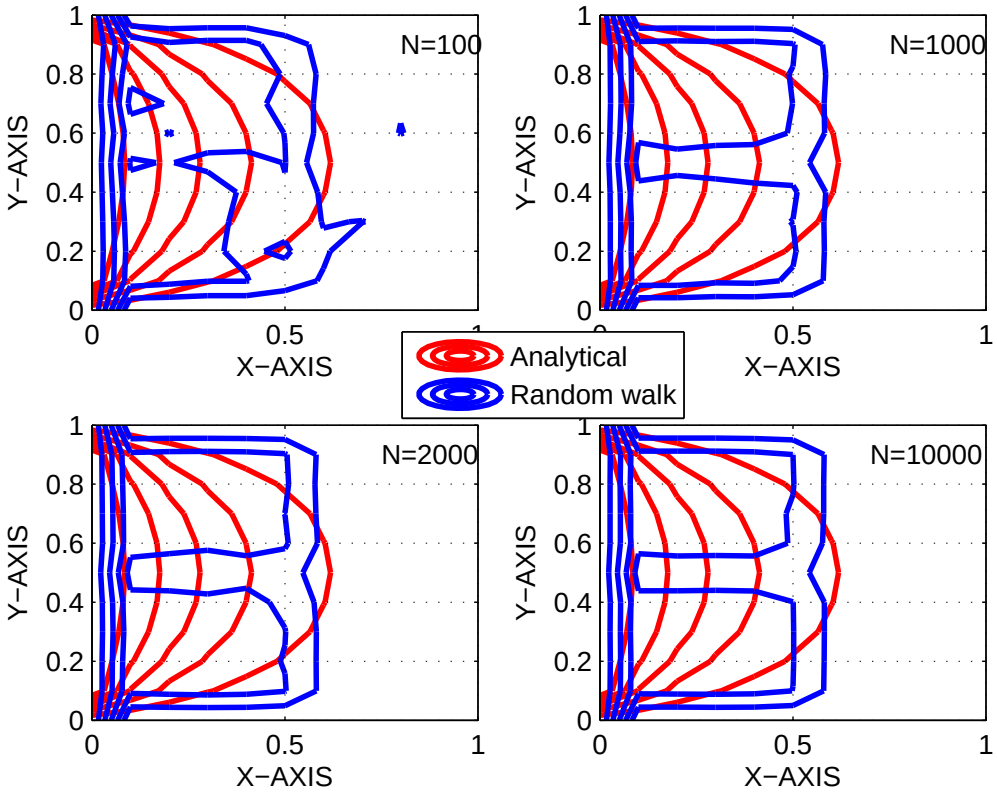

Figure 2.6. RW solution as a function of number of realizations :::: h=0.5

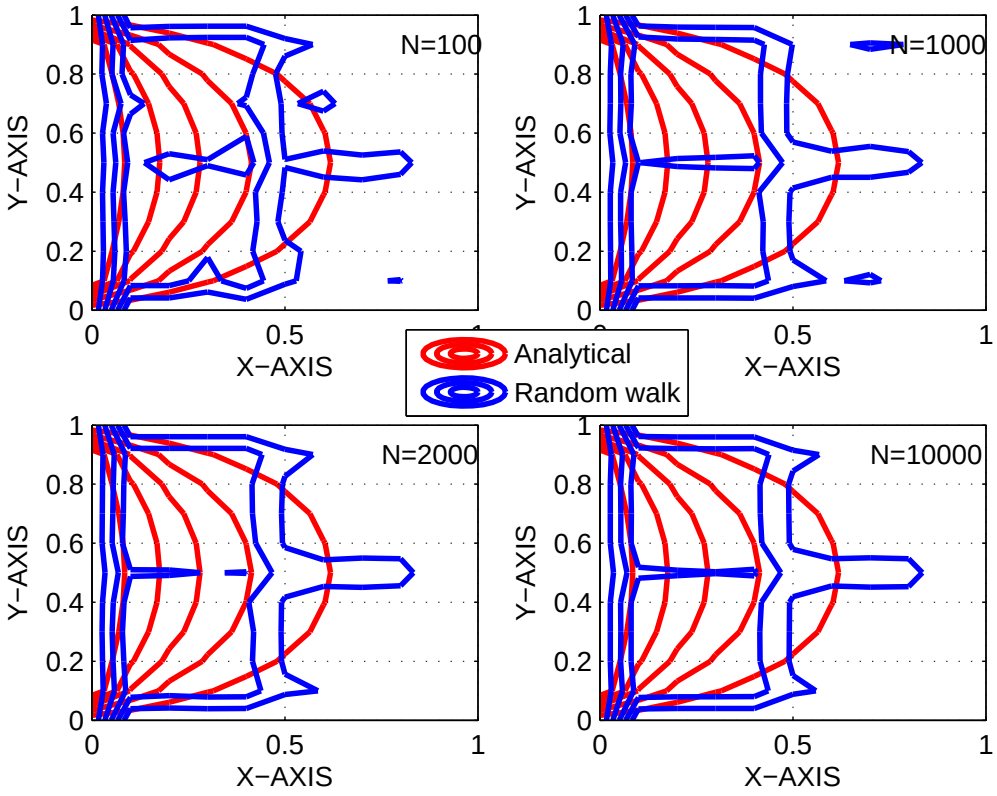

Figure 2.7. Random walk solution as a function of number of realizations :::: h=0.4

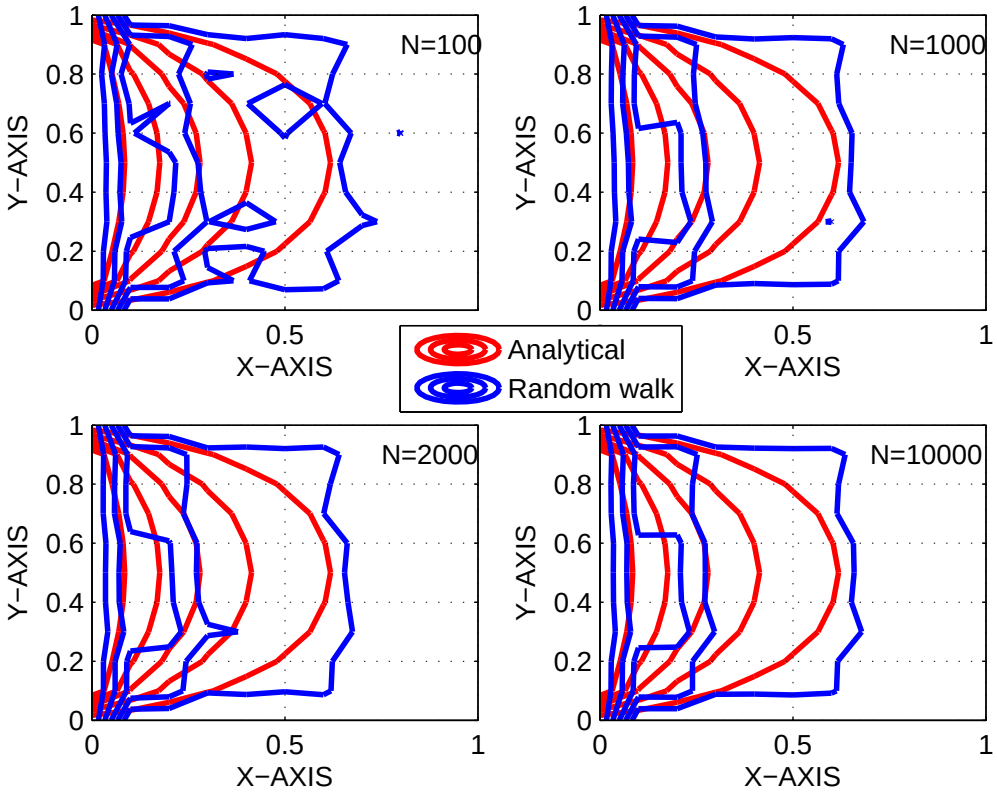

Figure 2.8. Random walk solution as a function of number of realizations :::: h=0.3

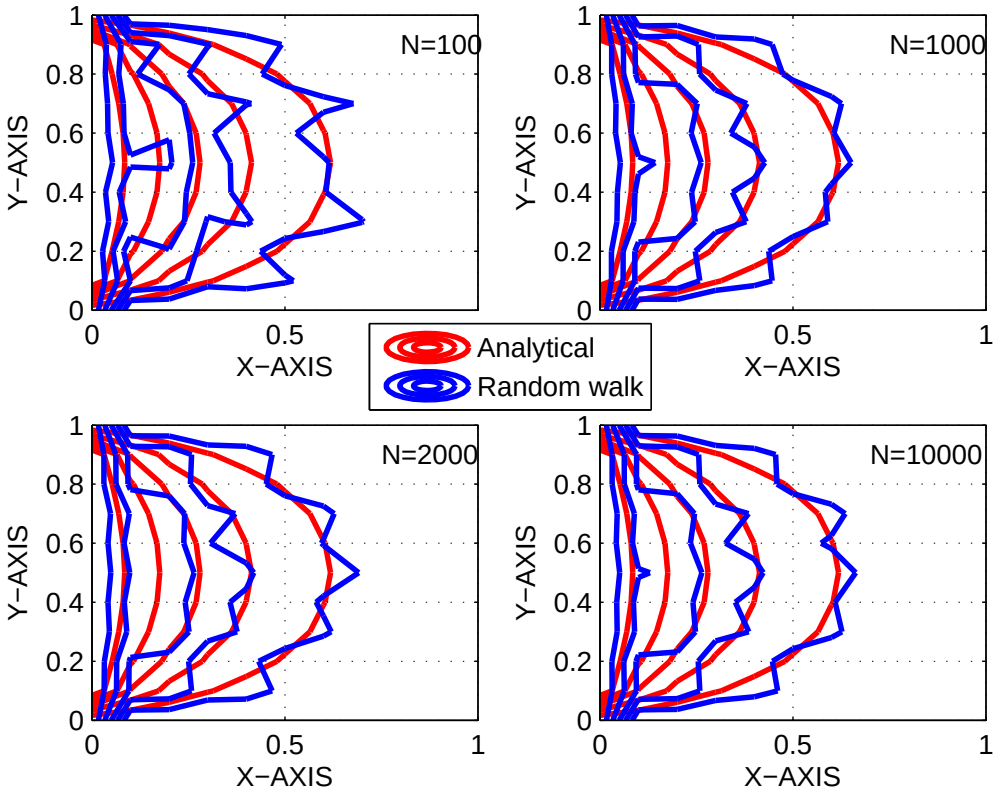

Figure 2.9. Random walk solution as a function of number of realizations :::: h=0.2

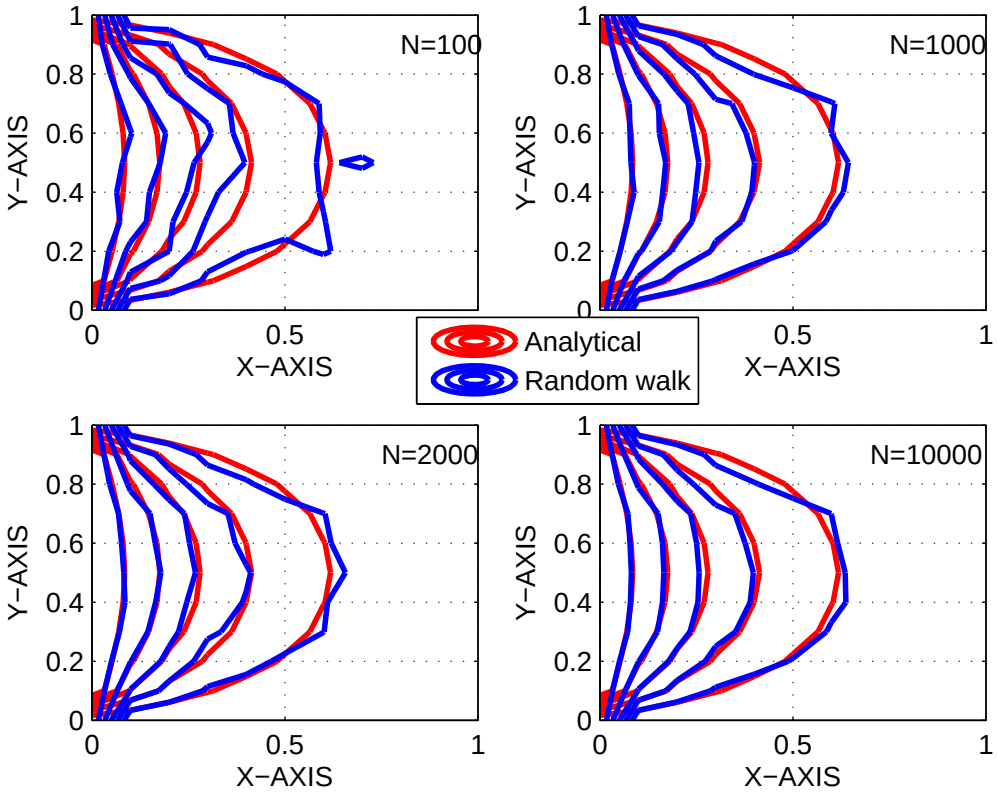

Figure 2.10. Random walk solution as a function of number of realizations :::: h=0.1

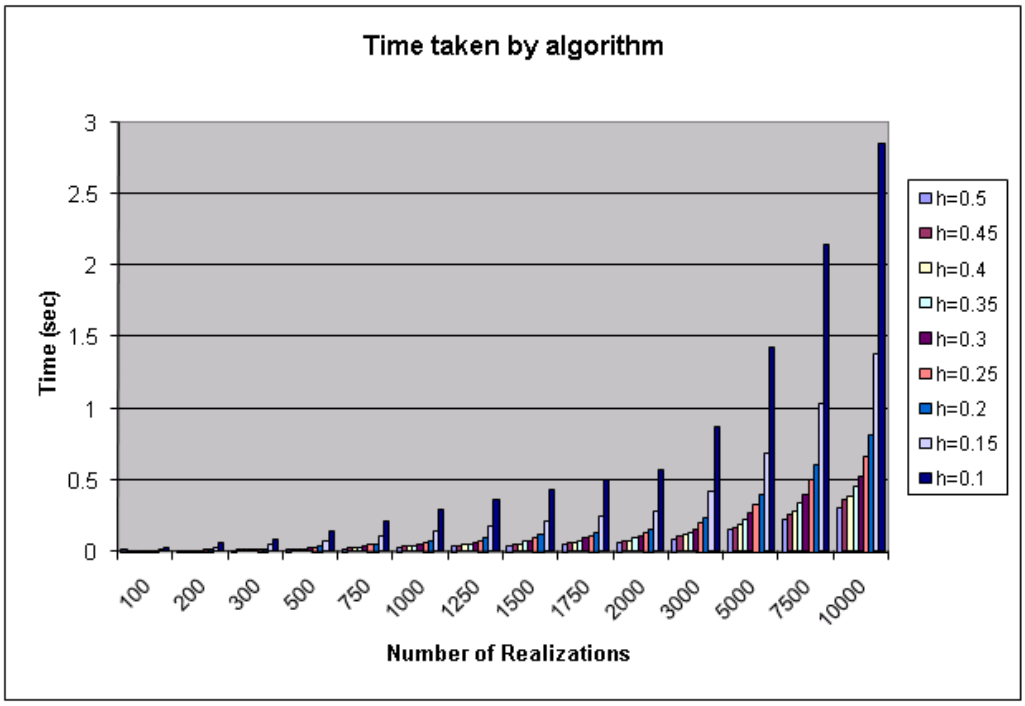

Figure 2.11. Time taken by the RW method to complete, N number of realizations on a grid size h

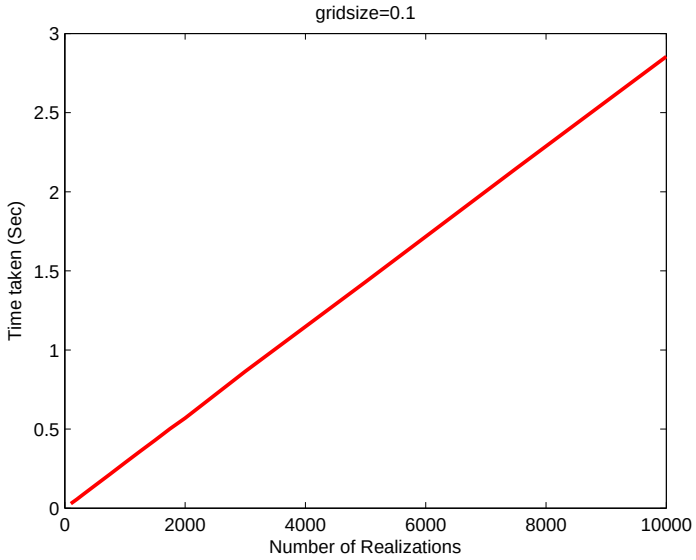

Figure 2.12. Time taken by RW algorithm as a function of number of realizations, N

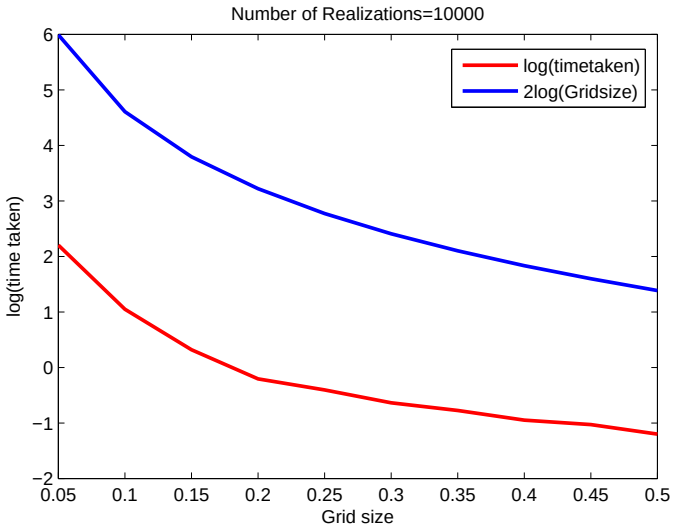

Figure 2.13. Time taken by RW algorithm as a function of grid size,h

Figure 2.14 indicates how the L_2 error varies as a function of number of realizations for different values of grid size. The L_2 error decreases as we decrease the grid size for a given number of realizations. For a given grid size, the error decreases with increase in number of realizations up to certain number of realizations and it gets saturated beyond that. For example, for grid size $h = 0.1$, the accuracy improves by increasing number of realizations up to $N = 2,000$ and the L_2 error curve stays flat beyond $N = 2,000$.

Figure 2.15 indicates how the L_2 error varies as a function of grid size for different values of number of realizations. This also depicts that accuracy increases with increase in number of realizations and decrease in grid size.

Figure 2.16 depicts how L_2 error decreases with increase in number of realizations, with grid size 0.1. In Figure 2.17, normalized L_2 error is plotted as function of number of realizations. The four curves drawn in blue show the normalized values of $N^{-1/4}, N^{-1/3}, N^{-1/2}$ and N^{-1} (labeled as $1, 2, 3$ and 4 respectively) as a function of number of realizations N. It can be observed that curve showing normalized L_2 error overlaps with that of $N^{-1/2}$, showing that error is inversely proportional to $\sqrt{N}$, where N is number of realizations, for small values of number of realizations. Therefore statistical error in random walk solution retains $\mathscr{O}(N^{-1/2})$ behavior expected in Monte Carlo simulations.

Figure 2.18 and 2.19 show the variation of L_2 error and normalized L_2 error as a function of grid size for $N = 10000$. The green curve in figure 2.16 is a straight line with slope 2.1. It can be observed from the figure how close the error curve and straight line for different

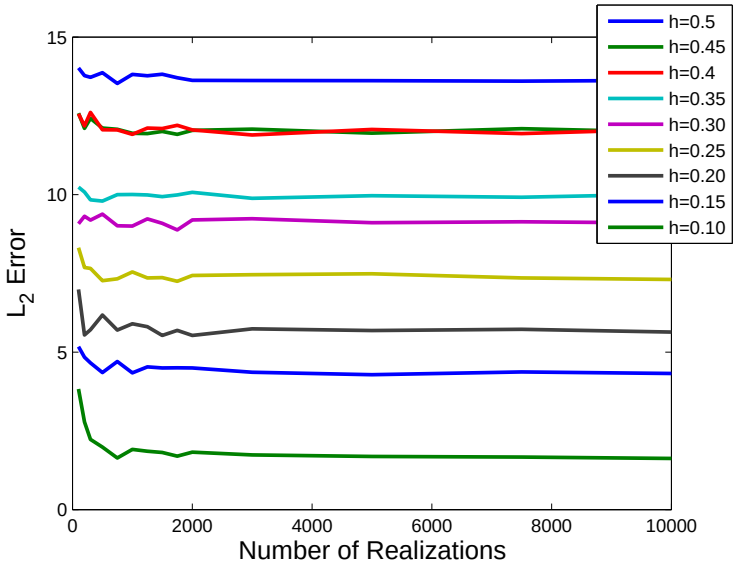

Figure 2.14. L_2 error variation with number of realizations for different grid sizes

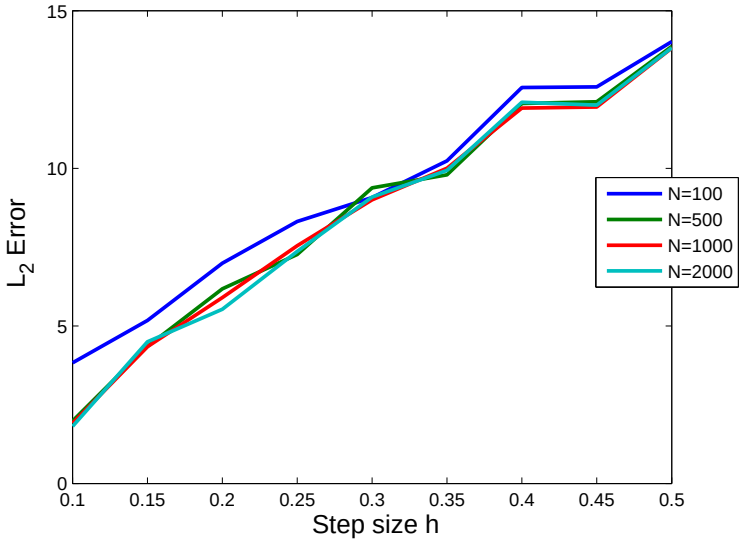

Figure 2.15. L_2 error variation with grid size for different values of N

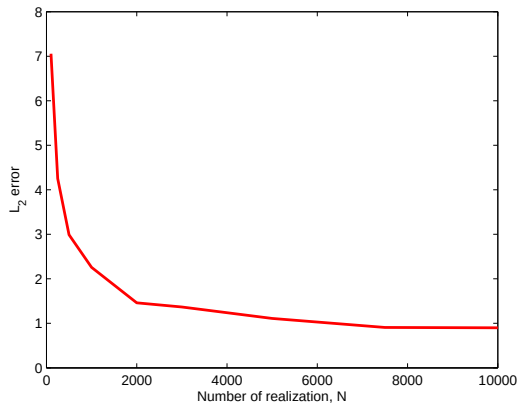

Figure 2.16. L_2 Error vs Number of Realizations

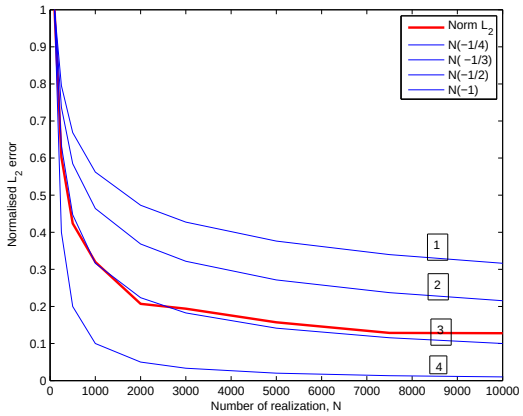

Figure 2.17. Normailzed L_2 error varying as $N^{-1/2}$

values of grid size are. From this plot we can conclude that L_2 error is directly proportional to grid size.

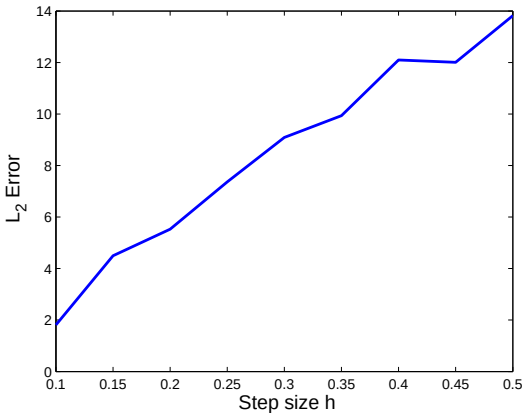

Figure 2.18. L_2 Error vs grid size

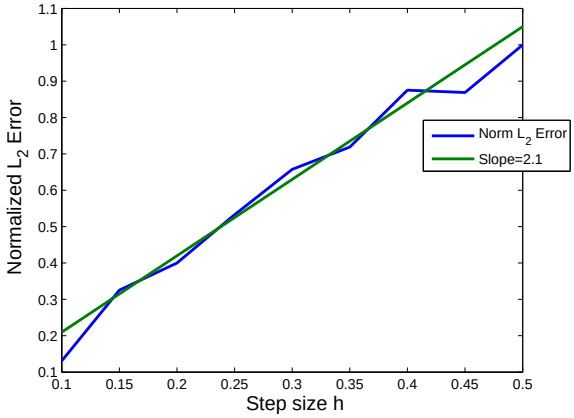

Figure 2.19. Normailzed L_2 error varying linearly with grid size

To summarize, normalized L_2 error is directly proportional to grid size h and inversely proportional to $\sqrt{N}$

$$\epsilon \propto \left(\frac{h}{\sqrt{N}}\right)$$

.

As a final exercise, we would like to answer the question, for a given accuracy, what set of parameters is to be chosen to obtain the solution with desired accuracy in minimum

amount of time $i.e$ to obtain solution with 2.5% L_2 error, there will be many combinations of grid size h and number of realizations N. But which set of parameters we should choose, to obtain results in time as small as possible.

Figure 2.20 shows the number of realizations for a given grid size to obtain results with an accuracy 2.5%. For grid size $h = 0.1$, we need about $2,200$ realizations, where as for $h = 0.05$, we need only 600 realizations (about one-fourth of that for $h = 0.1$).

Figure 2.21 shows how much time it takes to get 2.5% L_2 error for a given grid size. In other words, how much time it takes to complete number of realizations shown in previous figure for a given grid size. It can be observed from this figure, for all grid size the algorithm takes about same time of 0.63 sec. The reason for same time for all grid sizes is, because ϵ is directly proportional to h and inversely proportional to $\sqrt{N}$, whereas time taken to complete a given number of realizations N for a given grid size h is directly proportional to N and inversely proportional to $\sqrt{h}$. It can concluded the time taken to obtain a solution with given accuracy for different values of grid sizes to be very close to each other and the fluctuations can be accounted to the random nature of the stochastic process we are simulating. Therefore the best in time we can do with random walk to obtain solution to Laplace equation for the given problem with 2.5% L_2 error is 0.62 seconds.

The conclusion of this experiment is to obtain a solution with a given L_2 error, choose a grid size h using Figure 2.14. For example, for $\epsilon = 2.5\%$, $h = 0.5$ is a bad choice, as smallest error possible is about 12% for that case. Sizes $h < 0.1$ are good for this case. Once this is chosen, we can obtain the result with different accuracy by varying the number of realizations.

2.4 Brownian Motion Process: Continuous analog of random walk process

In the last section, investigation on how a random walk in a plane can be used to solve Laplace equation in $2D$ has been done. The question to ask is what will be the case if the point where the solution is needed is not on the grid chosen or how does the random walk behave as grid size shrinks to 0. If $(x(t), y(t))$ represents the position of the particle at time t, then how do we obtain $(x(t), y(t))$, if the starting point $(x(0), y(0))$ is known. These are the issues that will be investigated here [4].

The length of the space step between two points is h. The distance over which the particle moves in n steps becomes proportional to h. Let Δt represent discrete time step at which

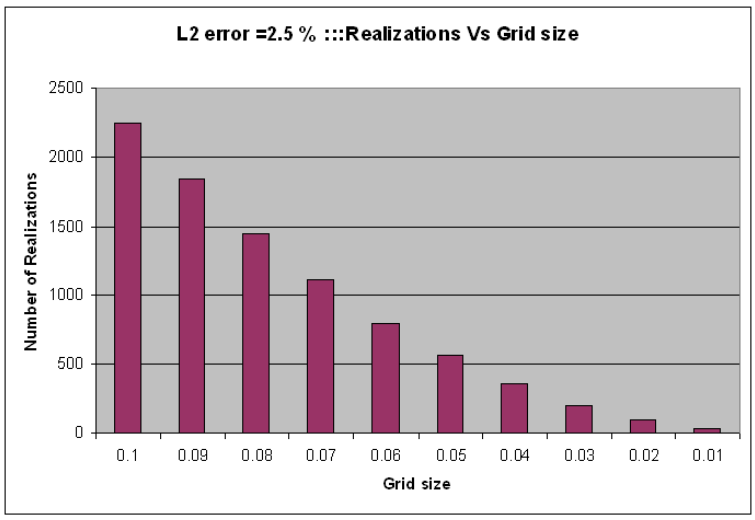

Figure 2.20. Number of realizations required to get L_2 error = 2.5% as a function of grid size

the jumps take place. *i.e* if the random walk starts at $t = 0$, the next jump takes place at Δt, next one at $2\Delta t$ and so on. Here h and Δt are parameters that can be varied. Suppose if h and Δt are simultaneously varied such that the particle will move, on the average, the same distance in the same period of time. For example, if we increase h alone, the distance that the particle moves in each time step increases. So, if the number of jumps made by the particle is decreased properly, then it is possible to maintain the average distance that the particle moves to be the same. The transition frequency, *i.e* number of times particle jumps in a unit time, should decrease. So Δt also has to increase. Thus in general, if h increases, Δt should increase and if h decreases, Δt should decrease. In the limit as $h \to 0$, a continuous random walk will result.

In order to find a proper relation between the shrinking parameter h and growing transition frequency (or may be Δt) and to obtain the limiting distribution of the particle displacement in time t, central limit theorem is to be applied. Let us assume that vector $\overline{\xi}_i (i = 1, 2, ...)$ represents the jump at i^{th} time step. For $2D$,

$$\overline{\xi}_i \;=\; +h\hat{a_x} \quad \text{or} \quad -h\hat{a_x} \quad \text{or} \quad +h\hat{a_y} \quad \text{or} \quad -h\hat{a_y}$$

$\overline{\xi}_i$ represents a random variable that are mutually independent, identically distributed and have zero expectations and finite second moments.

CENTRAL LIMIT THEOREM: Let $X_1, X_2, ...$ be independent, identically distributed random variables withe finite mean μ and finite variance σ^2. If Y_n is defined by

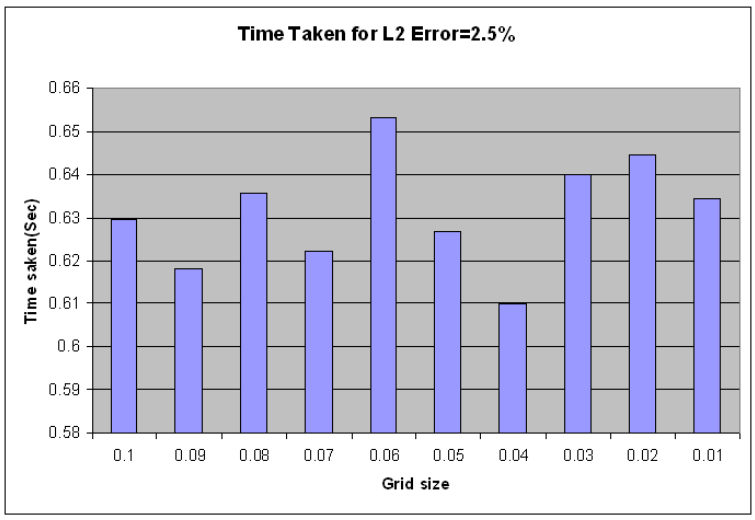

Figure 2.21. Time taken to obtain L_2 error = 2.5% for different grid sizes.

$$Y_n := \frac{1}{\sqrt{n}} \sum_{i=1}^{n} \left(\frac{X_i - \mu}{\sigma} \right) \tag{2.4}$$

Then, Y_n converges as $n \to \infty$ to a normal distribution with zero expectation and same matrix of second moments as that of the random vectors $\overline{\xi}_i$

As $\overline{\xi}_i$ denotes displacement in the i^{th} step of the particle executing a walk, expectation and variance are given by

$$E\{\overline{\xi}_i\} = 0$$
$$E\{\overline{\xi}_i^2\} = 1/l$$

where l denotes the dimension of the walk.

The displacement of the particle in n steps during a random walk with parameter h is given by

$$Y_n := h(\overline{\xi}_1 + ... + \overline{\xi}_n) \tag{2.5}$$

Comparing eqn(2.4) and eqn(2.5), it can be seen that for a reasonable limiting distribution, the parameter h must be of the order $1/\sqrt{n}$. As the number of steps is of the order of $1/h^2$ (as the random walk here is 2 dimensional), the interval between successive jumps of the particle is equal to h^2/l(the coefficient l is introduced to simplify the relation).

Consider a time t, at which the particle has executed n steps and thus:

$$t = n \times \Delta t \Rightarrow t = n \times h^2/l \Rightarrow n = lt/h^2$$

The position of the particle at time t in this random walk is denoted by

$$x(t) - x(0) = h(\overline{\xi}_1 + ...\overline{\xi}_n) = \sqrt{\frac{lt}{n}}(\overline{\xi}_1 + ...\overline{\xi}_n)$$

As it can be noticed the vector $x(t) - x(0)$ is derived from the vector 2.4 by multiplying by a constant $\sqrt{lt}$. In the limit as $h \to 0$ the increment $x(t) - x(0)$ has a symmetrical normal distribution with a variance equal to $1/l * (\sqrt{lt})^2 = t$ in any direction.

Therefore the probability density function

$$p(t, x) = \frac{1}{(2\pi t)^{l/2}} exp(-x^2/2t) \tag{2.6}$$

$$p(t, y) = \frac{1}{(2\pi t)^{l/2}} exp(-y^2/2t) \tag{2.7}$$

Once initial point $(x(0), y(0))$ is known, $(x(t), y(t))$ can be obtained using above pdf's.

Thus, a random walk on a grid goes over in the limit to a continuous process for which the random displacement of the particle during a time t has the density given by eqn(2.6). The mathematically correct formulation of the corresponding stochastic process has come to be known as Wiener process or Brownian motion process.

Hereafter we will be using only $x(t)$. Whatever applies to $x(t)$ also applies to $y(t)$.

2.5 Brownian Motion Process or Wiener Process : Definition and Properties

Let $\mathbf{W}(t); t \geq 0$ be Brownian motion process taking values in R^d (d-dimensional real space). The process starts at an arbitrary point $\mathbf{x} \in R^d$ and is characterized by stationary independent increments, that is, the increments of $\mathbf{W}$ over non-overlapping time intervals are independent and their statistics depend only on the duration of the time increment [11]. Specifically,

(1) the increment $\mathbf{W}(t) - \mathbf{W}(s)$ of $\mathbf{W}$ during the time interval (s, t), $s < t$, is an d-valued Gaussian vector with mean zero and covariance matrix $I(t-s)$, where I denotes the identity matrix and

(2) the increments $\mathbf{W}(t) - \mathbf{W}(v)$ and $\mathbf{W}(u) - \mathbf{W}(s)$, $s < u \leq v < t$, are independent.

Properties The Wiener process $\mathbf{W}(t)$ is characterized by three facts:

1. $\mathbf{W}(0) = 0$
2. $\mathbf{W}(t)$ is almost surely continuous
3. $\mathbf{W}(t)$ has independent increments with distribution $\mathbf{W}(t) - \mathbf{W}(s) \sim \mathcal{N}(0, t-s)$ for $(0 < s < t)$.

where $N(\mu, \sigma^2)$ denotes the normal distribution with expected value μ and variance σ^2. The condition that it has independent increments means that if $0 < s_1 < t_1 < s_2 < t_2$, then $\mathbf{W}(t_1) - \mathbf{W}(s_1)$ and $\mathbf{W}(t_2) - \mathbf{W}(s_2)$ are independent random variables.

For $\mathbf{W}(t)$ a Wiener process, $\mathbf{W}(0) = 0$ and $\mathbf{W}(t)$ has independent increments. It can be showed that this process $\mathbf{W}(t)$ also satisfies Markov property. Mathematically, if $X(t), t > 0$, is a stochastic process, the Markov property states that

$$\Pr\big[X(t+h) = y \,|\, X(s) = x(s), \forall s \leq t\big] = \Pr\big[X(t+h) = y \,|\, X(t) = x(t)\big], \quad \forall h > 0.$$

2.6 Algorithm

In this section, we describe the algorithm that can be applied to solve Laplace equation using Brownian motion.

1. Start
2. Set initial point $(x(0), y(0))$ of the Brownian motion or Wiener process (This is the point where the solution is to be obtained)
3. Perform next step using Brownian Motion Process

$$x(t + \Delta t) = x(t) + \text{pick a random number from } \sqrt{2}N(0, \Delta t)$$
$$y(t + \Delta t) = y(t) + \text{pick a random number from } \sqrt{2}N(0, \Delta t)$$

   where $N(\mu, \sigma^2)$ represents a normal distribution function with mean μ and variance σ^2.
4. Is boundary reached?
   If No : Repeat step 3
   If Yes : Proceed to next step
5. Record the potential at the boundary

6. Is number of realizations completed?
   If No : Repeat from Step 2
   If Yes : Proceed to Next step

7. Calculate the mean potential according to eqn (2.2)

8. Stop

2.7 Numerical Experiments

2.7.1 Problem setup and Analytical solution

We look at the same problem of finding the potential at a point inside a rectangular box with potential specified along the walls. This would facilitate us to draw comparisons between discrete and continuous stochastic processes, we have discussed so far. The analytical solution is same as presented in section [2.3.2].

2.7.2 Experimental Setup

The first step is to start with the point, where the solution is needed and apply the algorithm employing Brownian motion to obtain the potential at that point. After we are done with a point, we proceed to another point and solve for potential at that point. As in the discrete case, the potential at a point can be determined without the knowledge of the potential at the neighboring points. So the solution at different points can be obtained using different processors. However, in the discussion below, we obtained the solution serially at one point after one another.

The parameters that influence the performance of this method most are:
(i)The time step, Δt
(ii)The number of simulated random walks (called realizations), N

The effect of the number of realizations N has already been investigated. The more the number of realizations the better the accuracy. From the relationship $\Delta t = (\Delta x)^2/2$, it can be established that smaller the Δt, the better is the accuracy. The reason can be traced back to Taylor's series.

We set forth to see how the variation of these parameters effects the accuracy of the solution and time taken to obtain the solution, for a given accuracy.

2.7.3 Results and Discussion

To validate the approach using Brownian motion process, we are going to obtain the electrostatic potential distribution inside a rectangular box for the same problem we have solved in the previous section. The solution obtained by the Brownian motion process is presented here. Note that numerical solution for this problem has been presented before in [15]. The potential distribution inside the rectangular region obtained by analytical solution and Brownian motion process are shown in Figures 2.22 and 2.23 respectively. A comparison of the analytical solution and solution by Brownian motion process shows a good agreement between these two.

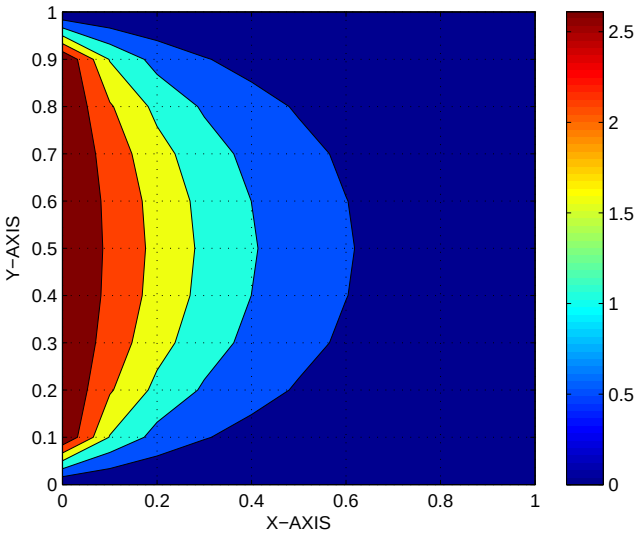

Figure 2.22. Analytical Solution

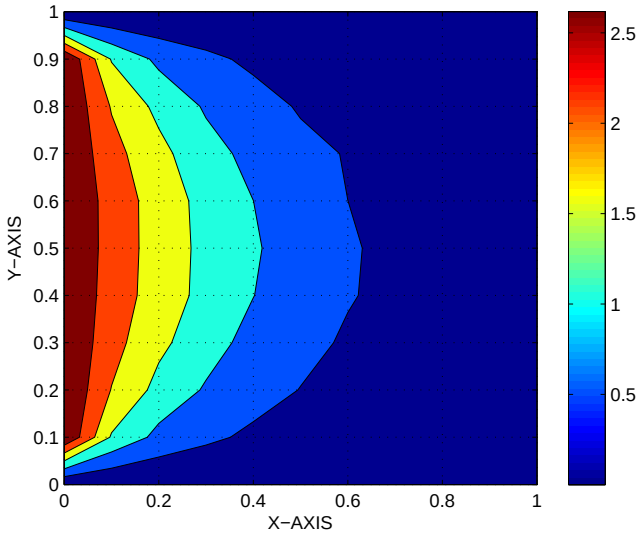

Figure 2.23. Brownian motion solution: N=4000 and $\Delta t = 0.1$

Figure 2.24 shows the contours of electrostatic potential obtained by analytical solution (red) and random walk method (blue), when $\Delta t = 1$. Figures 2.25, 2.26, 2.27 and 2.28 show the contours for different grid size $\Delta t = 0.1, 0.01, 0.001$ and 0.0001 respectively. These set of figures depict how the Brownian motion solution approaches analytical solution with increase in number of realizations and decrease in time step.

For the sake of completeness, time taken by the Brownian motion method to complete, say N number of realizations with time step Δt, for different values of N and Δt is presented in the Figure 2.29. It can be observed from the figure that time taken by the Brownian motion

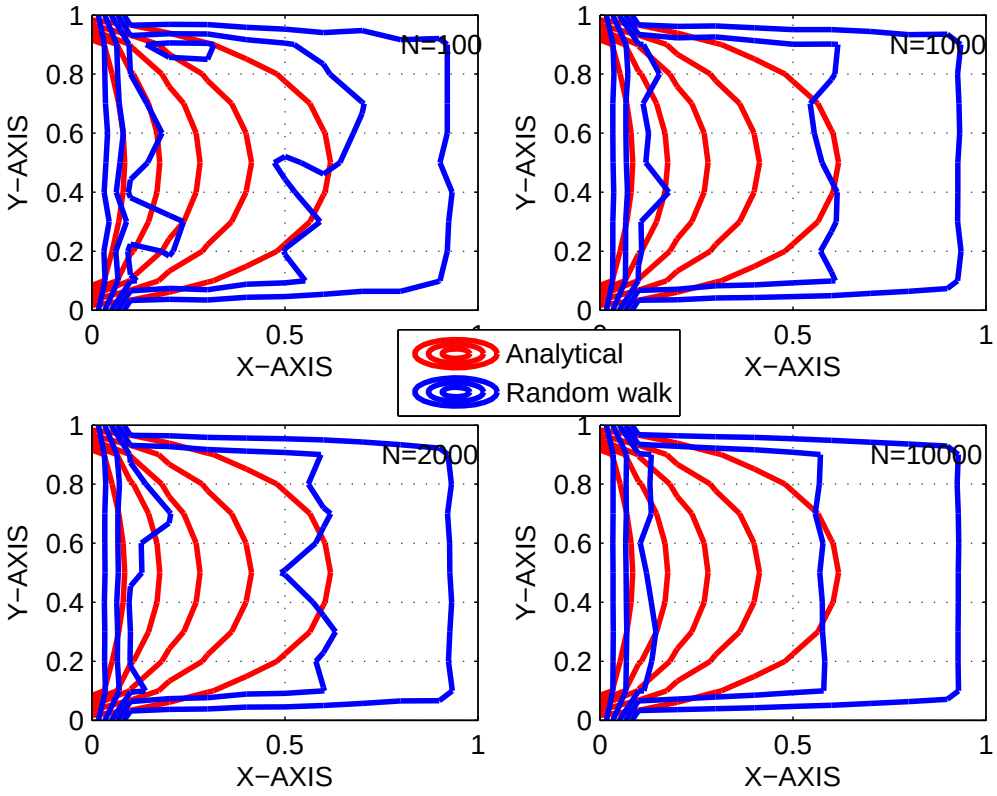

Figure 2.24. Brownian motion solution as a function of number of realizations:::: $\Delta t = 1$

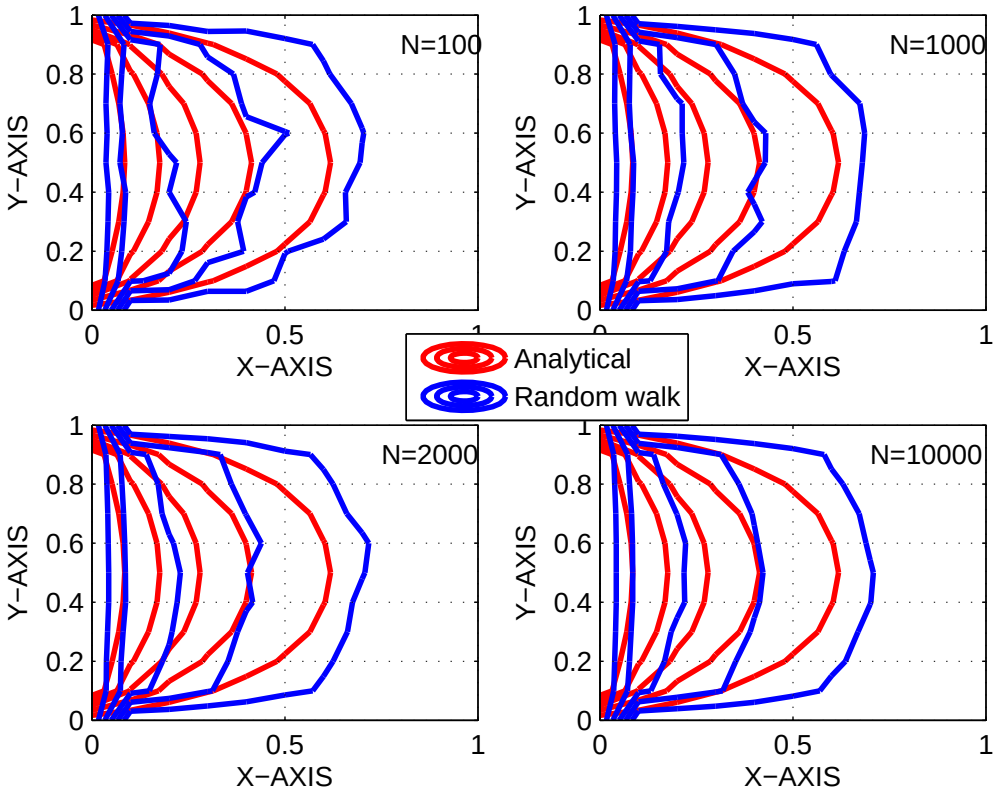

Figure 2.25. Brownian motion solution as a function of number of realizations:::: $\Delta t = 0.1$

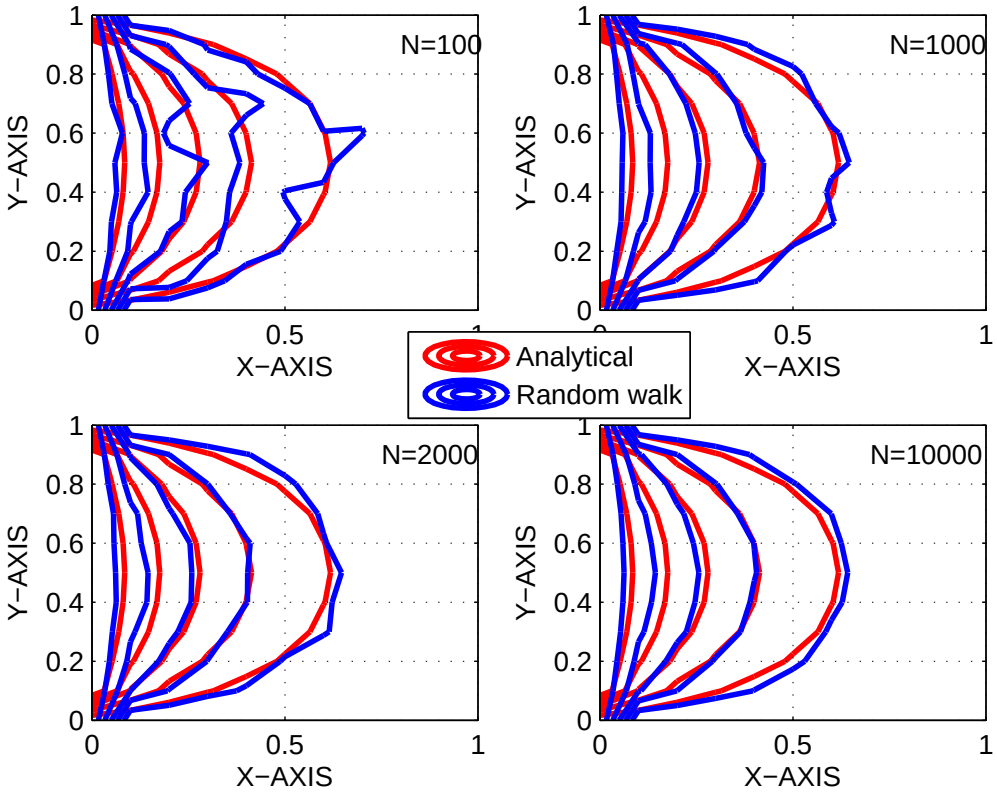

Figure 2.26. Brownian motion solution as a function of number of realizations:::: $\Delta t = 0.01$

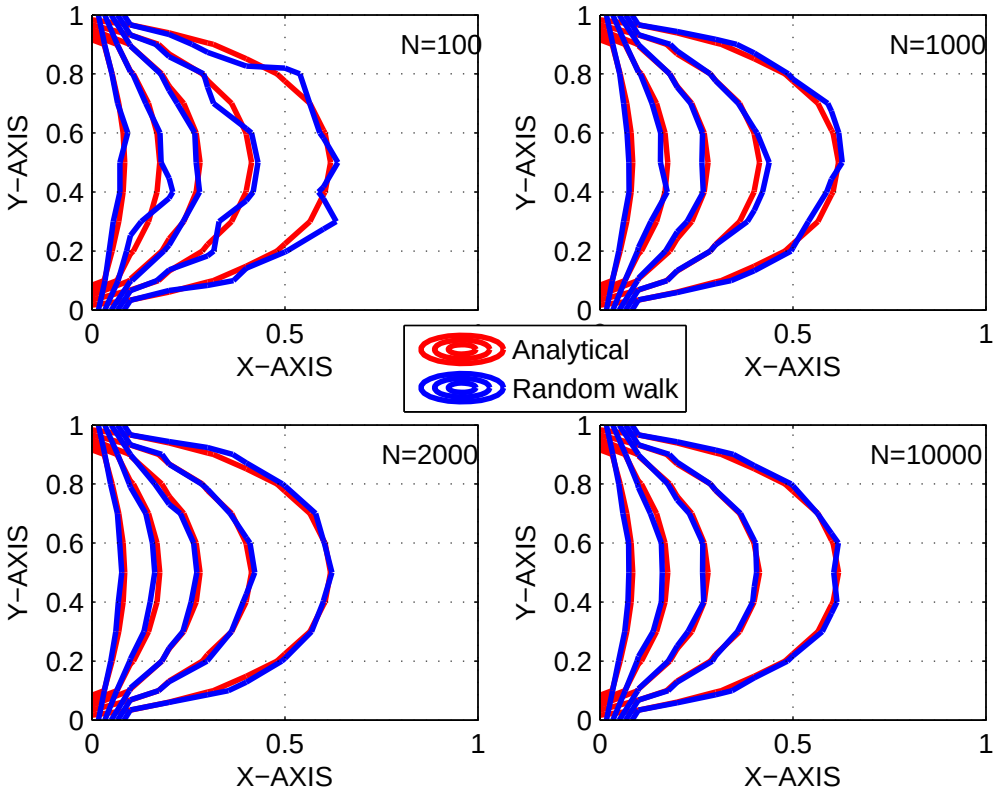

Figure 2.27. Brownian motion solution as a function of number of realizations :::: $\Delta t = 0.001$

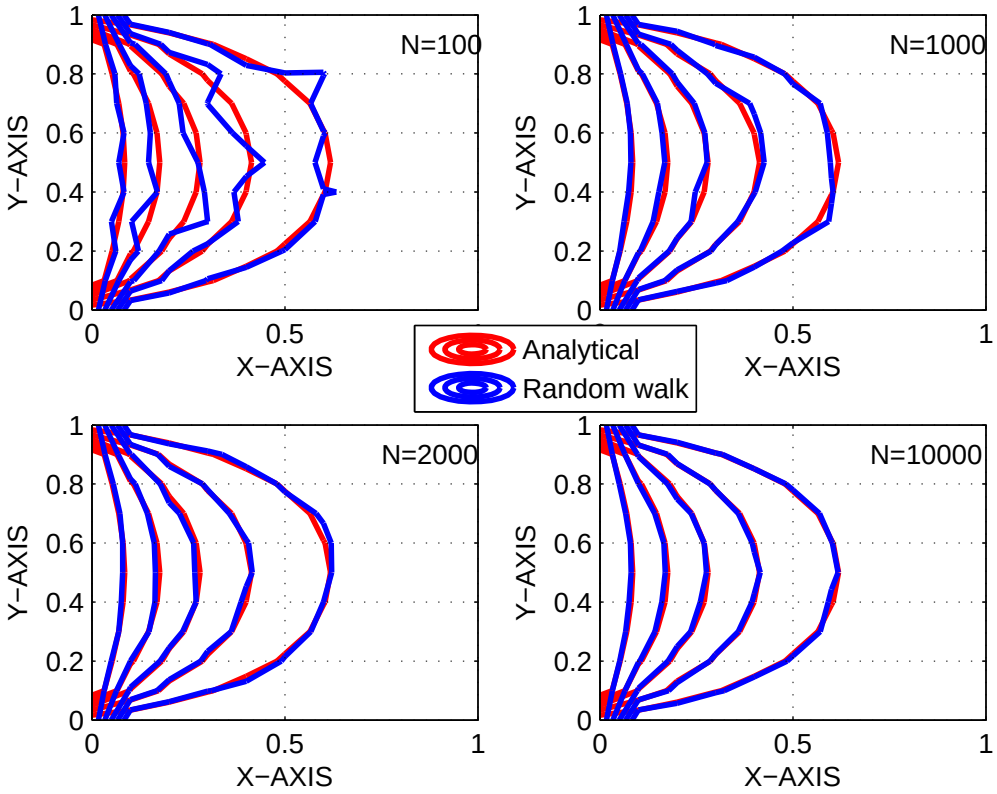

Figure 2.28. Brownian motion solution as a function of number of realizations:::: $\Delta t = 0.0001$

process increases with increase in number of realizations and decrease in time step. These results are presented to support our prediction by intuition.

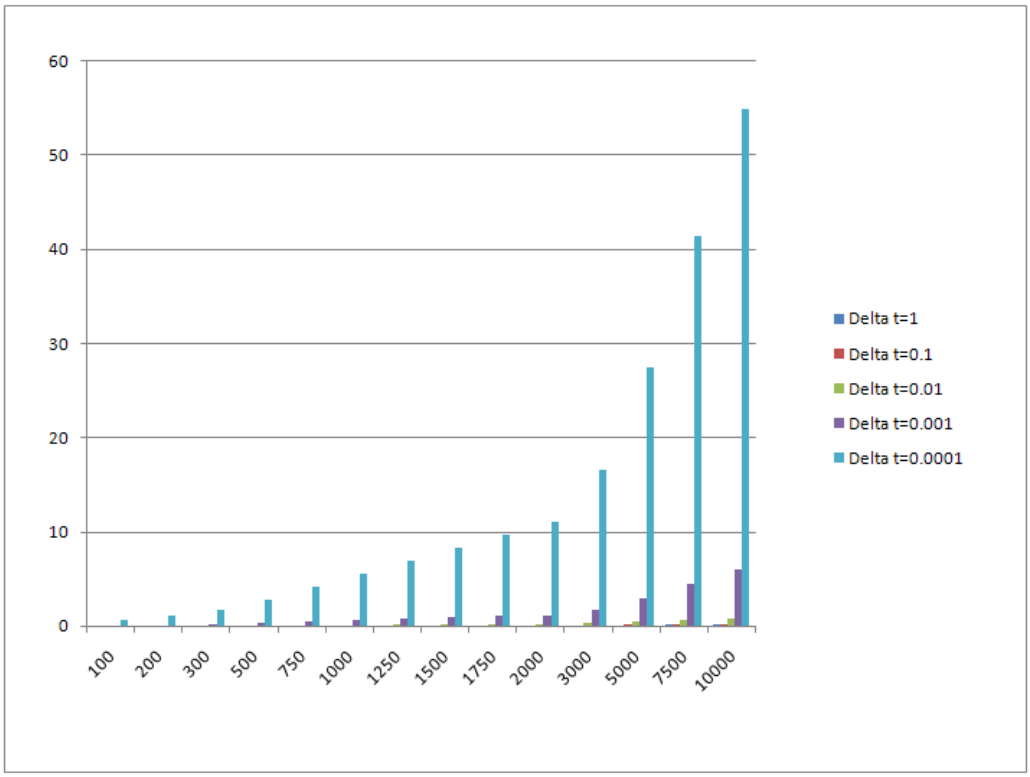

Figure 2.29. Time taken by the Brownian motion method to complete, N number of realizations with time step Δt

The time taken to complete N realizations with time step $\Delta t = 0.01$ is plotted as a function of N in the figure 2.30. It can be said that if the number of realizations is doubled, keeping Δt constant, then time taken by algorithm also increases by 2.

Figure 2.31 how the time taken to complete $N = 10,000$ realizations as a function of Δt. If Δt is increased 10 times, keeping number of realizations the same, the time taken decreases 10 times. For example, when $\Delta t = 10^{-4}$, time taken to complete $10,000$ realizations is about 50 sec, whereas for $\Delta t = 10^{-3}$, it is only about 5 sec. Therefore, for a constant number of realizations time taken by the Brownian motion process is inversely proportional to Δt. (This is also what we expect from the relationship $\Delta t = \frac{\Delta x^2}{2}$, as we have already established that time taken is inversely proportional to Δx^2 in the random walk case)

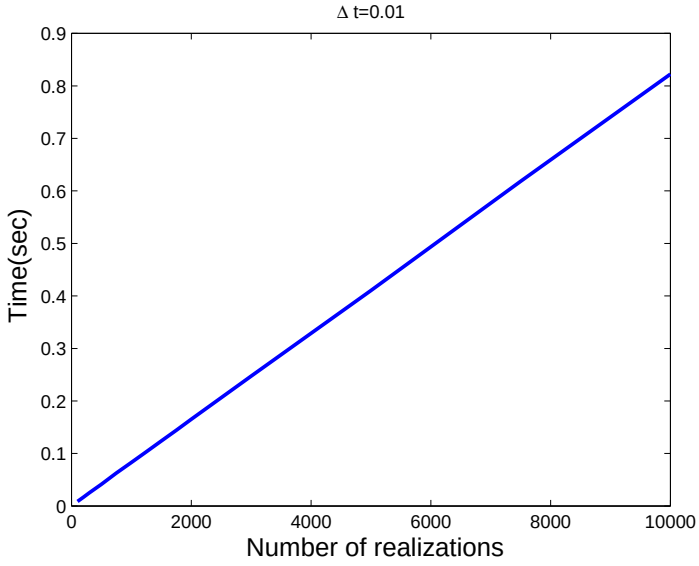

Figure 2.30. Time taken by Brownian motion algorithm as a function of number of realizations, N

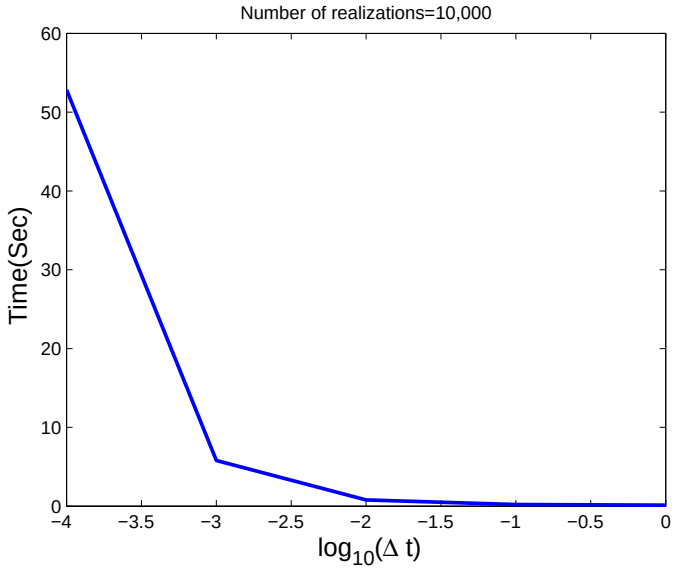

Figure 2.31. Time taken by Brownian motion algorithm as a function of time step,Δt

Experimental Error Analysis Here again we use an L_2 error norm as a measure of performance.

$$\epsilon(\%) = \frac{100}{|\psi_{max}|}\sqrt{\left(\frac{1}{M}\sum_{i=1}^{M}(\psi_i^n - \psi_i^e)^2\right)}$$

where ψ_i^e is the exact analytical solution, ψ_i^n is the Brownian motion solution and M is the number of randomly chosen points in the domain where the unknown ψ is evaluated.

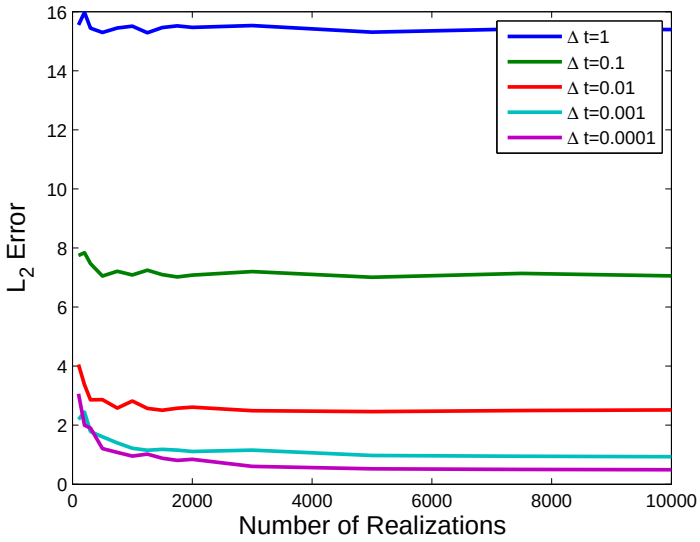

Figure 2.32. L_2 error variation with number of realizations for different Δt

Figure 2.32 indicates how the L_2 error varies as a function of number of realizations for different values of time step. The L_2 error decreases as we decrease the Δt for a given number of realizations. For a given Δt, the error decreases with increases in number of realizations up to certain number of realizations and it gets saturated beyond that. For example, for grid size $\Delta t = 0.001$, the accuracy improves by increasing number of realizations up to $N = 2000$ and the L_2 error curve stays flat beyond $N = 2000$.

Figure 2.33 indicates how the L_2 error varies as a function of Δt for different values of number of realizations. This also depicts that accuracy increases with increase in number of realizations and decrease in Δt. When Δt is changed from 10^{-2} to 10^{-1} *i.e* increased 10 times, the error changes from 2% to 6%, which is about 3 times ($\sqrt{10} = 3.16$). Therefore L_2 error increases with Δt as proportional to $\sqrt{\Delta t}$. (This is also what we expect from the

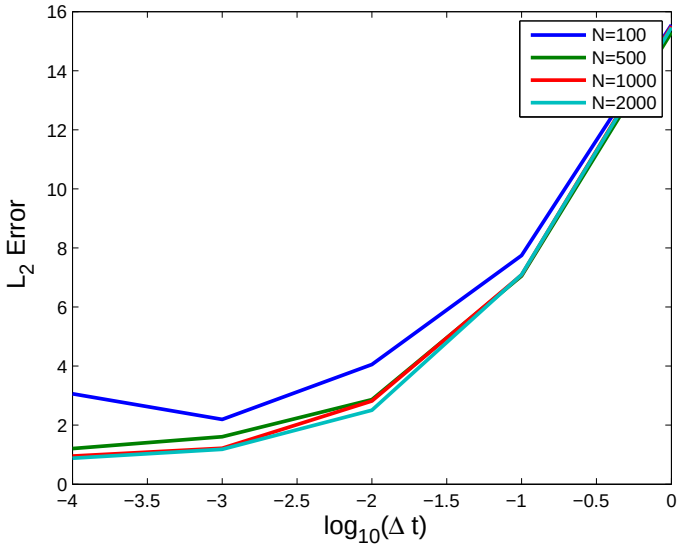

Figure 2.33. L_2 error variation with Δt for different values of N

relationship $\Delta t = \frac{\Delta x^2}{2}$, as we have already established that L_2 error is directly proportional to Δx in the Random walk case)

As a final exercise, we would like to answer the question, for a given accuracy, what set of parameters is to be chosen to obtain the solution with desired accuracy in minimum amount of time *i.e* say, to obtain solution with 2.5% L_2 error, there will be many combinations of Δt and number of realizations N. But which set of parameters we should choose, to obtain results in time as small as possible.

Figure 2.34 shows what should be number of realizations for a given grid size to obtain results with accuracy 2.5%. When $\Delta t = 0.005$, we need about 2000 realizations, where as for $\Delta t = 0.001$, we need only 400 realizations (about one-fifth of that for $\Delta t = 0.005$).

Figure 2.35 shows how much time it takes to get 2.5% L_2 error for a given Δt. In other words, how much time it takes to complete number of realizations shown in previous figure for a Δt. It can be observed from this figure, for all Δt the algorithm takes about same time 0.4 sec. The reason for same time is the same as that in random walk case.

The conclusion of this experiment is to obtain a solution with a given L_2 error, choose a Δt using Figure 2.32. For example, for $\epsilon = 2.5\%$, $\Delta t = 0.1$ is a bad choice, as smallest error possible is about 8% for that case, however Δt 0.001 are good for this case. Once this is chosen, we can obtain the result with different accuracy by varying number of realizations.

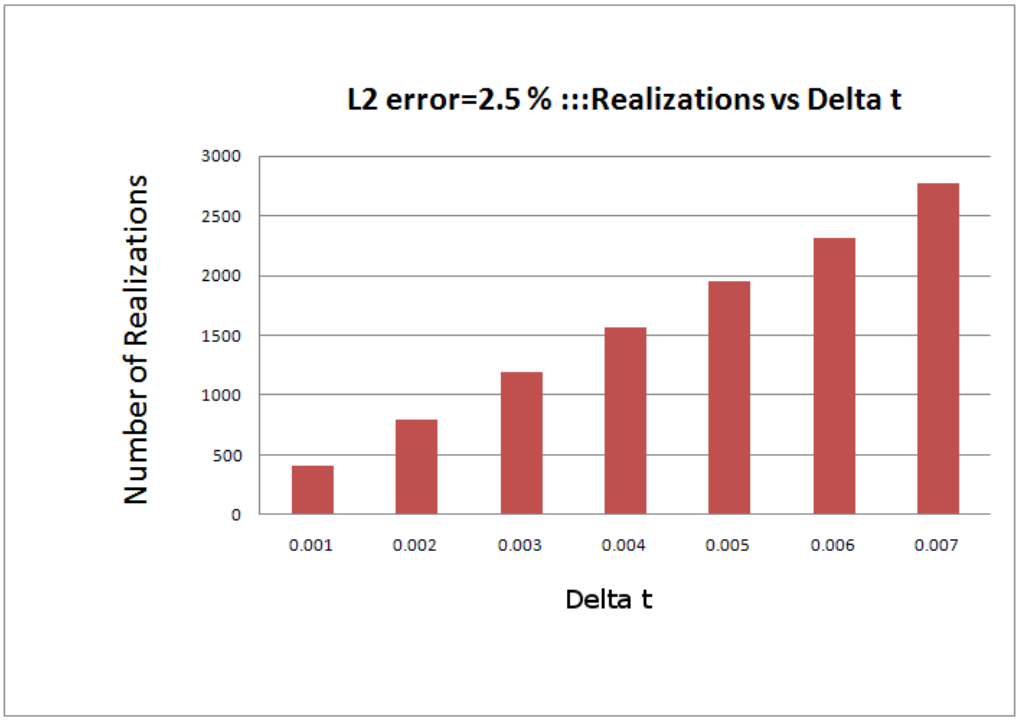

Figure 2.34. Number of realizations required to get L_2 error $= 2.5\%$ as a function of Δt

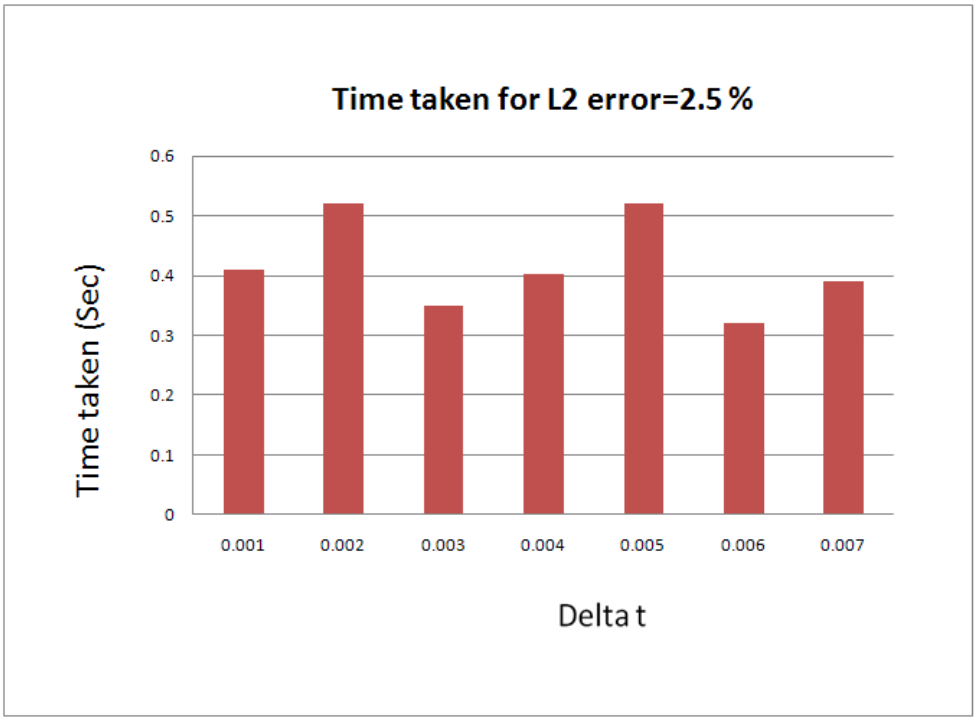

Figure 2.35. Time taken to obtain L_2 error = 2.5% for different Δt

We can conclude this chapter by comparing the time taken to obtain solution with a given accuracy by random walk and Brownian motion process. We have already observed that to obtain solution with 2.5% L_2 error, the best we can do in time with random walk is about 0.6 seconds and the best we can do with Brownian motion process is 0.4 seconds. Figure 2.36 shows the time taken to obtain solution with a given accuracy using random walk and Brownian motion process. For all accuracies, it can be observed that time taken by Brownian motion process is slightly smaller compared to that of Random walk method. Therefore Brownian motion process will be used through the rest of my thesis to carry out investigations on the stochastic method to solve Poisson's and parabolic wave equations, which are the topics of following chapters.

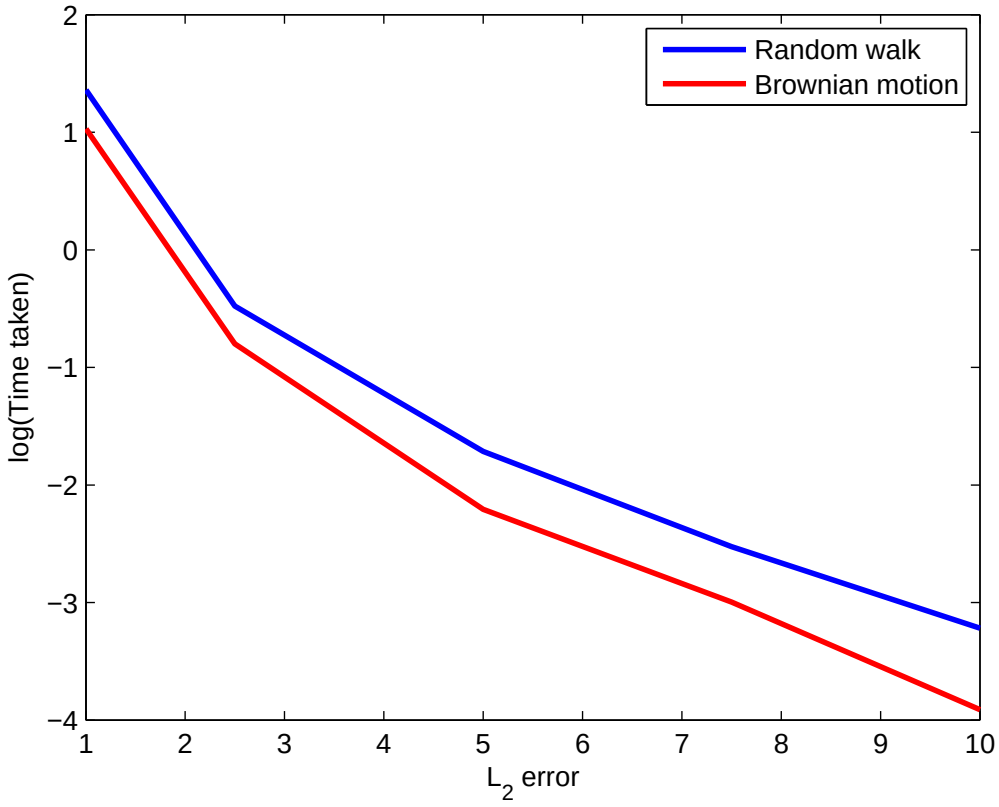

Figure 2.36. Time taken to obtain solution with different L_2 error using both Random walk and Brownian motion

CHAPTER 3

SOLUTION OF POISSON'S EQUATION

In chapter 1, a stochastic method which involves constructing either random walk or Brownian motion process is introduced. This method was used to obtain local solution to Laplace equation and numerical investigations were carried out to verify this method and to understand various parameters involved in the method. The theoretical considerations supporting this stochastic method are relatively complex and involve concepts of random process and stochastic integration such as Ito process and properties of Ito diffusion process. Some of the details are presented in this chapter, but for an elaborate explanation see references [11], [1], [4] and [7].

In this chapter, a stochastic method which is very similar to the one used in previous chapter is formulated to obtain local solution of Poisson's equation with Dirichlet boundary conditions and is investigated. This chapter is organized as follows. Ito's formula, which is an extension of change of variable formula in classical calculus is given in Section 3.1. In section 3.2, a relationship is established between the value of unknown function in the Poisson's equation, the boundary conditions and expectation depending on the sample paths of Brownian motion process. This derivation is based on properties of Brownian motion process and Ito's formula. An algorithm to obtain the local solution of Poisson's equation using this stochastic method is presented in section 3.3. Numerical experiments performed to verify the developed method and understand key parameters involved in the method are discussed in last section.

3.1 Ito Formula

Ito's formula extends the change of variable formula from classical calculus to stochastic integrals with stochastic integrators satisfying special properties [9].

One Dimensional case

If X is a random process with special properties [9], then the integral and differential form of Ito's formula are:

$$f(X(t)) - f(X(0)) = \int_0^t f'(X(s))dX(s) + \frac{1}{2}\int_0^t f''(X(s))d[X,X](s) \tag{3.1}$$

$$df(X(t)) = f'(X(s))dX(s) + \frac{1}{2}f''(X(s))d[X,X](s) \tag{3.2}$$

Multi Dimensional case

If X is a vector of d dimensions [9] and $f : R^d \to d$ has continuous second order, then the integral and differential form of Ito's formula are:

$$f(\mathbf{X}(t)) - f(\mathbf{X}(0)) = \sum_{i=1}^{d}\int_0^t \frac{\partial f}{\partial x_i}(\mathbf{X}(s))dX_i(s) + \sum_{i=1}^{d}\frac{1}{2}\int_0^t \frac{\partial^2 f}{\partial x_i \partial x_j}(\mathbf{X}(s))d[X_i,X_j](s) \tag{3.3}$$

$$df(\mathbf{X}(t)) = \sum_{i=1}^{d}\frac{\partial f}{\partial x_i}(\mathbf{X}(s))dX_i(s) + \sum_{i=1}^{d}\frac{1}{2}\frac{\partial^2 f}{\partial x_i \partial x_j}(\mathbf{X}(s))d[X_i,X_j](s) \tag{3.4}$$

3.2 Local solution of Poisson's equation

3.2.1 Evaluating expectation of sample paths of Brownian motion process

Let us consider Brownian motion process, a diffusion processes which we have discussed in the last chapter. Let $\mathbf{W}(t); t \geq 0$ be Brownian motion process taking values in R^d. The process starts at an arbitrary point $x \in R^d$ and is characterized by stationary independent increments, that is, the increments of $\mathbf{W}$ over non-overlapping time intervals are independent and their statistics depend only on the duration of the time increment [11].

Consider a function $u : R^d \to R$ with continuous partial second derivatives. Infinitesimal generator of the process $W(t)$ *i.e* average rate of change of $u(\mathbf{W}(t))$ at $t = 0$ given that $\mathbf{W}(0) = \mathbf{x}$ is

$$\mathscr{A}u(\mathbf{x}) = \lim_{t\to 0}\frac{E^x\{u(\mathbf{W}(t))\} - u(\mathbf{x})}{t} \tag{3.5}$$

Here, $E^x[\ ]$=$E[\ |\mathbf{W}(0) = \mathbf{x}]$. Considering the Ito formula

$$f(\mathbf{X}(t)) - f(\mathbf{X}(0)) = \sum_{i=1}^{d}\int_0^t \frac{\partial f}{\partial x_i}(\mathbf{X}(s))dX_i(s) + \sum_{i=1}^{d}\frac{1}{2}\int_0^t \frac{\partial^2 f}{\partial x_i \partial x_j}(\mathbf{X}(s))d[X_i,X_j](s)$$

Replacing f by u and $\mathbf{X}(t)$ by $\mathbf{W}(t)$ and using

$$d[W_i, W_j] = ds \quad \forall i = j$$
$$d[W_i, W_j] = 0 \quad \text{otherwise}$$

in the Ito formula, we get

$$u(\mathbf{W}(t)) - u(\mathbf{W}(0)) = \sum_{i=1}^{d} \int_0^t \frac{\partial u}{\partial W_i}(\mathbf{X}(s))dW_i(s) + \sum_{i=1}^{d} \frac{1}{2} \int_0^t \frac{\partial^2 u}{\partial W_i^2}(\mathbf{X}(s))ds \tag{3.6}$$

Taking the expectation of the Ito formula applied to the function $u(\mathbf{W}(s))$, conditional on $\mathbf{W}(0) = \mathbf{x}$, gives

$$E^x\{u(\mathbf{W}(t))\} - u(\mathbf{W}(0)) = E^x\{\sum_{i=1}^{d} \int_0^t \frac{\partial u}{\partial W_i}(\mathbf{X}(s))dW_i(s)\} + E^x\{\sum_{i=1}^{d} \frac{1}{2} \int_0^t \frac{\partial^2 u}{\partial W_i^2}(\mathbf{X}(s))ds\}$$

It can be shown that expectation of first term on the right hand side is zero. The equation becomes

$$E^x\{u(\mathbf{W}(t))\} - u(\mathbf{W}(0)) = E^x\{\sum_{i=1}^{d} \frac{1}{2} \int_0^t \frac{\partial^2 u(\mathbf{W}(s))}{\partial W_i^2} ds\}$$

This formula can be generalized by replacing t with a random time. For example, let G be a bounded open subset of R^d and suppose that the Brownian motion $\mathbf{W}$ starts at $\mathbf{x} \in G$. Define

$$\tau = inf\{t \geq 0 : \mathbf{W}(t) \notin G, \mathbf{W}(0) = \mathbf{x} \in G\} \tag{3.7}$$

to be the time when $\mathbf{W}$, starting at $\mathbf{x} \in G$, leaves this set. The time τ is a random variable because its value depends on the particular sample of the Brownian motion. The averaged Ito formula with t replaced by τ becomes [11]

$$E^x\{u(\mathbf{W}(\tau))\} - u(\mathbf{x}) = \frac{1}{2} E^x\{\int_0^\tau \nabla^2 u(\mathbf{W}(s))ds\} \tag{3.8}$$

This equation is essential for obtaining local solutions of the Laplace and Poisson's equation.

3.2.2 Local solution of Laplace and Poisson's equation

Let $u : R^d \to R$ be the solution of the Poisson equation

$$\begin{aligned} \nabla^2 u(\mathbf{x}) + p(\mathbf{x}) = 0 \qquad & \mathbf{x} \in G \\ u(\mathbf{x}) = g(\mathbf{x}) \qquad & \mathbf{x} \in \partial G \end{aligned} \tag{3.9}$$

satisfying the Dirichlet boundary conditions. where p and g are specified functions.

Suppose that the objective is to find the local solution of Equations 3.9 at an arbitrary point x of the domain of definition G. Because u has continuous second-order partial derivatives, Equation 4.6 applies and gives

$$E^x\{u(\mathbf{W}(\tau))\} - u(\mathbf{x}) = \frac{1}{2}E^x\{\int_0^\tau p(\mathbf{W}(s))ds\}$$

because $u(\mathbf{W}(\tau)) \in \partial G$ so that it is equal to the boundary value $g(W(\tau))$ and $\mathbf{W}(s) \in G$ for $s \in (0, \tau)$ so that $\nabla^2 u(\mathbf{W}(s)) = p(\mathbf{W}(s))$ by Equation 3.9. Hence, the value of the unknown function u at $\mathbf{x} \in G$ is [11]

$$u(\mathbf{x}) = E^x[g(\mathbf{W}(\tau))] + \frac{1}{2}E^x\{\int_0^\tau p(\mathbf{W}(s))ds\} \tag{3.10}$$

The right-hand side of Equation depends on expectations of known functions, the functions g and p and samples of the Brownian motion W in the time interval $(0, \tau)$. Generally, these expectations cannot be obtained analytically. However, they can be estimated by Monte Carlo simulation as demonstrated in the following sections.

If $p = 0$ in Equation 3.9 , the equation considered for solution is a Laplace equation and the local solution of this equation is given by

$$u(\mathbf{x}) = E^x[g(\mathbf{W}(\tau))] \tag{3.11}$$

that is, Equation 4.6 with p=0. This is the equation that is evaluated to obtain local solution to Laplace equation with Dirichlet boundary condition in the previous chapter.

3.3 Algorithm

The algorithm that can be used to obtain local solution of Poisson's equation using Equation (4.6) can be specified in the following way.

1. Set the initial point of the Brownian motion process to the point where the value of u in Equation (3.9) is to be found.

2. Start Brownian motions and continue according to Equations (3.12) and (3.13)

$$x(t + \Delta t) = x(t) + \text{Pick a random number with distribution } \sqrt{2}N(0, \Delta t) \tag{3.12}$$

$$y(t + \Delta t) = y(t) + \text{Pick a random number with distribution } \sqrt{2}N(0, \Delta t) \tag{3.13}$$

3. Note the time spent by the Brownian motion inside the source before exiting domain G

4. Is boundary reached?
   If Yes: Stop the Brownian motion and proceed to next step
   If No: proceed to step 3

5. Record the potential at the boundary.

6. Is number of realizations completed?
   If No: Repeat step 2
   If Yes: Proceed to next step

7. Find the value of $u(x, y)$ as given by Equation (4.6)

3.4 Numerical Experiments

3.4.1 Problem setup

The problem of interest is to find the potential between two parallel plates located at $y = 0$ and $y = a$, which are infinite in extent along x-axis and z-axis, given a charge distribution in its interior. Its cross section is shown in Figure 3.1. A square cylindrical charge distribution with its axis along z-axis is present at $x = 0, y = b$. The geometry of interest is inside the rectangle defined by $x = -a, x = +a, y = 0, y = +a$. The dimension of the square cylinder is as shown given by $h \times h$. This is an electrostatic, deterministic, interior boundary value problem.

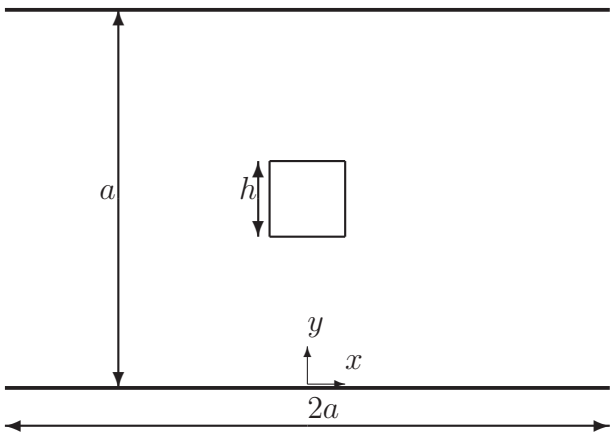

Figure 3.1. Two parallel plates with a square cylinder charge distribution

3.4.2 Analytical Solution

The analytical solution to the problem specified is obtained by solving Poisson's equation. The Poisson's equation for a homogeneous region is given by

$$\nabla^2\psi = -\frac{\rho_v}{\epsilon} \tag{3.14}$$

where ψ - potential, ρ_v - volume charge density, ϵ - permitivity of the medium. However instead of solving the Poisson's equation directly for the square cylindrical charge distribution, potential as a function of (x, y) is first found for a line source and this expression is used to evaluate the analytical solution of the current problem using linear superposition.

The potential at any point (x, y) due to a line source present at (x_0, y_0) of linear charge density ρ_l is given by [17]

$$\psi_l(x, y; x_0, y_0) = \frac{\rho_l}{2\pi\epsilon} \tanh^{-1}\left(\frac{\sin(\frac{\pi y_0}{a})\sin(\frac{\pi y}{a})}{-\cos(\frac{\pi y_0}{a})\cos(\frac{\pi y}{a}) + \cosh\left(\frac{\pi(x-x_0)}{a}\right)}\right) \tag{3.15}$$

The potential as a function of (x, y) for a square cylindrical charge distribution with boundaries given by $x = xs1$, $x = xs2$, $y = ys1$ and $y = ys2$, is obtained by integrating the Equation (3.15) from $xs1$ to $xs2$ along x-axis and from $ys1$ to $ys2$ along y-axis as shown below.

$$\psi(x, y) = \frac{1}{h^2}\int_{xs1}^{xs2}\int_{ys1}^{ys2} \psi_l(x, y; x_0, y_0)\mathrm{d}x_0\mathrm{d}y_0 \tag{3.16}$$

As it is difficult to evaluate this integral in a closed form, we compute it numerically using MATLAB.

3.4.3 Results and Discussions

Figure 3.2 shows the average number of jumps made by a particle undergoing Brownian motion as a function of its starting point. For example, it can be observed that a particle starting at $(-0.5, 0.5)$ makes about 140 jumps on average for each realization before reaching the boundary. The Brownian motion process is generated with $\Delta t = 0.0001$ and $N = 10,000$ realizations are used here.

Number of jumps made by a particle starting its Brownian motion close to the boundary will be smaller than that made by a particle starting its Brownian motion relatively farther to the boundary. This trend is shown in the Figure 3.2. Moreover as the boundaries are parallel to x-axis, we expect the particles starting their motion on same y-coordinate, to

make same number of jumps on average. This is also shown in the figure as the same color areas are also parallel to $x-$axis. Thus, it can be observed from the Figure 3.2 average number of jumps is high for Brownian motions originating along the center i.e $y = 0.5$ and it decreases as we move closer to the boundary.

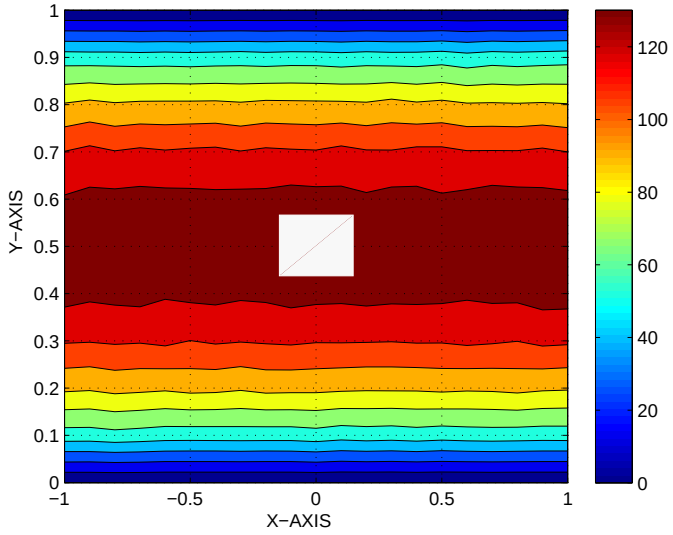

Figure 3.2. The average number of jumps in Brownian motions originating at (x, y)

The electrostatic potential distributions $\psi(x, y)$ obtained using analytical and stochastic solution are plotted in the Figure 3.3 and Figure 3.4 respectively.A comparison of the analytic solution and stochastic solution shows a good agreement between these two.

Figure 3.5 shows the contours of electrostatic potential obtained by analytical solution (red) and stochastic solution (blue), when $\Delta t = 0.1$. Figures 3.6, 3.7 and 3.8 show the contours for different time steps $\Delta t = 0.01, 0.001$ and 0.0001 respectively. These set of figures depict how the stochastic solution approaches analytical solution with increase in number of realizations and decrease in time step.

Similar to the error analysis in the previous chapter, as a measure of the performance of this method, an L_2 error norm is constructed as shown below.

$$\epsilon = \frac{100}{|\psi_{max}|}\sqrt{\left(\frac{1}{M}\sum_{i=1}^{M}(\psi_i^n - \psi_i^e)^2\right)}$$

where ψ_i^e is the exact analytical solution, ψ_i^n is the stochastic solution and M is the number of randomly chosen points in the domain where the unknown ψ is evaluated.

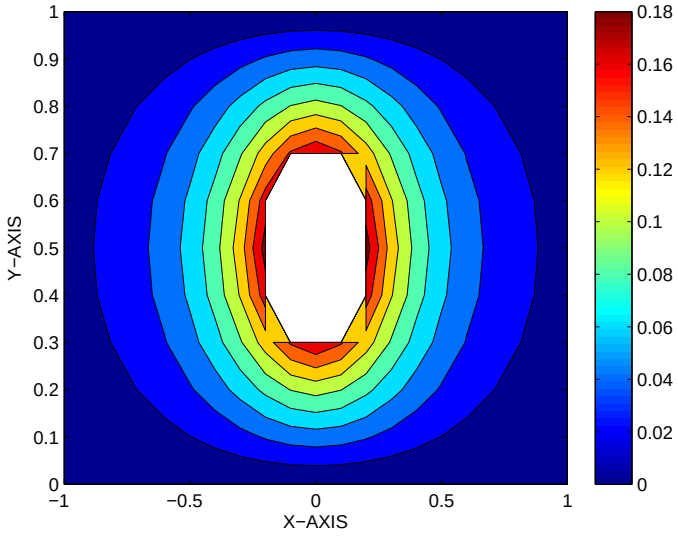

Figure 3.3. Analytical Solution potential $\psi(x, y)$

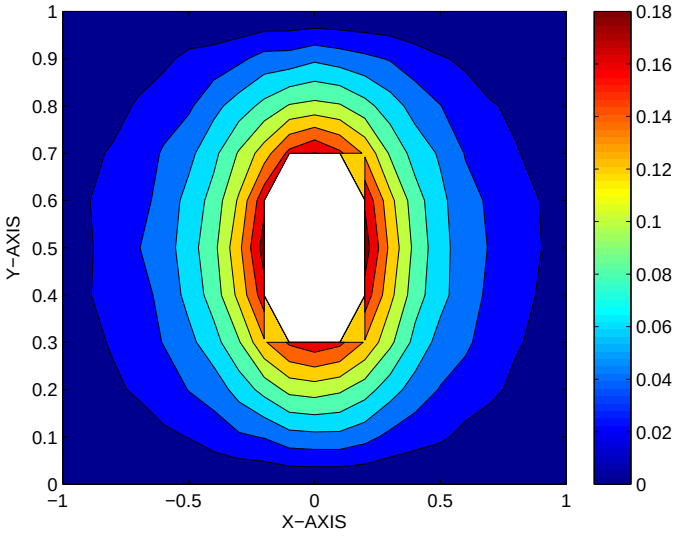

Figure 3.4. Stochastic Solution potential $\psi(x, y)$

Figure 3.9 indicates how the L_2 error varies as a function of number of realizations for different values of time step Δt. For a given time step Δt, the error decreases with increase in number of realizations. The L_2 error decreases as we decrease the time step Δt for a given number of realizations. Figure 3.10 indicates how the L_2 error varies as a function of time step for different values of number of realizations. This also depicts that accuracy increases with increase in number of realizations as well as decrease in time step Δt.

For the sake of completeness, time taken by the stochastic method to complete, say N number of realizations using time step Δt, for different values of N and Δt is presented in the Figure 3.11. It can be observed from the figure that time taken by the stochastic solution increases with increase in number of realizations as well as decrease in time step. It has already been shown is figure 3.9that for the case using $N = 10,000$ and $\Delta t = 0.0001$, we obtain a stochastic solution with an error $\epsilon = 3\%$. Therefore, from figure 3.11to obtain a solution with $\epsilon = 3\%$, it takes about 350 seconds. These results are similar to those presented in the previous chapter and give the reader a sense of time taken to obtain stochastic solution for this problem.

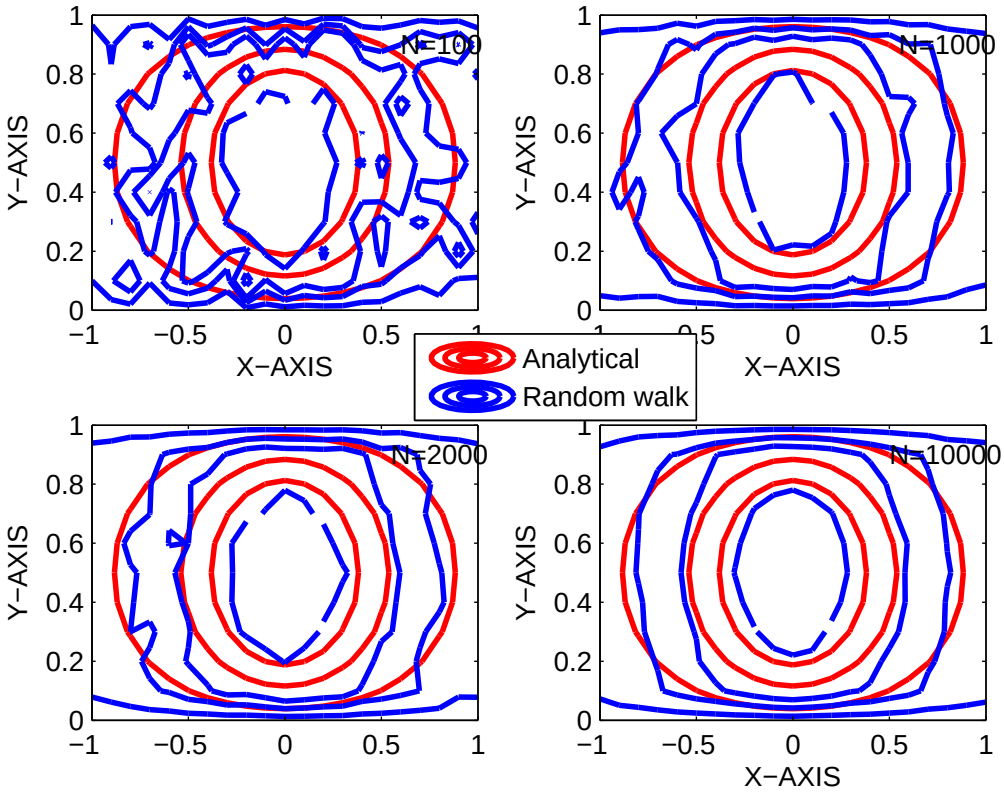

Figure 3.5. Stochastic solution as a function of number of realizations :::: Δt=0.1

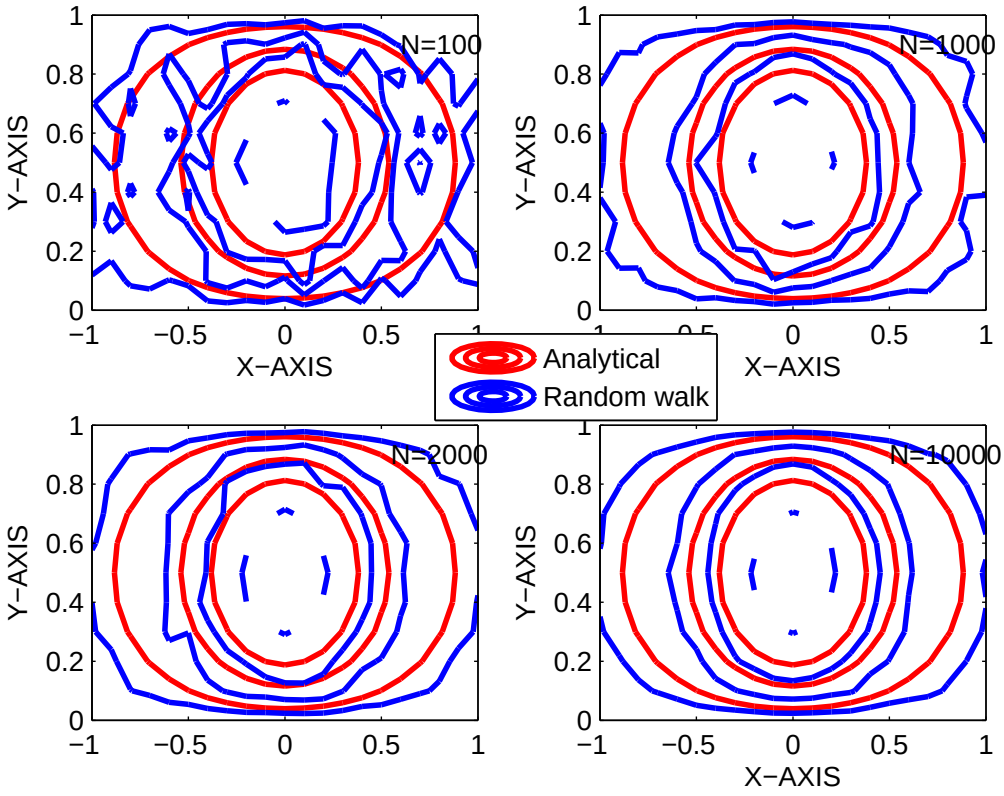

Figure 3.6. Stochastic solution as a function of number of realizations :::: Δt=0.01

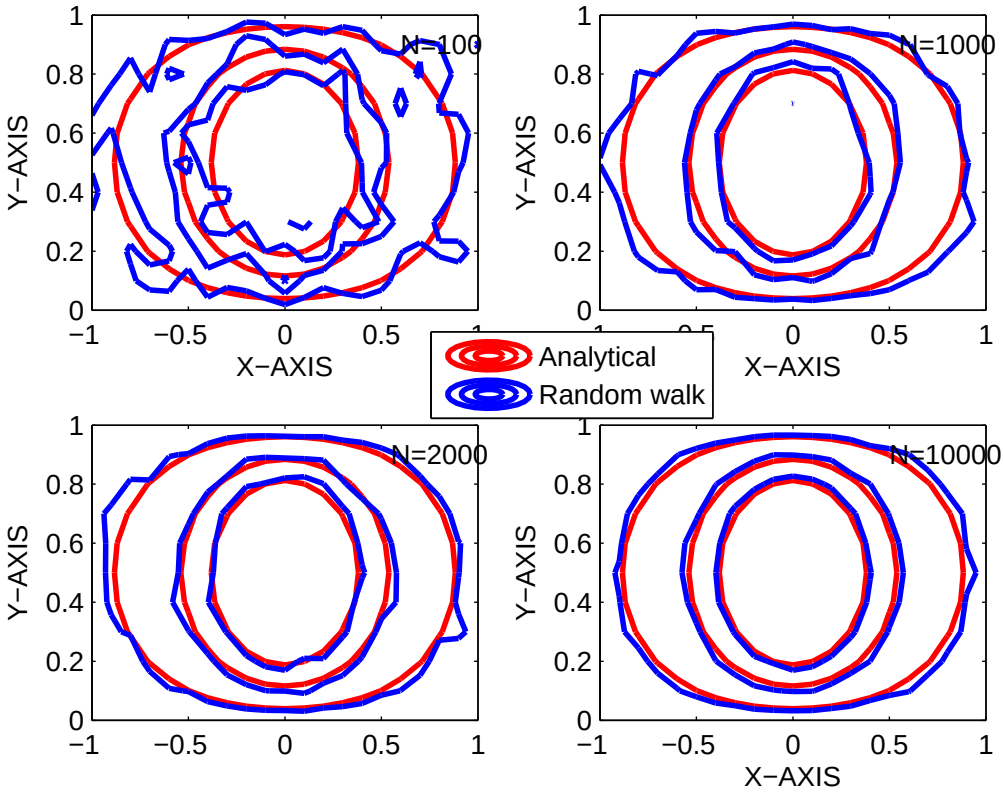

Figure 3.7. Stochastic solution as a function of number of realizations :::: Δt=0.001

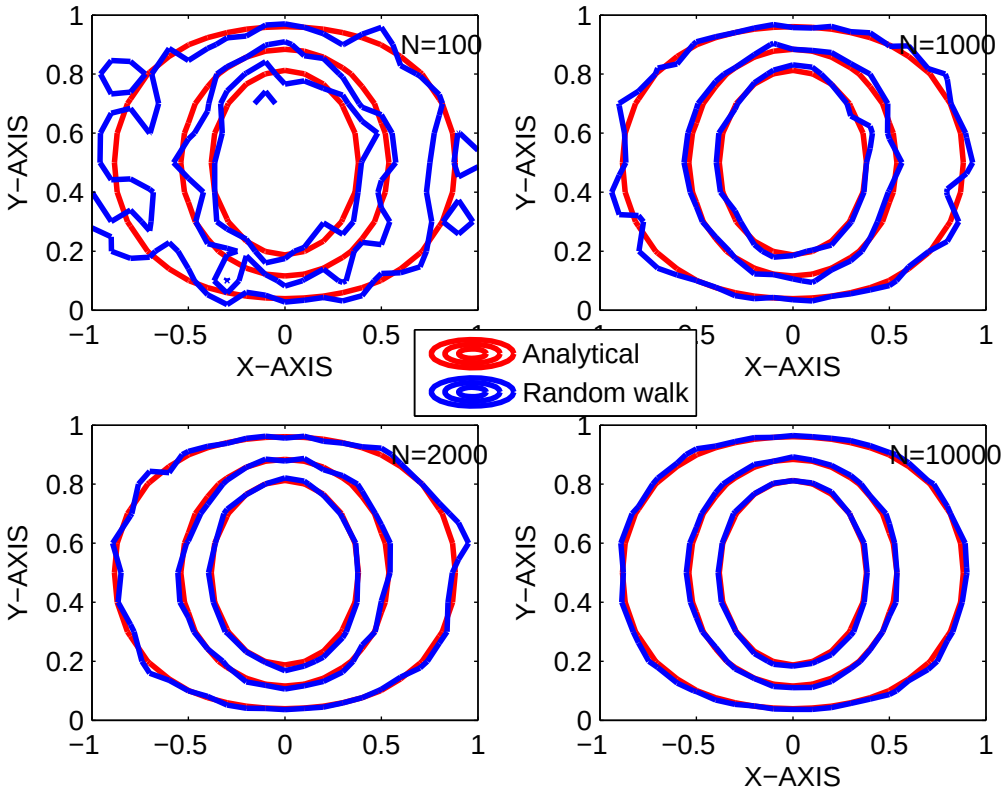

Figure 3.8. Stochastic solution as a function of number of realizations :::: Δt=0.0001

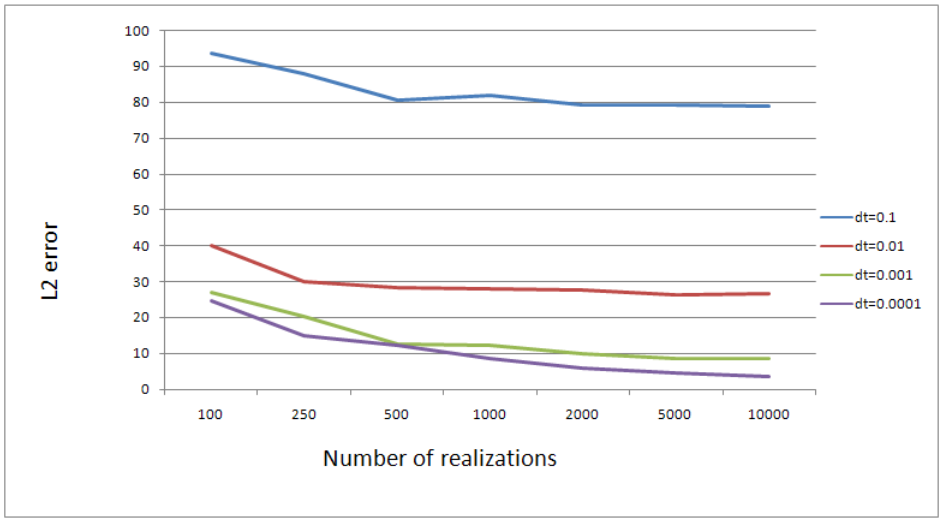

Figure 3.9. L_2 error variation with number of realizations for different Δt

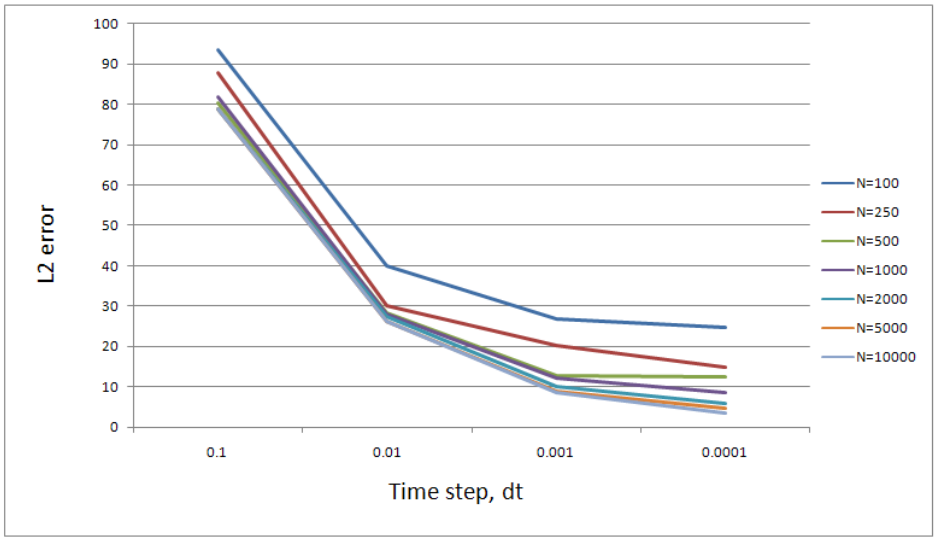

Figure 3.10. L_2 error variation with time step Δt for different values of N

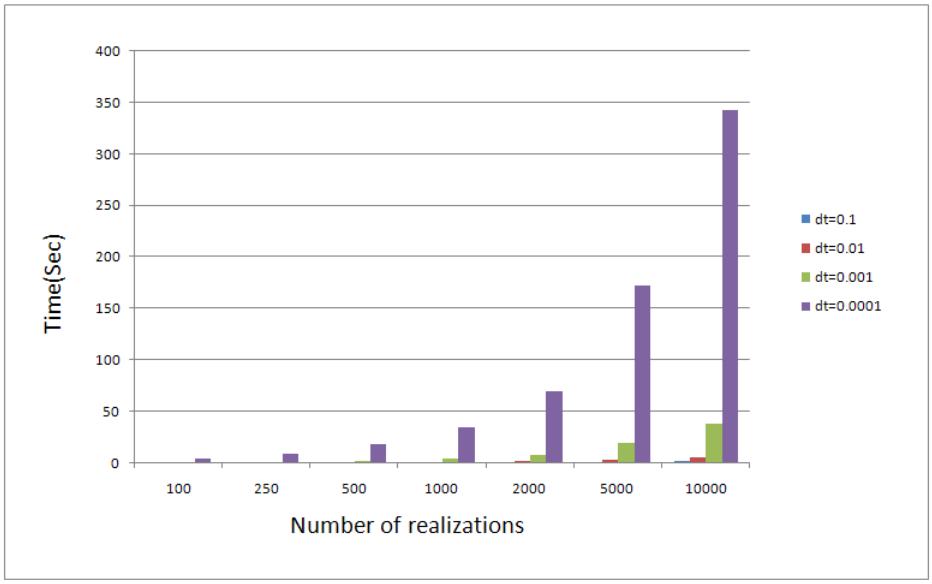

Figure 3.11. Time taken by the stochastic method to complete, N number of realizations using time step Δt

CHAPTER 4

SOLUTION OF PARABOLIC WAVE EQUATION WITH DIRICHLET BOUNDARY CONDITION

In this chapter, the stochastic method is used to obtain local solution of an electrodynamic problem. The problem under consideration is problem of propagation of time harmonic waves inside a parallel plate waveguide with perfectly conducting walls boundaries at the top and bottom. A brief theory in the context of this problem is presented here and this approach is validated by favorable comparisons between stochastic and analytical solutions. The stochastic approach to obtain solution to this problem has originally been presented in [15].

The class of partial differential equations considered in this chapter are

$$\sum_{i=1}^{d} \alpha_i(\mathbf{x}) \frac{\partial \mathbf{u}(\mathbf{x})}{\partial x_i} + \frac{1}{2} \sum_{i,j=1}^{d} \beta_{ij}(\mathbf{x}) \frac{\partial^2 \mathbf{u}(\mathbf{x})}{\partial x_i \partial x_j} = 0 \tag{4.1}$$

in which $\alpha = \{\alpha_i\}$ and $\beta = \{\beta_{ij}\}$ are smooth functions of $\mathbf{x}$. These equations are defined in an open bounded subset G of R^d, where d is the dimension of the region R and satisfy Dirichlet boundary conditions. To obtain local solution of this class of partial differential equations, the Brownian motion process, which was considered in the previous chapter is itself not sufficient. For the reasons which we will be explained later, we need to consider a special type of diffusion process called Ito process.

4.1 Ito process and Local solution by stochastic method

Let $\mathbf{X}(t) \in R^d$, $t \geq 0$, be an Ito diffusion process defined by [8]

$$\mathbf{X}(t) = \mathbf{X}(0) + \int_0^t a(\mathbf{X}(s))ds + \int_0^t b(\mathbf{X}(s))d\mathbf{W}(s) \tag{4.2}$$

where the d by 1 and d by d_b matrices a and b give the drift and the diffusion coefficients of $\mathbf{X}$ respectively, and the Brownian motion process $\mathbf{W}$ consists of d_b independent standard

Brownian motion processes. It can also be stated that $\mathbf{X}$ defined by Equation (4.2) is the solution of the stochastic differential equation.

$$d\mathbf{X}(t) = \mathbf{a}(\mathbf{X}(t))dt + \mathbf{b}(\mathbf{X}(t))d\mathbf{W}(t) \tag{4.3}$$

It can be proved that the infinitesimal generator $\mathscr{A}$ of the Ito process $\mathbf{X}$ defined by

$$\mathscr{A}u(\mathbf{X}) \;=\; \lim_{t\to 0}\frac{E^x[u(\mathbf{X}(t))] - u(\mathbf{x})}{t}$$

is equal to

$$\mathscr{A}u(\mathbf{X}) \;=\; \left[\sum_{i=1}^{d}\int_0^t a_i(\mathbf{X}(s))\frac{\partial}{\partial x_i} + \sum_{i,j=1}^{d}\frac{1}{2}\int_0^t (\mathbf{b}(\mathbf{X}(s)\mathbf{b}(\mathbf{X}(s)))_{i,j}\frac{\partial^2}{\partial x_i \partial x_j}\right] u(\mathbf{X}(s)) \tag{4.4}$$

This generator has the same functional form as the left hand side of the Equation (4.1) and coincides with for $\alpha = \mathbf{a}$ and $\beta = \mathbf{bb'}$. Therefore Ito process is chosen to obtain local solution of the partial differential equations of general form of Equation (4.1).

If $u : R^d \to R$ is the solution of the partial differential equation

$$\begin{aligned} \mathscr{A}u(\mathbf{x}) + p(\mathbf{x}) = 0 \qquad & \mathbf{x} \in G \\ u(\mathbf{x}) = g(\mathbf{x}) \qquad & \mathbf{x} \in \partial G \end{aligned} \tag{4.5}$$

satisfying the Dirichlet boundary conditions, where p and g are specified functions, the objective is to find the local solution of Equations (4.5) at an arbitrary point $\mathbf{x}$ of the domain of definition G. If τ denotes the first exit time from domain G

$$\tau = inf\{t \geq 0 : \mathbf{X}(t) \notin G, \mathbf{X}(0) = \mathbf{x} \in G\}$$

It can be shown that the value of the unknown function u at $\mathbf{x} \in G$ is [9]

$$u(\mathbf{x}) = E^x[g(\mathbf{X}(\tau))] + \frac{1}{2}E^x\{\int_0^\tau p(\mathbf{X}(s))ds\} \tag{4.6}$$

The right-hand side of equation depends on expectations of known functions, the functions g and p and samples of the Ito process $\mathbf{X}$ in the time interval $(0, \tau)$. As mentioned before, in general, these expectations cannot be obtained analytically and so they can be estimated by Monte Carlo simulation.

If $p = 0$ in Equation (4.5), the equation considered for solution is a diffusion equation and the local solution of this equation is given by

$$u(\mathbf{x}) = E^x[g(\mathbf{X}(\tau))] \tag{4.7}$$

that is, Equation (4.6) with p=0.

4.2 Local solution of parabolic wave equation

In this section, we would like to obtain local solution of standard parabolic wave equation given by

$$\begin{aligned} \frac{\partial u}{\partial x} &= \frac{i}{2k_0}\frac{\partial^2 u}{\partial z^2} && (x,z) \in G \\ u(x,z) &= g(x,z) && (x,z) \in \partial G \end{aligned} \tag{4.8}$$

with Dirichlet boundary conditions. We would like to compare Equation (4.8) with those of form given by Equation (4.1), however Equation (4.8) has coefficients which are complex numbers. Therefore the corresponding Ito process to be used to obtain local solution of this PDE will also be complex valued. Alternatively, we can say heuristically, absorb the imaginary term i in the coefficient of the partial differential equation into the coordinates or axis so that the problem of interest is defined in complex space $(x, z = \xi + i\eta)$. The Ito process has two components, the drift component is only along x direction and diffusion component is only along z direction. This problem has been treated in [15] and the differential paths of $z(s)$ and $x(s)$ are given by the stochastic differential equations

$$dz(s) = \frac{i}{\sqrt{k_0}} dW(s) \qquad z(0) = \xi \tag{4.9}$$

$$dx(s) = -ds \qquad x(0) = x \tag{4.10}$$

Analytic Continuation In order to solve the boundary value problem defined by the Equation (4.8), we need to augment the random paths given by (4.9) by Dirichlet boundary condition.

Let G^c and ∂G^c be a domain and its boundary in a complex space C^2 satisfying,

$$G^c \cap R^2 = G \tag{4.11}$$

$$\partial G^c \cap R^2 = \partial G \tag{4.12}$$

so that intersection of G^c and ∂G^c with real space R^2 coincide with the domain G and the boundary ∂G of the Dirichlet problem given by (4.8). Assuming $g^c(x,z)$ is the value of $u(x,z)$ on the boundary ∂G^c, such that $g^c(x,z)$ is extension of $g(x,z)$ from real space to complex space. The local solution can be obtained by the formula [1]

$$u(\mathbf{x}) = E^x[g^c(\mathbf{X}(\tau))] \tag{4.13}$$

which is identical to (4.6) except that paths are in complex space.

As can be observed, to obtain local solution of the parabolic wave equation, one need the value $g^c(x,z)$ on the boundary ∂G^c, where as boundary value $g(x,z)$ is given only on ∂G. However the above formula can still be used because in some cases there is a unique extension of the analytic boundary value $g(x,z)$ from real space ∂G to complex space ∂G^c [1]. This is demonstrated in the example problem solved in the next section.

Having formulated how to obtain local solution of Dirichlet problem of Equation (4.8), let us demonstrate how this method can be used with an example[15].

4.3 Numerical Experiments

4.3.1 Problem Definition

In this section, we would like to consider a problem where an equation of form (4.8) needs to be solved for an unknown function whose values are given on boundary.

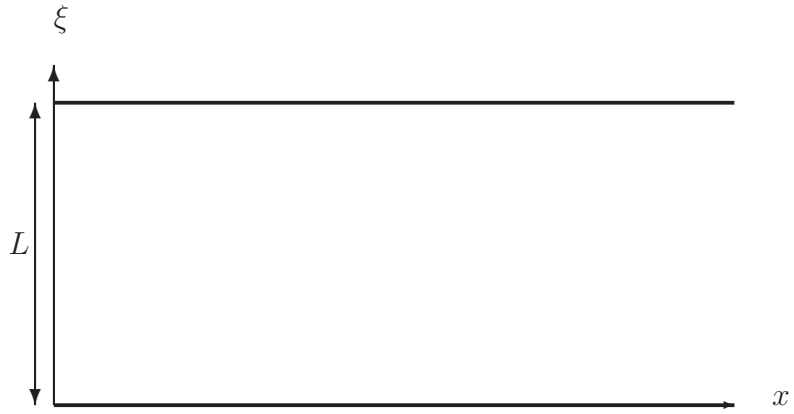

Figure 4.1. Parallel plate waveguide with conducting walls

Consider propagation of time harmonic waves inside an infinite parallel plate waveguide with PEC boundaries at $z = 0$ and $z = L$. Assuming paraxial propagation, the reduced field $u(x,z) = v(x,z)exp(-ik_0x)$, where $v(x,z)$satisfies the Helmholtz equation in $2D$.

$$\begin{aligned} \frac{\partial u}{\partial x} &= \frac{i}{2k_0}\frac{\partial^2 u}{\partial z^2} \qquad (x,z) \in G \\ u(x,0) &= 0 = u(x,L) \\ u(0,z) &= u_0(z) \end{aligned} \tag{4.14}$$

4.3.2 Analytical Solution

In order to propagate solutions of the standard parabolic wave equation satisfying Dirichlet boundary condition, the appropriate transform is the Fourier sine transform. However continuous sine transform doesn't match the boundary condition at the top boundary $z = L$. Therefore a discrete sine transform matching the boundaries at the top and bottom boundary is considered [15]:

$$\begin{aligned} U(x, m\Delta p) &= \sum_{n=1}^{N-1} u(x, n\Delta z) sin\left(\frac{mn\pi}{N}\right) \\ u(x, n\Delta z) &= \frac{2}{N} \sum_{m=1}^{N-1} U(x, m\Delta p) sin\left(\frac{mn\pi}{N}\right) \end{aligned}$$

Given $u(0, z) = u_0(z)$

$$\begin{aligned} U(0, m\Delta p) &= \sum_{n=1}^{N-1} u(0, n\Delta z) sin\left(\frac{mn\pi}{N}\right) \\ U(x, m\Delta p) &= U(0, m\Delta p) e^{\frac{i\lambda_m x}{2k_0}} \qquad \text{where } \lambda_m = \frac{cos\left(\frac{\pi m}{N}\right) - 1}{(\Delta\xi)^2} \\ u(x, n\Delta z) &= \frac{2}{N} \sum_{m=1}^{N-1} U(x, m\Delta p) sin\left(\frac{mn\pi}{N}\right) \end{aligned}$$

This gives the field at advanced range x and height z. This result is used in analytic continuation of data and also to compare results obtained stochastically.

4.3.3 Solution Setup

Local solution of the Equation (4.14) is given by

$$u(\mathbf{x}) = E^x[g^c(\mathbf{X}(\tau))] \tag{4.15}$$

Here, the unknown function u is a function of $z = \xi + i\eta$ and x. Given $u(0, z = \xi + 0) = u_0$ along a line and $u(x, z = \xi + i\eta = 0) = u(x, z = \xi + i\eta = L) = 0$ along top and bottom lines. However we need the values $u(0, z = \xi + i\eta)$ along the source plane and $u(x, i\eta)$ and $u(x, L + i\eta)$ along top and bottom planes. These are obtained using analytic continuation:

$$u(0, z = \xi + i\eta) = \frac{2}{N}\sum_{m=1}^{N-1} U(0, m\Delta p) sin\left(\frac{m\pi z}{L}\right) \tag{4.16}$$

$$u(x, 0 + i\eta) = \frac{2i}{N}\sum_{m=1}^{N-1} U(x, m\Delta p) sinh\left(\frac{m\eta\pi}{L}\right) \tag{4.17}$$

$$u(x, L + i\eta) = \frac{2i}{N}\sum_{m=1}^{N-1} (-1)^m U(x, m\Delta p) sinh\left(\frac{m\eta\pi}{L}\right) \tag{4.18}$$

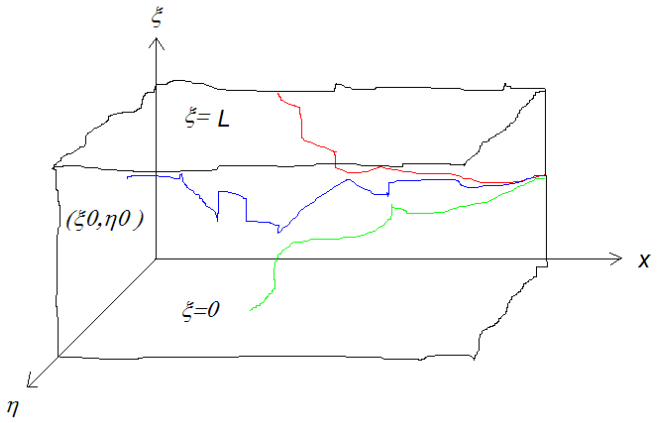

Figure 4.2. Random paths generated by Ito process

4.3.4 Algorithm

1. Start random process at (x, ξ) according to Equations

$$dz(s) = \frac{i}{\sqrt{k_0}} dW(s) \qquad z(0) = \xi$$
$$dx(s) = -ds \qquad x(0) = x$$

2. If it hits bottom or top boundaries, stop the random motion and use the values given by Equation (4.18) and (4.17) in Equation (4.15) to obtain the expectation.

3. If it doesn't hit any boundaries, continue till it hits the boundary $x = 0$ *i.e* the source plane. Terminate the random motion and use Equation (4.16) to obtain the expectation.

4. Repeat the same procedure for all points, where solution is required

4.3.5 Validation and Results

The results are computed for Gaussian initial field with peak at $\xi = H_t$ and standard deviation σ_ξ. The Figure 4.3 depicts how well the analytic and stochastic solutions compare with each other. As presented in the last chapter, a careful choice of Δt and number of realizations, N will result in favorable comparisons.

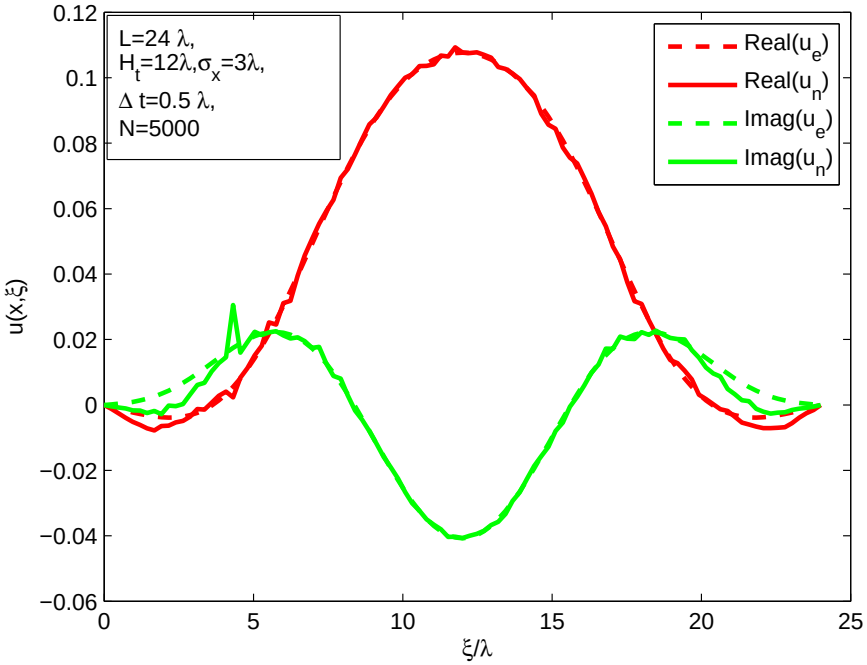

Figure 4.3. Field at range 50λ from source plane

CHAPTER 5

SOLUTION OF PARABOLIC EQUATION WITH IMPEDANCE BOUNDARY CONDITIONS

In previous chapters, a stochastic method to obtain local solution of second order partial differential equations was demonstrated by considering simple examples. In all the problems we have considered so far, value of unknown function u is specified on the boundary (Dirichlet boundary condition). To reiterate the procedure to obtain local solution of such problems:

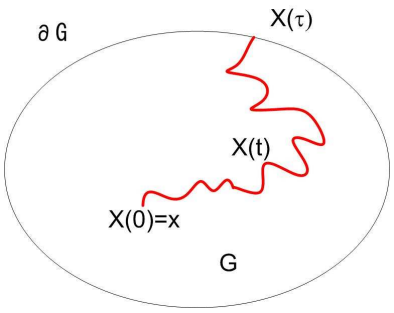

Figure 5.1. Dirichlet boundary condition

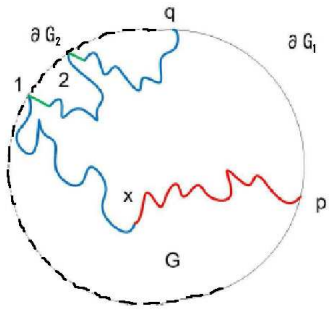

Figure 5.2. Impedance boundary condition

- Start a diffusion process **X** with generator coinciding with the differential operator of the PDE under consideration, for example, parabolic wave equation, at the point where the solution is needed.
- Continue the process till it hits the boundary.
- Once it hits the boundary, as we know the value of u at this point on the boundary, terminate the process and use this boundary value to obtain expectation using Monte Carlo algorithm.

But for the problems in which unknown function is not specified at boundaries, this method obviously will not work. In this last chapter, we would like to look at such problems, where u is specified only on a subset of the boundary and is given by either Neumann boundary condition or impedance boundary condition on the rest of it. The outline of the procedure used to solve such problems discussed in this chapter is as follows

- Start a diffusion process X with generator coinciding with the differential operator of the PDE under consideration at the point where the solution is needed
- Sample paths can be divided into two groups as shown in figure 5.2. (∂G_1 is the region on the boundary where unknown function u is specified and ∂G_2 is the region on the boundary where u is given by either Neumann boundary condition or impedance boundary condition)
  - Sample paths that reach ∂G_1 for the first time before reaching ∂G_2.
    As the value of unknown function u is known on the boundary ∂G_1, we terminate them and use the boundary value to obtain the expectation.
  - Sample paths that reach ∂G_2 for the first time before reaching ∂G_1.
    In this case, the value of unknown function u is not known on ∂G_2, but is given by impedance boundary condition. Therefore, now
    - Reflect X at the point 1, where it hits the boundary by a selected amount in a direction that is consistent with the boundary condition at that point to point 2, as shown in figure 5.2.
    - Restart the diffusion process from point 2 and find the point where it hits ∂G_1.
    - If it hits ∂G_2 again, repeat the above procedure until it hits ∂G_1, but keep a record of the point where it hits ∂G_2.
    - Here a relationship needs to be established between unknown function u, boundary condition and expectation depending on the sample paths using formula, which is called as extended form of Feynman-Kac formula.
- Compute the expectation using Monte Carlo simulations to obtain the value of unknown function.

This chapter is organized as follows. It begins with Feynman-Kac formula which is needed to solve problems with impedance boundary condition using stochastic method. Next, the

model problem we are trying to solve in this chapter is defined and its analytical solution is presented. This is followed by the discussion about local solution in the context of this problem. In the next section, an outline of the algorithm using this approach is given. This chapter concludes with the discussion about the results obtained using this stochastic method.

5.1 Feynman-Kac Formula

Consider a boundary value problem with the unknown function u formulated in a domain G with the boundary $\partial G = \partial G_1 \cup \partial G_2$ as shown in the figure 5.2. Here $u : R^d \rightarrow R$ is the solution of the partial differential equation satisfying

$$\begin{aligned} \sum_{i=1}^{d} \alpha_i(\mathbf{x}) \frac{\partial u(\mathbf{x})}{\partial x_i} + \frac{1}{2} \sum_{i,j=1}^{d} \beta_{ij}(\mathbf{x}) \frac{\partial^2 u(\mathbf{x})}{\partial x_i \partial x_j} + q(\mathbf{x}) u(\mathbf{x}) &= 0 \qquad \mathbf{x} \in G \\ u(\mathbf{x}) &= g(\mathbf{x}) \qquad \mathbf{x} \in \partial G_1 \\ \sum_{i=1}^{d} \frac{\partial u(\mathbf{x})}{\partial x_i} + b(\mathbf{x})(u(\mathbf{x})) &= 0 \qquad \mathbf{x} \in \partial G_2 \end{aligned} \tag{5.1}$$

where α_i, β_{ij} and q are defined inside G, while g and b are specified on ∂G and let $\mathscr{A}$ be

$$\begin{aligned} \mathscr{A}u(\mathbf{x}) &= \sum_{i=1}^{d} \alpha_i(\mathbf{x}) \frac{\partial u(\mathbf{x})}{\partial x_i} + \frac{1}{2} \sum_{i,j=1}^{d} \beta_{ij}(\mathbf{x}) \frac{\partial^2 u(\mathbf{x})}{\partial x_i \partial x_j} \\ \mathscr{B}u(\mathbf{x}) &= \sum_{i=1}^{d} \frac{\partial u(\mathbf{x})}{\partial x_i} \end{aligned}$$

In order to obtain local solution to this problem using stochastic method, random motions are to be defined on the closure $G \cup \partial G$ whose behavior inside G corresponds to the operator $L_G = \mathscr{A}$ and whose behavior on the boundary ∂G_2 corresponds to the first-order operator $L_{\partial G} = \mathscr{B}$. Since both operators L_G and $L_{\partial G}$ are particular cases of the general second-order operator discussed in the previous chapter, it is natural to expect that inside G the random motion should be a Brownian motion with a drift, and on the boundary ∂G_2, it should be a deterministic motion. The random motions of this type are called random process with reflection or reflected diffusion process.

It has been shown that the solution to this problem *i.e* value of the unknown function u at $\mathbf{x} \in G$ is [2]

$$u(\mathbf{x}) = E^x \left[\int_0^\tau g(\mathbf{X}(t)) e^{\left(\int_0^t q(\mathbf{X}(s))ds + b(\mathbf{X}(s))d\lambda_s \right)} d\lambda_t \right] \tag{5.2}$$

The right-hand side of equation depends on expectations of known functions, the functions g, q and b and samples of the reflected diffusion process X, in the time interval $(0, \tau)$. Therefore the local solution can be obtained by Monte Carlo simulations. Here, λ_t is a continuous non-decreasing stochastic process, called local time process increasing only at the intervals where $\mathbf{X}(t)$ touches the boundary ∂G_2 by one. A brief discussion about reflected diffusion process and local times in the context of the problem under consideration is given below.

5.2 Parabolic wave equation with impedance boundary condition

5.2.1 Problem Definition

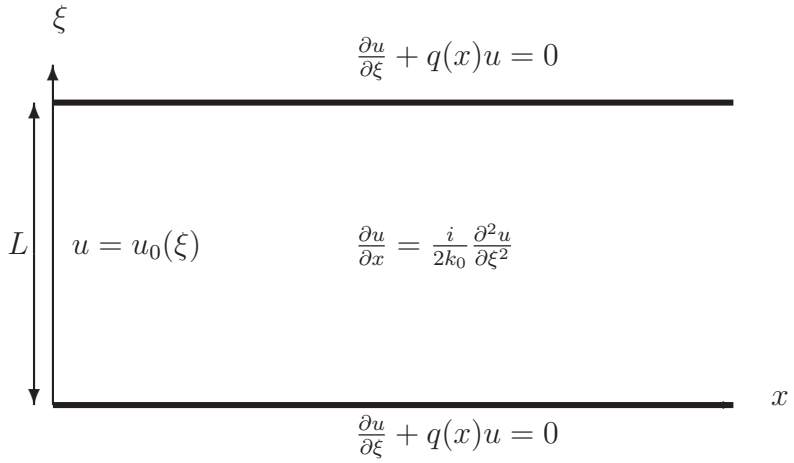

Figure 5.3. Parallel plate waveguide with impedance walls

We will consider a problem of propagation of time harmonic waves inside an infinite parallel plate waveguide with impedance walls.This model problem approximately describes propagation over an impedance ground plane with a periodic boundary condition enforced at the top plate, considering paraxial propagation and neglecting back scattering.

The reduced field $u(x,\xi) = v(x,\xi)exp(-ik_0x)$ satisfies parabolic wave equation

$$\begin{aligned} \frac{\partial u}{\partial x} &= \frac{i}{2k_0}\frac{\partial^2 u}{\partial \xi^2} \qquad (x,\xi) \in G \\ u(0,\xi) &= u_0(\xi) \end{aligned} \tag{5.3}$$

where $v(x,z)$ is the true field, k_0 is wavenumber and u_0 is known initial field.

The unknown u is given by the following impedance boundary condition at top boundary $\xi = L$ and bottom boundary $\xi = 0$.

$$\frac{\partial u}{\partial \xi} + q(x)u = 0 \quad \text{at} \quad \xi = 0 \quad \text{and} \quad \xi = L \tag{5.4}$$

5.2.2 Analytical Solution

The analytical solution to this model problem can be obtained by applying Discrete Mixed Fourier Transform. The algorithm to obtain solution at range R, given the initial field is discussed below [12].

1. Start with solution $u(x, n\Delta\xi)$ where $n = 0, 1, ...N$ and $L = N\Delta\xi$ at range $x = 0$

2. Compute Discrete Mixed Fourier Transform of this discretized solution. The discrete MFT of $u(x, n\Delta\xi)$ is given by

$$\begin{aligned} U(x,0) &= A\sum_{n=0}^{N}{}' r^n u(x,n\Delta\xi) \\ U(x,m\Delta p) &= \sum_{n=1}^{N-1} u(x,n\Delta\xi)\left[q\sin\left(\frac{mn\pi}{N}\right) - \frac{\sin(\frac{\pi m}{N})}{\Delta\xi}\cos\left(\frac{\pi mn}{N}\right)\right] \quad m = 1, ...N-1 \\ U(x,N\Delta p) &= A\sum_{n=0}^{N}{}' (-r)^{N-n} u(x,n\Delta\xi) \end{aligned}$$

   where the prime superscript on the sum indicates that the first and last terms are weighted with coefficient $\frac{1}{2}$ and the following quantities are needed to complete the definition of transform

$$A = \frac{2(1-r^2)}{(1+r^2)(1-r^{2N})}$$

   Here r and r^{-1} are the roots of the quadratic equation $r^2 + 2rq\Delta\xi - 1 = 0$
   When q has a positive real part (vertical polarization), the desired root is
   $r = \sqrt{1+(q\Delta\xi)^2} - q\Delta\xi$, while for a negative real part (horizontal polarization)
   $r = -\sqrt{1+(q\Delta\xi)^2} - q\Delta\xi$

3. Advance the DMFT function to range $x + \Delta x$ using the system of equations

$$\begin{aligned} U(x+\Delta x, 0) &= \exp\left\{\frac{i\Delta x}{2k\Delta\xi^2}\frac{(r-1)^2}{r}\right\}U(x,0) \\ U(x+\Delta x, m\Delta p) &= \exp\left\{\frac{i\Delta x}{k\Delta\xi^2}\left(\cos\frac{\pi m}{N}-1\right)\right\}U(x,m\Delta p) \\ U(x+\Delta x, N\Delta p) &= \exp\left\{-\frac{i\Delta x}{2k\Delta\xi^2}\frac{(r+1)^2}{r}\right\}U(x,m\Delta p) \end{aligned}$$

4. Compute inverse discrete mixed Fourier transform which is given by

$$\begin{aligned} u(x,n\Delta\xi) &= r^n U(x,0) + \frac{2}{N}\sum_{m=1}^{N-1} U(x,m\Delta p)\left[\frac{q\sin\left(\frac{mn\pi}{N}\right) - \frac{\sin(\frac{\pi m}{N})}{\Delta\xi}\cos\left(\frac{\pi mn}{N}\right)}{q^2 + \left(\frac{\sin(\frac{\pi m}{N})}{\Delta\xi}\right)^2}\right] \\ &+ (-r)^{N-n}U(x,N\Delta p) \end{aligned}$$

This gives the field at advanced range $x = R$ and height ξ. This result is used in analytic continuation of data and also to compare results obtained stochastically.

5.3 Local Solution of parabolic wave equation with impedance boundary condition

In this section, the procedure to obtain local solution of this problem using a stochastic method is discussed. Most of the steps for this problem coincide with those of the Dirichlet problem described in the previous chapter and considered in [15]. In order to obtain a local solution to this problem, we need to generate random motions in complex space ($x, z = \xi + i\eta$). Start random processes, $x(s)$ and $z(s)$, at $x(0) = x$ and $z(0) = \xi$ respectively and continue the random processes according to the stochastic differential equations given below:

$$dx(s) = -ds \tag{5.5}$$

$$dz(s) = \sqrt{\frac{i}{k_0}}dW(s) \tag{5.6}$$

In the previous chapter, to obtain local solution, we terminated the random process at the first exit time τ from the domain G

$$\tau = inf\{t \geq 0 : (x(t), z(t)) \notin G, (x(0), z(0)) = (x, \xi) \in G\}$$

and obtained the local solution by using the following equation

$$u(x,z) = E^x[g^c(x(\tau), z(\tau))] \tag{5.7}$$

where $g^c(x,z)$ is analytically continued boundary as explained in the previous chapter.

Analytical continuation of field on the source plane, $x = 0$:
The value of u is given only along the line, $x = 0, z = 0 + i\eta$. To obtain the field on the entire source plane, the expression for $u(x, \xi)$ given in eqn 5.8 can be analytically continued to complex space by writing $z = \xi + i\eta$ as shown in eqn 5.9.

$$\begin{aligned} u(x,\xi) = r^n U(x,0) &+ \frac{2}{N}\sum_{m=1}^{N-1} U(x, m\Delta p)\left[\frac{q\sin\left(\frac{m\pi\xi}{L}\right) - \frac{\sin(\frac{\pi m}{N})}{\Delta\xi}\cos\left(\frac{\pi m\xi}{L}\right)}{q^2 + \left(\frac{sin(\frac{\pi m}{N})}{\Delta\xi}\right)^2}\right] \\ &+ (-r)^{N-n} U(x, N\Delta p) \end{aligned} \tag{5.8}$$

$$\begin{aligned} u(x, z = \xi + i\eta) = r^n U(x,0) &+ \frac{2}{N}\sum_{m=1}^{N-1} U(x, m\Delta p)\left[\frac{q\sin\left(\frac{m\pi z}{L}\right) - \frac{\sin(\frac{\pi m}{N})}{\Delta\xi}cos\left(\frac{\pi m z}{L}\right)}{q^2 + \left(\frac{\sin(\frac{\pi m}{N})}{\Delta\xi}\right)^2}\right] \\ &+ (-r)^{N-n} U(x, N\Delta p) \end{aligned} \tag{5.9}$$

Thus the value of intial field u along the source plane $(0, z = \xi + i\eta)$ can be obtained by analytical continuation.

If the value of u on the top plane $\xi = L$ and bottom plane $\xi = 0$ is known as well, we would have used eqn (5.7) to obtain local solution. However, on the top and bottom planes, u is given by the boundary condition (5.4). Therefore, the value of $u(x, z)$ in the right hand side of equation (5.7) is not known at all points $(x(\tau), z(\tau))$, to compute the expectation. An alternative approach to obtain local solution of this problem is discussed below.

- The sample paths of the random process starting at (x, ξ) can be divided into two groups as shown in figure 5.4.

    1. Sample paths that reach source plane $x = 0$, before reaching top or bottom planes. As we know that value of u on source plane, we terminate them and its contribution to the expectation will be this value of u on source plane.
    2. Sample paths that reach either top plane or bottom plane before reaching source plane. Since the boundary values on the top and bottom planes are not known, we cannot terminate these paths. These sample paths must be modified such that they obey impedance boundary condition as given by (5.4).

- On the bottom plane given by $z = 0$, the unknown function u is given by $\frac{\partial u}{\partial z} + q(x)u = 0$. Therefore, modify the random process on this plane, such that the infinitesimal

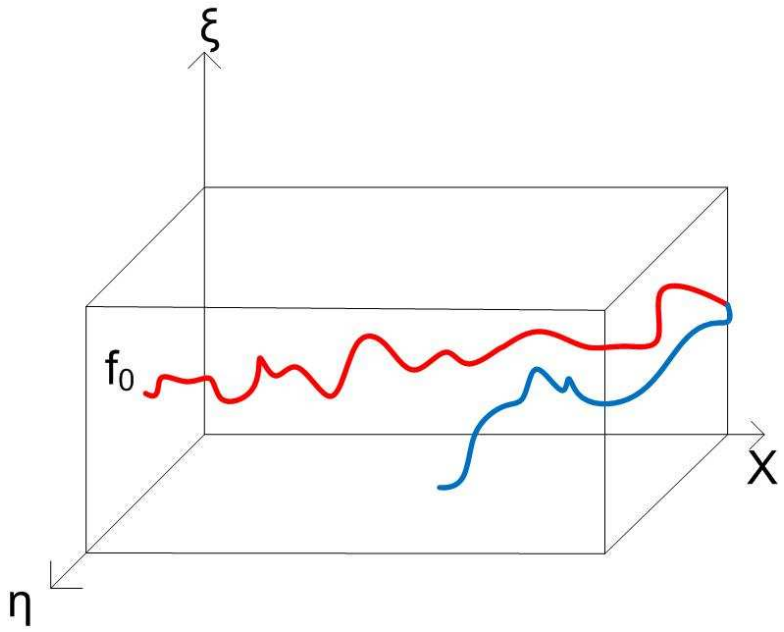

Figure 5.4. Two types of sample paths

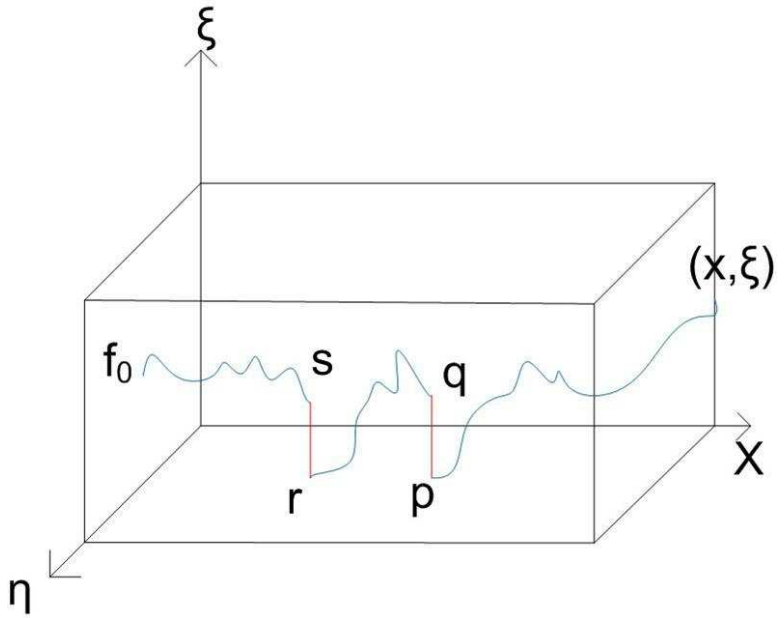

Figure 5.5. Reflections at impedance wall on bottom plane

generator of the random process matches with $\frac{\partial u}{\partial z} + q(x)u = 0$ as shown in figure 5.5. On the bottom plane, the random motion is governed by

$$dz(s) = +ds \tag{5.10}$$

$$dx(s) = 0 \tag{5.11}$$

Notice that only real part of $z(s)$ is changing.

- Once the particle is inside the waveguide, restart the random motion according to the Equations (5.5) and (5.6). If the particle reaches the bottom plane again, repeat the process as discussed above until it reaches the source plane.

- Once the particle reaches source plane, as the value of u is known, terminate the random motions. However this value cannot be used to obtain u at point a as given by (5.7) because Ito formula presented in the last chapter, which is used to obtain the expectation, is valid only for twice differentiable functions and $u(x(s), z(s))$ is not a twice differentiable function as $x(s)$ and $z(s)$ are reflected diffusion processes. Therefore a modified form of Ito formula needs to be used to obtain the expectation and thus we will be using the extended Feynman-Kac formula given by Equation (5.2).

- The contribution of this sample path to the expectation is given $f_0 e^{(q(p)+q(r))}$

- If the random motion reaches the top plane, perform a similar process. On the top plane, the unknown function u is approximately given by $\frac{\partial u}{\partial z} + q(x)u = 0$, which can also be written as $-\frac{\partial u}{\partial z} - q(x)u = 0$ as shown in figure 5.6. Inside the region, the random motion is governed by

$$dz(s) = -ds \tag{5.12}$$

$$dx(s) = 0 \tag{5.13}$$

- Once the particle is inside the waveguide, restart the random motion according to the Equations (5.5) and (5.6). If the particle reaches the top plane again, repeat the process as discussed above until it reaches the source plane. The contribution of this sample path to the expectation is given $f_0 e^{(-q(p)-q(r))}$

- The contribution in the case where random motion reaches both bottom and top planes as shown in figure 5.7 is $f_0 e^{(q(1)-q(2))}$

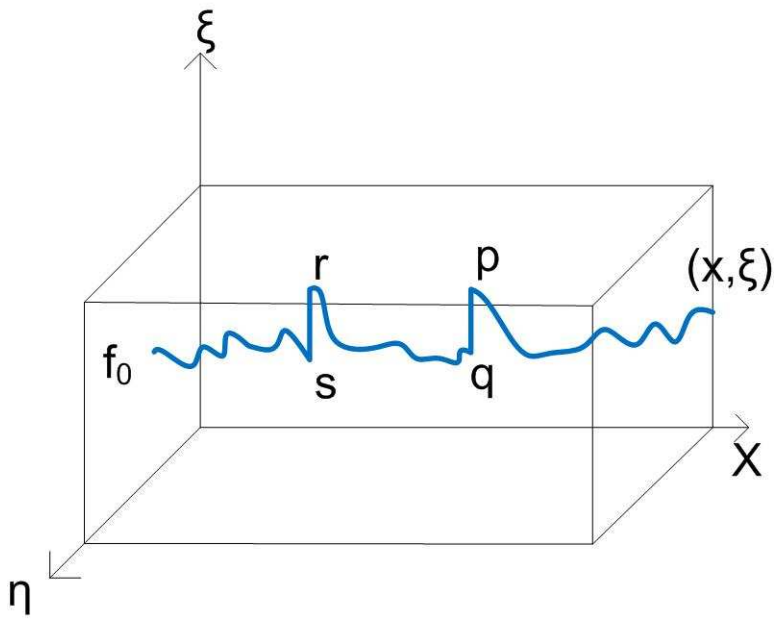

Figure 5.6. Reflections at impedance wall on top plane

5.4 Algorithm

The algorithm that can be used to solve this problem is given by

1. Initialize
   counter $NOOFHITS\_TOP \leftarrow 0$
   counter $NOOFHITS\_BOTTOM \leftarrow 0$
   variable representing contribution from each sample path $ANSWER \leftarrow 0$

2. Start random motion at (x, ξ)

3. Continue random motion inside G according to the following stochastic differential equations

$$\begin{aligned} dx(s) &= -ds \\ d\xi(s) &= \frac{1}{2k_0} dW(s) \\ d\eta(s) &= \frac{1}{2k_0} dW(s) \end{aligned}$$

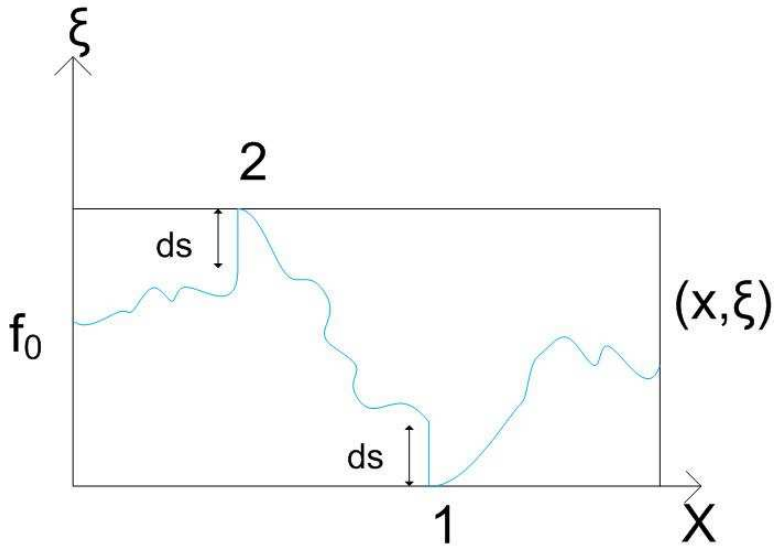

Figure 5.7. Reflections at impedance walls on top and bottom planes

4. If it hits top plane, random motions are given by

$$\begin{aligned} dx(s) &= 0 \\ d\xi(s) &= -ds \\ d\eta(s) &= 0 \end{aligned}$$

   Update counter $NOOFHITS\_TOP$

5. If it hits bottom plane, random motions are given by

$$\begin{aligned} dx(s) &= 0 \\ d\xi(s) &= +ds \\ d\eta(s) &= 0 \end{aligned}$$

   Update counter $NOOFHITS\_BOTTOM$

6. Once it hits source plane at $z = \xi_0 + i\eta_0$, note $f(\xi_0 + i\eta_0)$

7. Update ANSWER
   ANSWER $\leftarrow$ ANSWER + $f(\xi_0 + i\eta_0)$ X $e^{q(NOOFHITS\_BOTTOM - NOOFHITS\_TOP)}$

8. Repeat this procedure for large number of realizations to obtain accurate result.

9. Compute expectation of the contribution from each sample path, which is the desired solution at the point (x, ξ).

5.5 Numerical Experiments

5.5.1 Experimental Setup

In all the computations performed in this chapter, frequency of $f = 300$ MHz, which is equivalent to $\lambda = 1$m, is used. The height of waveguide is taken to be $L = 24\lambda$ and a Gaussian initial field with peak at $\xi = H_t = 12\lambda$ and standard deviation $\sigma_\xi = 3\lambda$ is applied at source plane, $x = 0$. The boundary condition on the top and bottom planes are given by $\frac{\partial u}{\partial z} + q(x)u = 0$, where $q = j\omega\epsilon_0 Z_s$ and $Z_s = \sqrt{\frac{\mu}{\epsilon}}$ and $\epsilon = \epsilon_r\epsilon_0 + j\frac{\sigma}{\omega}$. The electrical constants of the boundaries are taken to be $\epsilon_r = 80$ and $\sigma = 4S/m$. All of the results presented here are obtained using 10^5 realizations.

To find the field along the line $x = R$ (R is called range) and $z = \xi + i0$, start random motions at a given point (R, ξ) and generate random motions in complex space $(x, z = \xi + i\eta)$ and obtain the expectation using the algorithm described in the previous section.

5.5.2 Results and Discussion

5.5.2.1 *a)*What is marching algorithm? Why is it needed here? Determining good marching step for this problem

These are the questions we are trying to answer in this section using numerical results. Figures 5.8, 5.9 and 5.10 show the real (red) and imaginary (green) parts of analytical solution (solid line) and the stochastic solution (shown with $*$) computed using the algorithm discussed above at a distance of $R = 10\lambda, 20\lambda.....100\lambda$ from source plane. It can be observed that stochastic solutions show a good match with analytical solution until $R = 50\lambda$, and beyond this range, the stochastic solutions begin to blow up.

The reason for this is explained below. If range R is increased, then the number of possible sample paths also increases. Therefore more number of realizations are needed to obtain good match between stochastic and analytical solutions. In addition to this, the farther the range R (where the random motions are started) , the more is that probability that these random motions hit the source plane $x = 0$ at large distances along η axis. From the analytic continuation expression which is used to obtain the field on this source plane at any given point $(x = 0, z = \xi + i\eta)$, it can be observed that the field increases exponentially with η. If the random motions hit at large distances along η axis, there is a good chance that very large values are used in the expectation calculations. If not enough realizations are used, there is a good chance that stochastic solution jump from very small value to very large value or vice versa in just one realization. Therefore, to obtain good agreement

between stochastic and analytical fields, at large values of range, more number of realizations are needed, which will take more time.

To obtain field at large distances, say $R = 1000\lambda$, direct computation of field by using the procedure discussed above obviously will take very large amount of time. An alternative procedure is outlined here

1. Start computing the field at a distance, say at $R = 50\lambda$, where the stochastic solution shows good match with analytical solution.

2. Using this stochastic solution at 50λ as the initial field, compute the field at $R = 100\lambda$ by using the algorithm discussed above and using this field at 100λ, obtain the stochastic solution at $R = 150\lambda$ and so on.

Therefore to overcome the problem mentioned above, the marching algorithm is used. Having understood why a marching algorithm is needed, we proceed further to answer the question, what is a good marching step ($Mstep$) in this case. For obvious reasons, we don't want smaller $Mstep$. On the other hand it shouldn't be large that large exponential values are encountered in the expectation calculations as discussed above. From figures 5.8, 5.9 and 5.10, it can be observed that stochastic solutions until $R = 50\lambda$ show good match with analytical solutions. The above problem seems to creep in when field is computed at ranges greater than $R = 60\lambda$. Therefore in all the computations performed from here on, marching step $Mstep = 50\lambda$ will be used.

5.5.2.2 b) Field at a given range from the aperture source

Figures 5.11 to 5.17 show the real (red) and imaginary (blue) parts of analytical solution (solid line) and the stochastic solution (line with $*$) at the range from $R = 50\lambda$ to $R = 1600\lambda$ in steps of $R = 50\lambda$. These are computed using marching algorithm with marching step $Mstep = 50\lambda$ and $\Delta t = 0.1\lambda$. A good agreement is seen between the analytical and stochastic solution until $R = 1200\lambda$. Beyond this range $R = 1200\lambda$ the stochastic solutions do not compare well with analytical solution. The reason for this is explained below.

To reiterate the marching algorithm, in order to obtain solution, say at $R = 250\lambda$, as a first step compute the solution at the $R = 50\lambda$, stochastically. This stochastic solution, however accurate it might be, is always an approximation to the true field at this range (A very good agreement between the stochastic and analytical solution implies the error is very very small, nevertheless it will not be 0). If this (approximate) computed field, which lets say is 99.9% accurate, is used to compute the stochastic solution at the next step, then this

stochastic solution will include error which is caused not only by stochastic algorithm but also by the approximation of initial field. If this solution is used again as initial field to compute the field at the next step, the error due to the approximation increases. Therefore, if marching algorithm is used, then the error due to approximation of true field by the stochastic solution at the previous step propagates with marching. Therefore at large values of range, approximation error is large as more number of marchings are done and hence the stochastic solutions at these ranges do not compare well with the analytical solutions.

5.5.2.3 c) Stochastic solutions with different values of Δt

To support the above discussion, we present the following analysis. Figures 5.18, 5.19, 5.20 and 5.21 show the real and imaginary parts of analytical and stochastic solution at ranges $R = 250\lambda, R = 500\lambda, R = 750\lambda$ and $R = 1000\lambda$. Each of these figures includes four subfigures, three of which show the comparison between analytical solution and stochastic solution computed with $\Delta t = 0.1\lambda$, $\Delta t = 0.25\lambda$ and $\Delta t = 0.5\lambda$ respectively. The fourth subfigure shows the stochastic solution computed at the given range, when a true analytical field is used at the previous step instead of stochastic solution.

It has already been concluded in the previous chapters that the accuracy of the solution increases with decrease in Δt. Therefore, we expect the stochastic solution computed with $\Delta t = 0.1\lambda$ to be more accurate among these three cases, followed by $\Delta t = 0.25\lambda$ case. So, at each step, as the stochastic solution using $\Delta t = 0.1\lambda$ is more accurate than other, the approximation error for this will be smaller that other two. If marching algorithm is employed for these three cases, we expect the stochastic solution computed with larger Δt to show unfavorable comparisons with analytical solution at small ranges compared to that of smaller Δt case.

Even though figure 5.18 shows good agreement between stochastic and analytical solution for all cases, it can be observed from figure 5.19, the accuracy is better for the case $\Delta t = 0.1\lambda$ followed by $\Delta t = 0.25\lambda$. From figure 5.20, it can be observed that at range $R = 750\lambda$, stochastic solution with $\Delta t = 0.5\lambda$ is worse than the other two. Figure 5.21 shows that at range $R = 1000\lambda$, stochastic solution with $\Delta t = 0.25\lambda$ also does not show good agreement with analytical solution. However, the solution at range $R = 1000\lambda$ computed using one marching step (*i.e* using true field at the previous step), shows better comparisons to that of the stochastic solution with $\Delta t = 0.1\lambda$. From this experiment, it can be concluded that decreasing Δt can increase the maximum range at which the stochastic solution computed using marching algorithm still exhibits favorable comparisons with analytical solution.

However, an agreeable solution may not be obtained for large Δt, even when range is small enough.

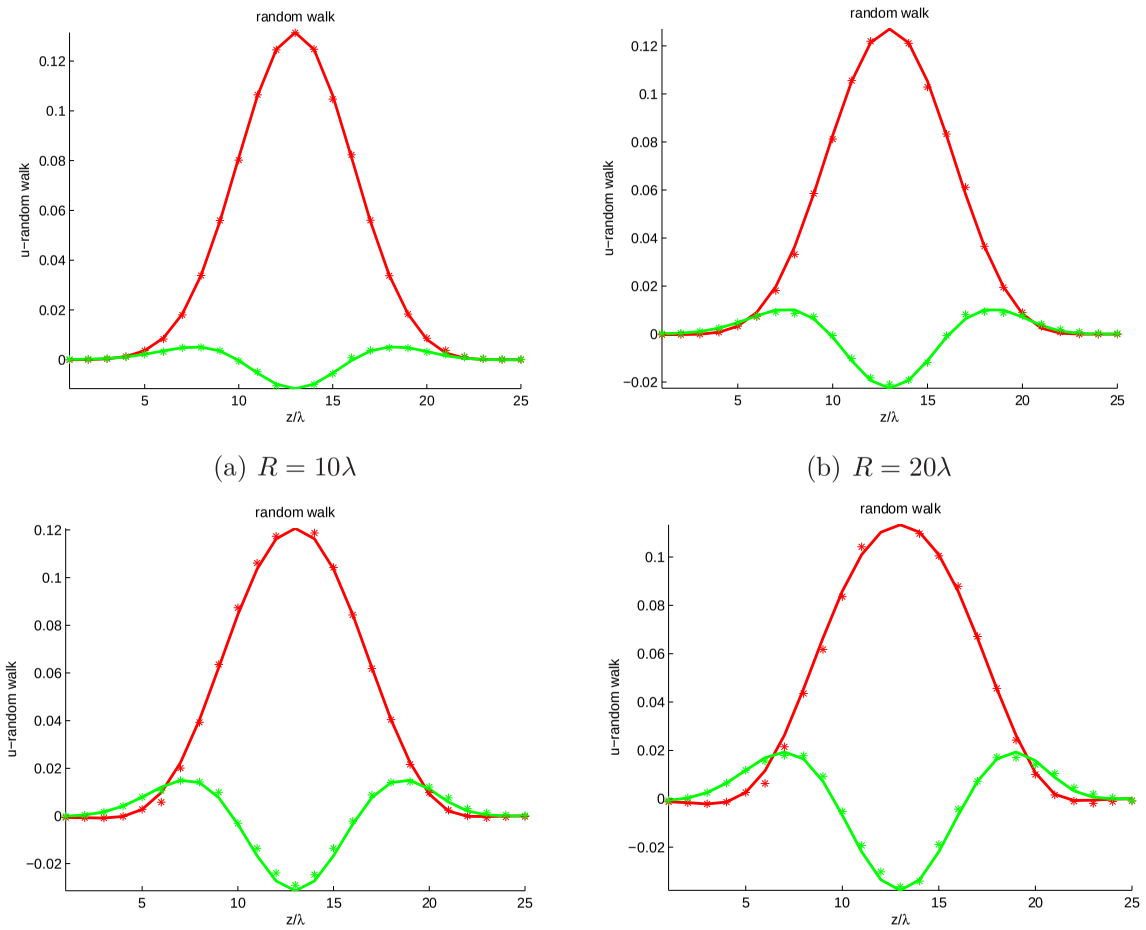

(a) $R = 10\lambda$

(b) $R = 20\lambda$

(c) $R = 30\lambda$

(d) $R = 40\lambda$

Figure 5.8. Field at a distance of R from source plane $x = 0$

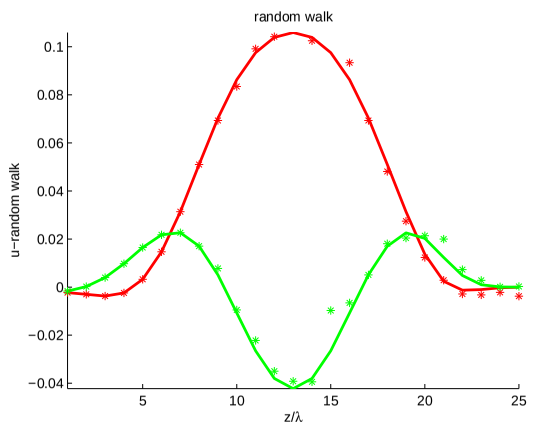

(a) $R = 50\lambda$

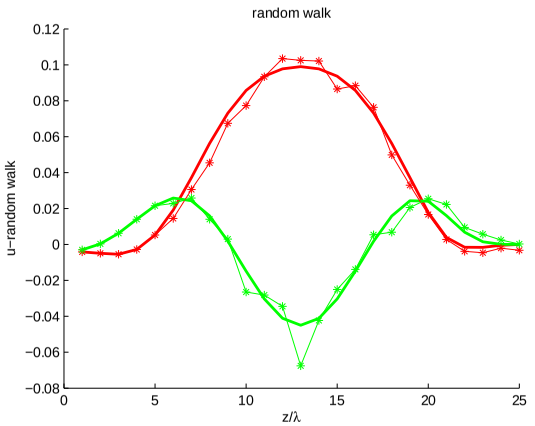

(b) $R = 60\lambda$

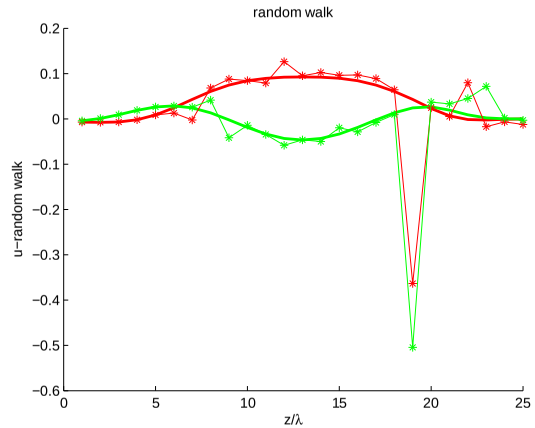

(c) $R = 70\lambda$

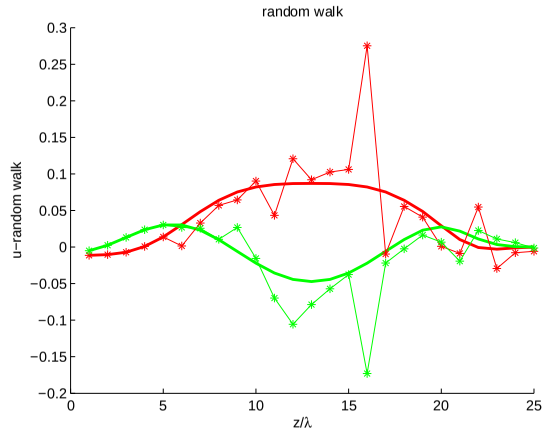

(d) $R = 80\lambda$

Figure 5.9. Field at a distance of R from source plane $x = 0$

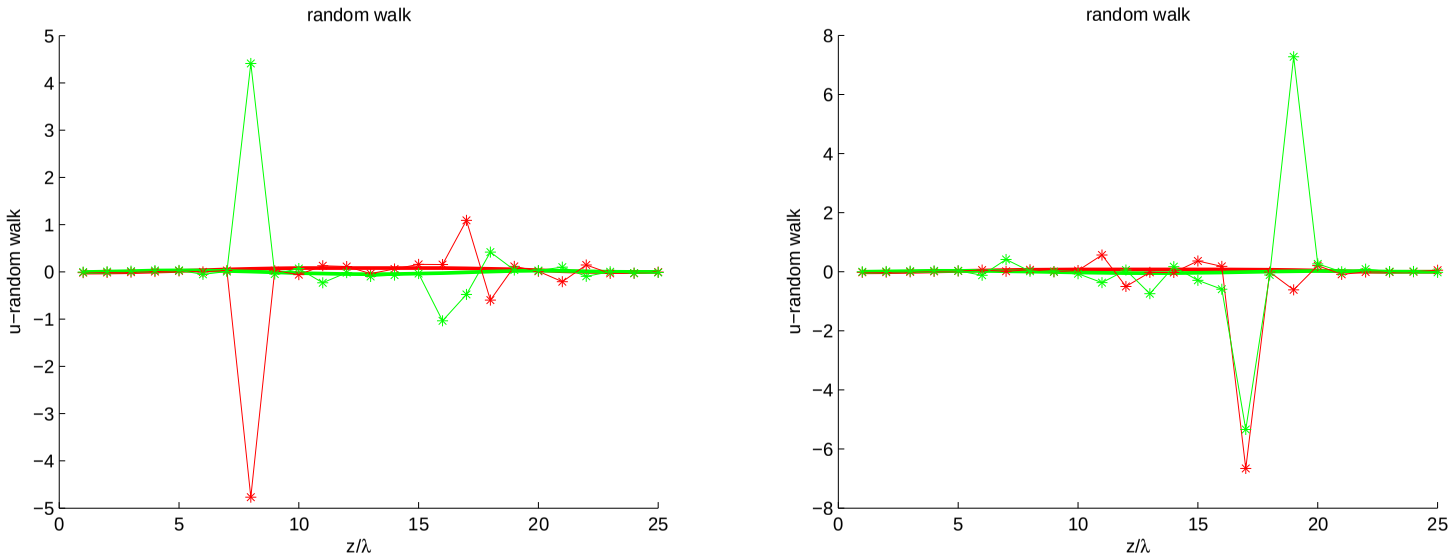

(a) $R = 90\lambda$ (b) $R = 100\lambda$

Figure 5.10. Field at a distance of R from source plane $x = 0$

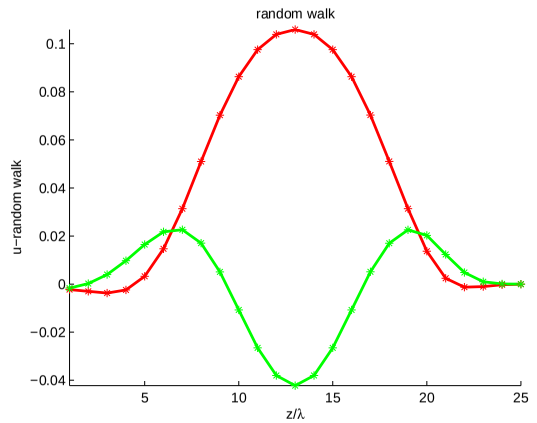

(a) $R = 50\lambda$

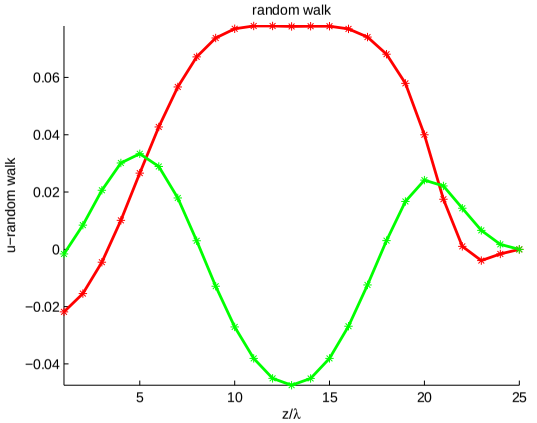

(b) $R = 100\lambda$

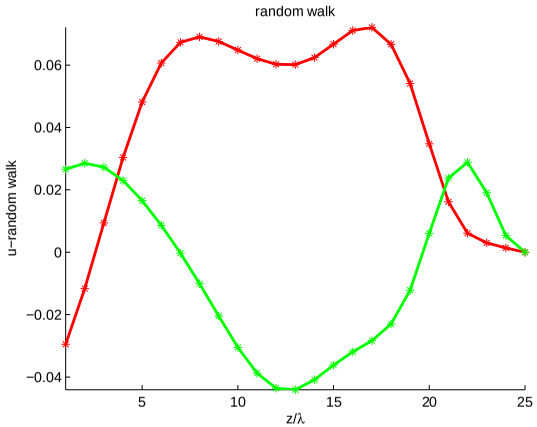

(c) $R = 150\lambda$

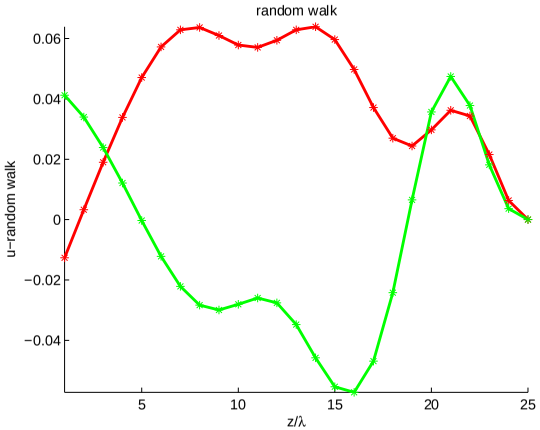

(d) $R = 200\lambda$

Figure 5.11. Field at a distance of R from original source plane $x = 0$ using marching algorithm and $\Delta t = 0.1\lambda$

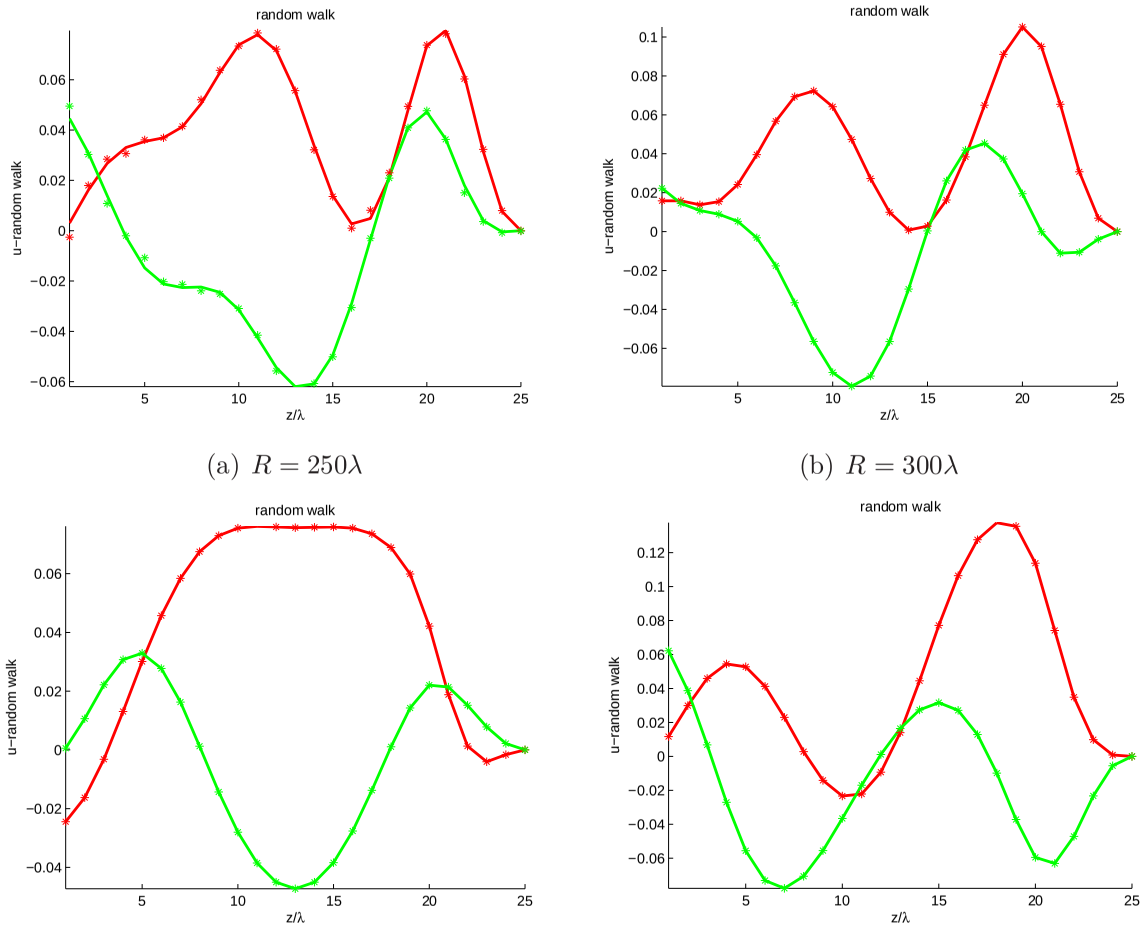

(a) $R = 250\lambda$ (b) $R = 300\lambda$

(c) $R = 350\lambda$ (d) $R = 400\lambda$

Figure 5.12. Field at a distance of R from original source plane $x = 0$ using marching algorithm and $\Delta t = 0.1\lambda$

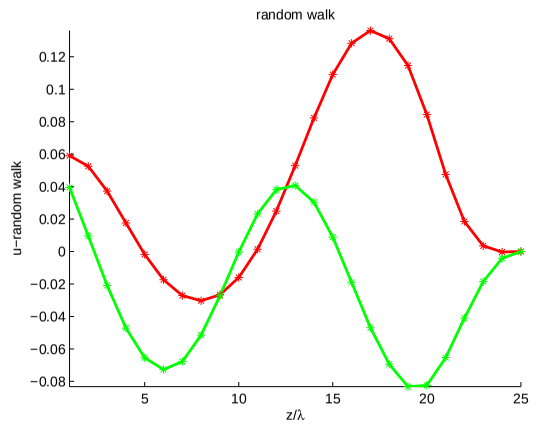

(a) $R = 450\lambda$

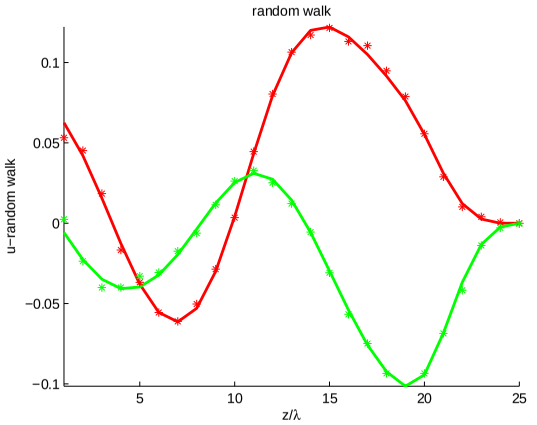

(b) $R = 500\lambda$

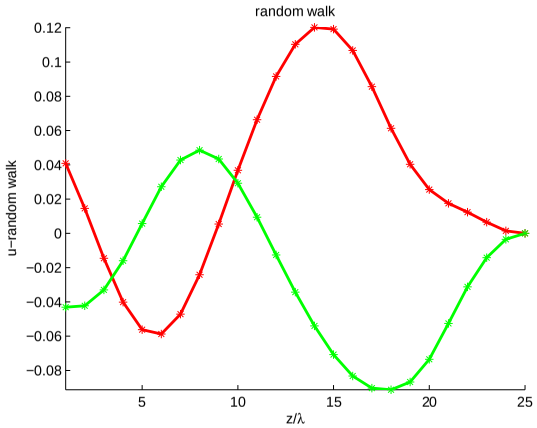

(c) $R = 550\lambda$

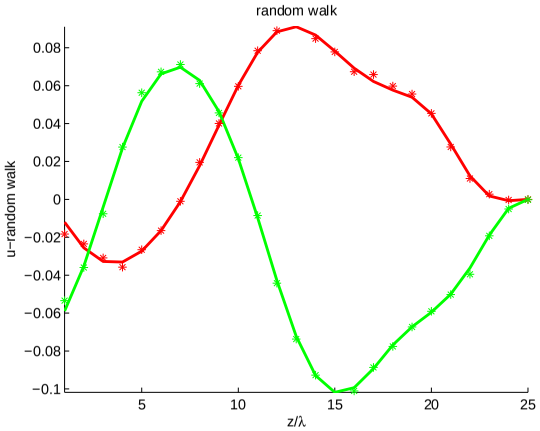

(d) $R = 600\lambda$

Figure 5.13. Field at a distance of R from original source plane $x = 0$ using marching algorithm and $\Delta t = 0.1\lambda$

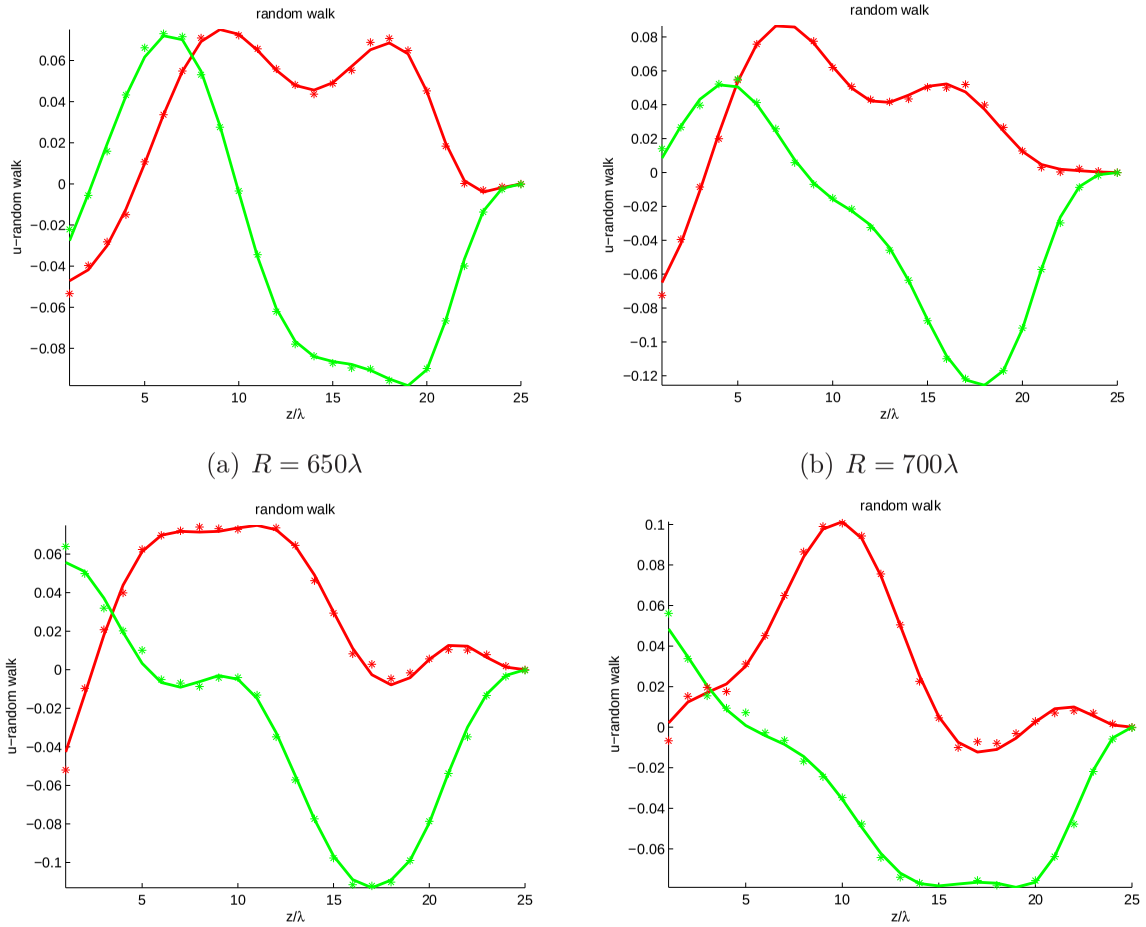

(a) $R = 650\lambda$ (b) $R = 700\lambda$

(c) $R = 750\lambda$ (d) $R = 800\lambda$

Figure 5.14. Field at a distance of R from original source plane $x = 0$ using marching algorithm and $\Delta t = 0.1\lambda$

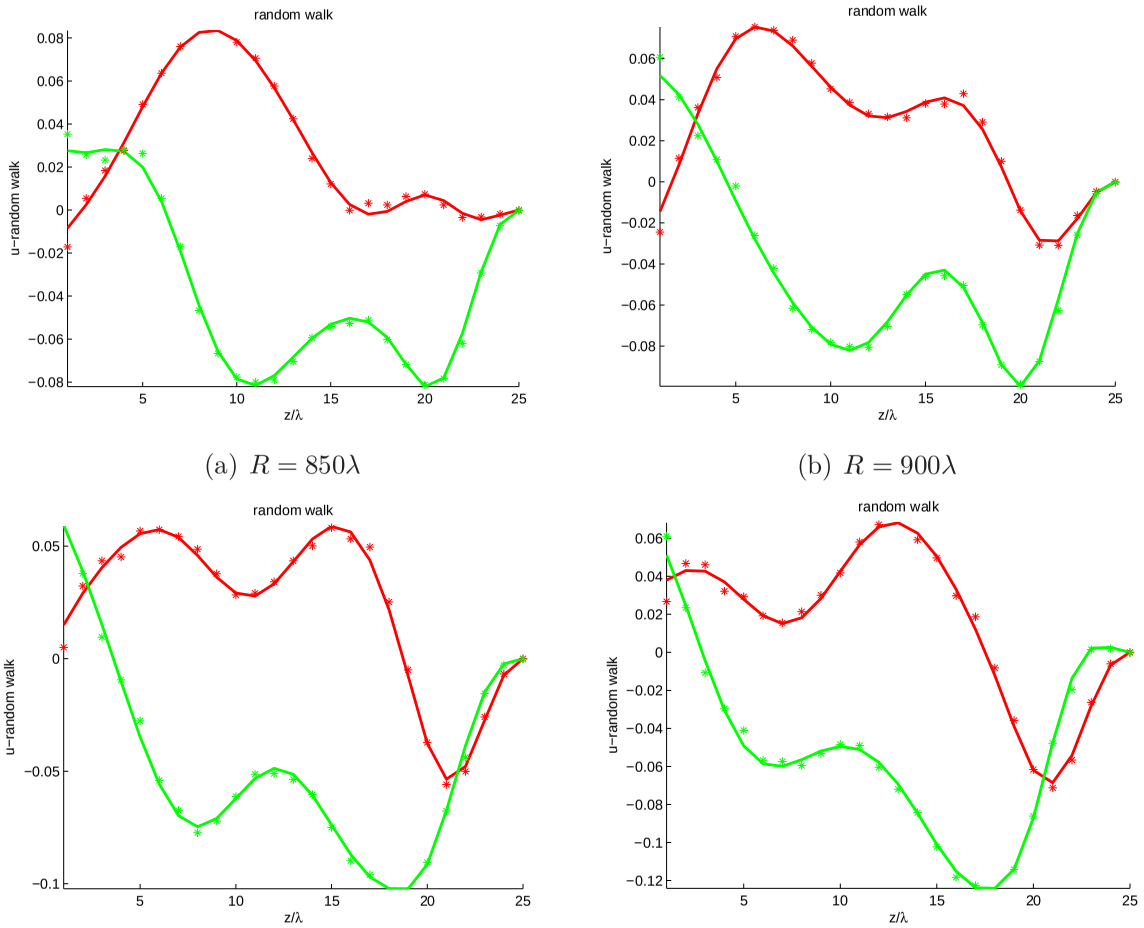

(a) $R = 850\lambda$

(b) $R = 900\lambda$

(c) $R = 950\lambda$

(d) $R = 1000\lambda$

Figure 5.15. Field at a distance of R from original source plane $x = 0$ using marching algorithm and $\Delta t = 0.1\lambda$

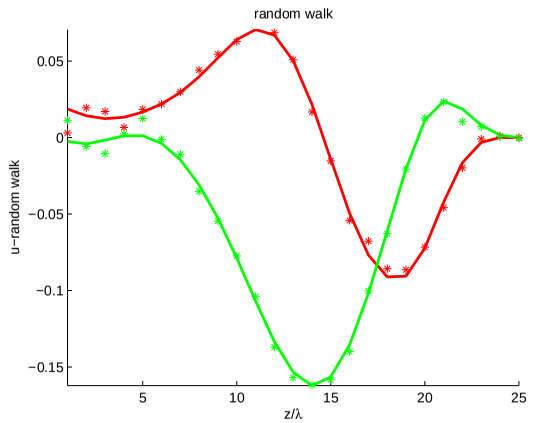

(a) $R = 1100\lambda$

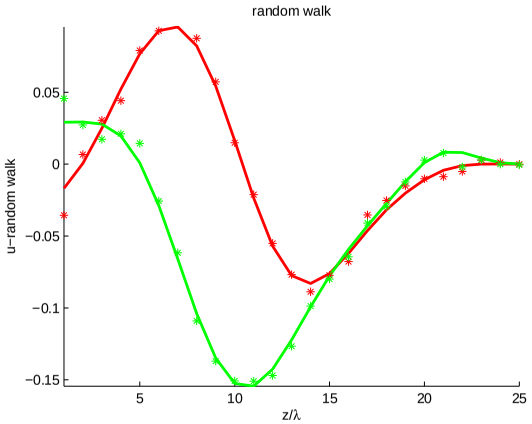

(b) $R = 1200\lambda$

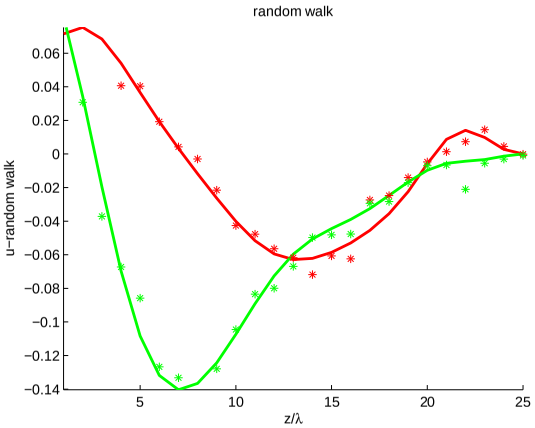

(c) $R = 1300\lambda$

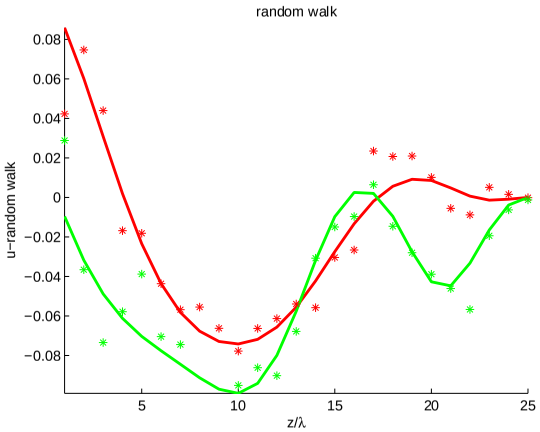

(d) $R = 1400\lambda$

Figure 5.16. Field at a distance of R from original source plane $x = 0$ using marching algorithm and $\Delta t = 0.1\lambda$

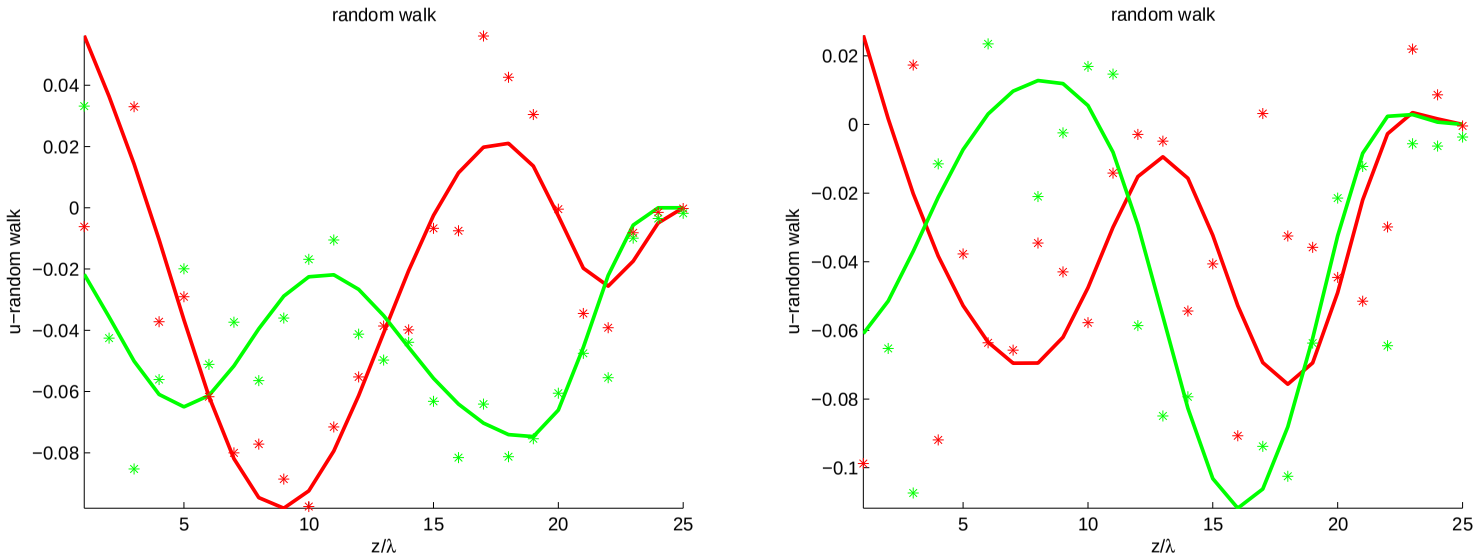

(a) $R = 1500\lambda$ (b) $R = 1600\lambda$

Figure 5.17. Field at a distance of R from original source plane $x = 0$ using marching algorithm and $\Delta t = 0.1\lambda$

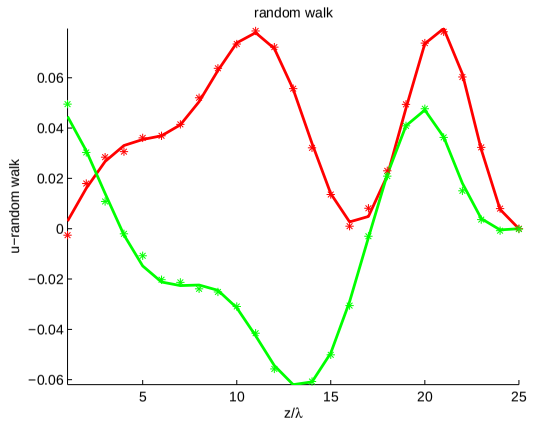

(a) $\Delta t = 0.1\lambda$

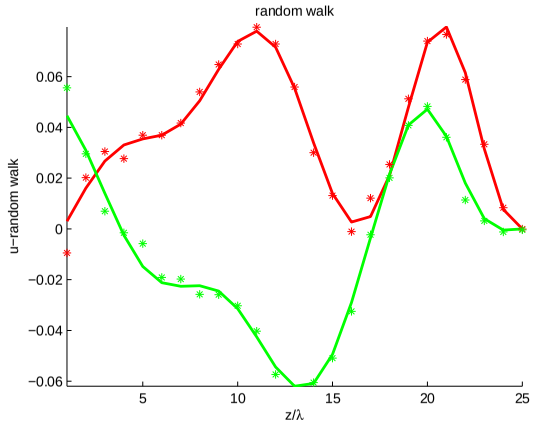

(b) $\Delta t = 0.25\lambda$

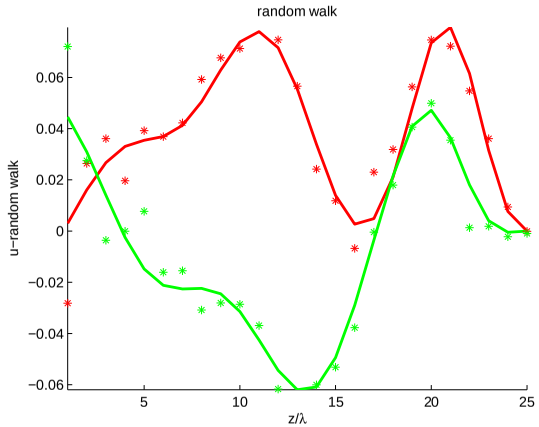

(c) $\Delta t = 0.5\lambda$

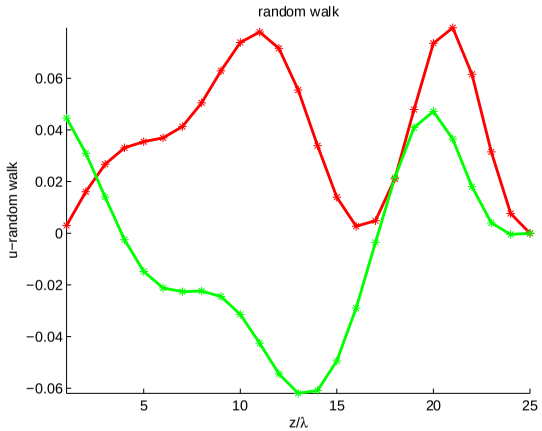

(d) Analytical solution is used as virtual source at the previous step

Figure 5.18. Field at 250λ

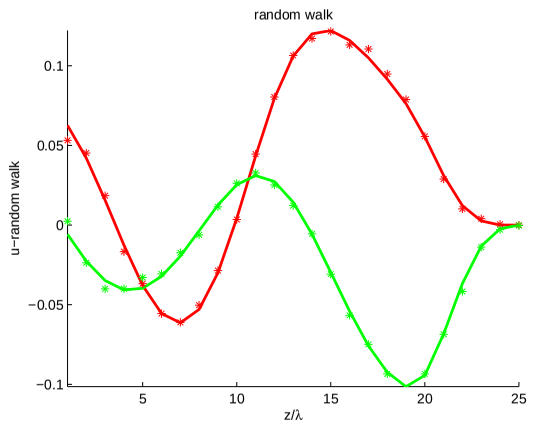

(a) $\Delta t = 0.1\lambda$

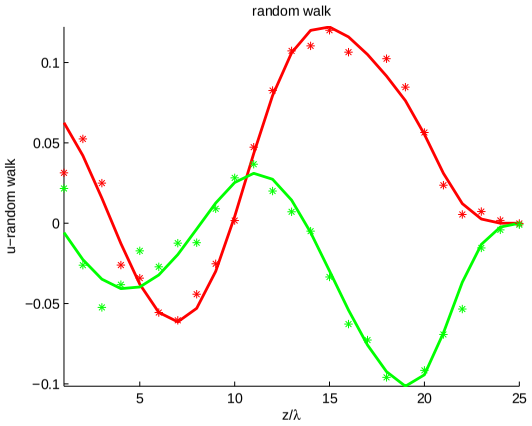

(b) $\Delta t = 0.25\lambda$

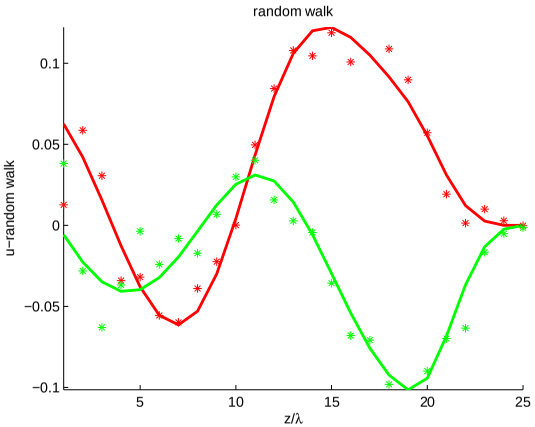

(c) $\Delta t = 0.5\lambda$

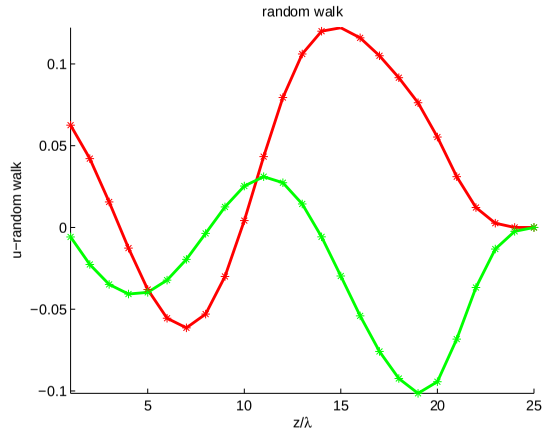

(d) Analytical solution is used as virtual source at the previous step

Figure 5.19. Field at 500λ

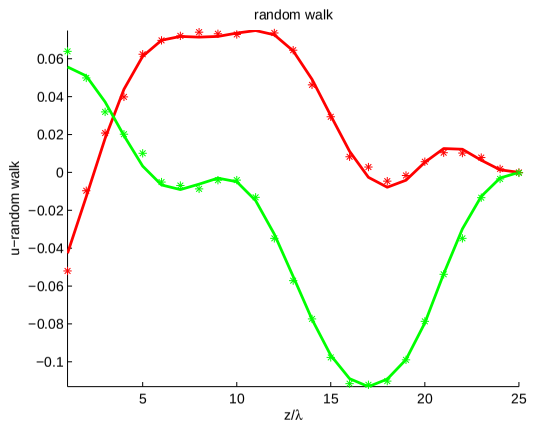

(a) $\Delta t = 0.1\lambda$

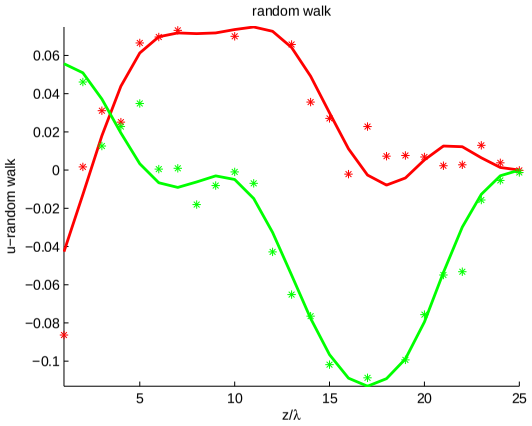

(b) $\Delta t = 0.25\lambda$

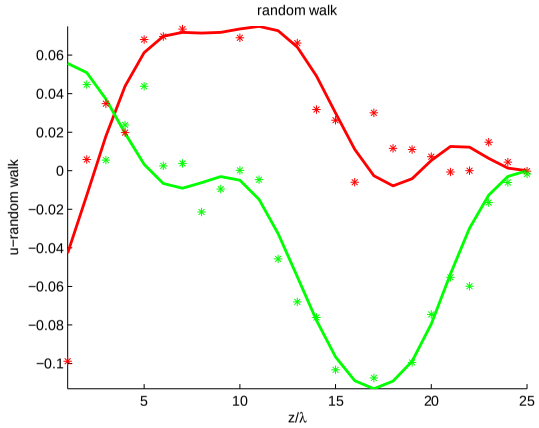

(c) $\Delta t = 0.5\lambda$

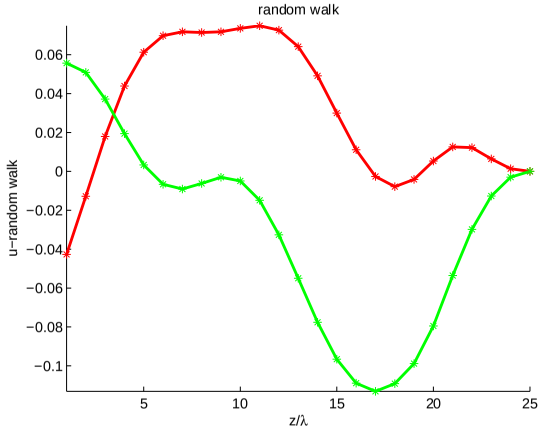

(d) Analytical solution is used as virtual source at the previous step

Figure 5.20. Field at 750λ

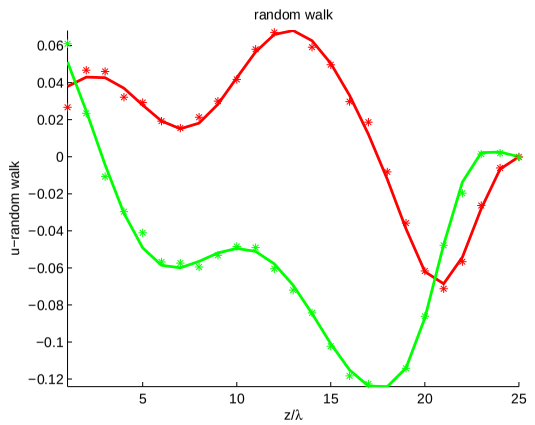

(a) $\Delta t = 0.1\lambda$

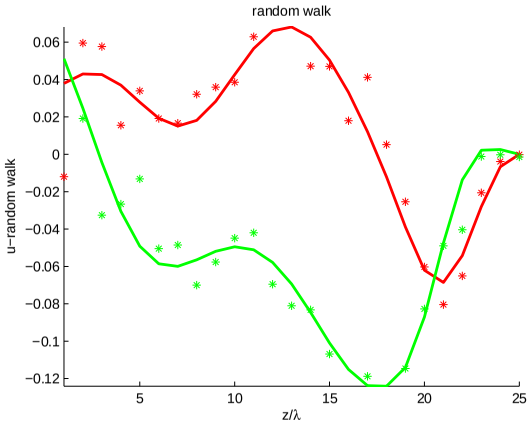

(b) $\Delta t = 0.25\lambda$

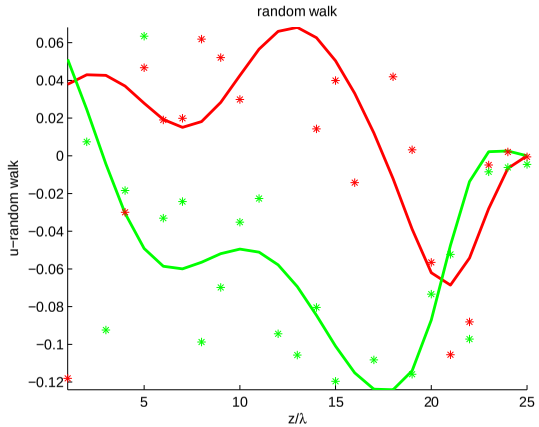

(c) $\Delta t = 0.5\lambda$

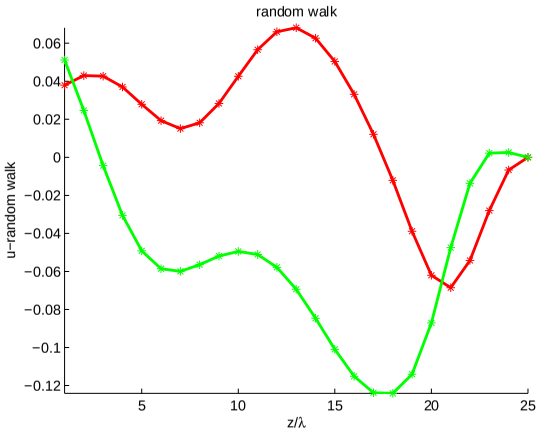

(d) Analytical solution is used as virtual source at the previous step

Figure 5.21. Field at 1000λ

CHAPTER 6

CONCLUSION AND FUTURE WORK

A stochastic method based on properties of diffusion process, Ito formula, Dynkin formula, Feynman-Kac functional and Monte Carlo simulations that can be used to obtain local solution of electromagnetic problems was studied with the objective of understanding the efficacy and limitations of it. Field computation by this method was demonstrated for electrostatic and electrodynamic propagation problems by considering simple problems. Numerical investigations were carried out to understand the effect of various parameters involved in this method. To summarize:

As the first step, the stochastic method was applied to solve Laplace equation to obtain the potential inside a rectangular region when the potential on the walls was given. The stochastic method which involves constructing either random walk or Brownian motion process was discussed and favorable comparisons between analytical and stochastic solutions were presented for both cases.

The parameters that effect the accuracy and time taken by the algorithm most, for random walk method, are grid size and number of realizations and, for Brownian motion process, are time step and number of realizations. It has been observed that accuracy increases with increase in number of realizations as well as decrease in either grid size or time step for the respective methods. It has been reported that with a choice of grid size $h = 0.01$ and number of realizations $N = 2000$, stochastic solution with an L_2 error $\epsilon = 1\%$ can be obtained in about 4 seconds. For Brownian motion process, a choice of $\Delta t = 0.001$ and number of realizations $N = 2500$ is adequate to obtain the solution with an L_2 error $\epsilon = 1\%$ in about 3.5 seconds. For a given accuracy, time taken by Brownian motion process was slightly small compared to that using random walk method.

Local solution to Poisson's equations was also obtained for the problem of finding potential between two parallel plates with square cylindrical charge distribution at the center. The effect of time step and number of realizations on accuracy and time taken to obtain the solution showed a similar trend as previously mentioned *i.e.* accuracy increases with increase

in number of realizations as well as decrease in time step. It has been concluded that with time step, $\Delta t = 0.0001$ and number of realizations, $N = 10,000$, a stochastic solution can be obtained with an accuracy of $\epsilon = 2\%$ in about 350 seconds.

To demonstrate this method for the electrodynamic case, a parabolic wave equation that is encountered in wave propagation problem over terrain was considered. As the stochastic method involves constructing a complex valued wiener process, analytical continuation methods have been used for field computations. This approach was validated first for the propagation problem inside an infinite parallel plate waveguide with perfectly conducting boundaries at the top and bottom.

Finally, a stochastic method was developed for the problem of propagation of time harmonic waves inside a parallel plate waveguide with impedance boundaries at the top and bottom. A brief theory in the context of obtaining local solution to the parabolic wave equation with impedance boundary conditions was discussed. Instead of computing the field at a given range in a single step, a marching algorithm was used with an optimum marching step of $Mstep = 50\lambda$.

Field computations using this marching algorithm with marching step $Mstep = 50\lambda$ and $\Delta t = 0.1\lambda$ has resulted in good agreement between the analytical and stochastic solution until $R = 1200\lambda$. This is because, at large values of range, approximation error due approximation of true field by the stochastic solution at each step is large as more number of marchings are done and hence the stochastic solutions at these ranges do not compare well with the analytical solutions. Experiments were carried out to the effect of Δt on this maximum range at which stochastic solutions are still accurate. It has been observed that decreasing Δt can increase the maximum range at which the stochastic solution computed using marching algorithm still exhibits favorable comparisons with analytical solution.

As mentioned above, analytical solutions were used to provide us with boundary conditions on analytically continued boundaries in the complex plane. For the simple problems considered here within the scope of the thesis, as the focus is on demonstrating the ideas of stochastic method, this approach was used. In more general case, other approaches may have to be found for specifying boundaries on the analytically continued boundaries.

Application of the stochastic method developed here which involves constructing a complex valued Wiener process with reflections, to solve problems with material boundaries at the top and bottom and problems with rough surfaces might provide more insight into reflection approach at impedance boundaries. Numerical investigations on this method for

more complex problems may help understand the usability of this method for more practical problems.

BIBLIOGRAPHY

[1] B.V.Budaev, and D.B.Bogy. Application of random walk methods to wave propagation. *Q. J. Mech. Appl. Math. 55*, 2 (2002), 209–226.

[2] B.V.Budaev, and D.B.Bogy. A probabilistic approach to wave propagation and scattering. *Radio Science 40* (2005).

[3] Doyle, P.G., and Snell, J.L. *Random Walks and Electrical Networks*. Mathematical Association of America, 1984.

[4] E.B.Dynkin, and A.A.Yushkevich. *Markov Processes : Theorems and Problems*. Plenum press, New York, 1969.

[5] J.B.Keller. Geometrical theory of diffraction. *J. Opt. Soc. Amer. 52*, 2 (Feb 1962), 116–130.

[6] J.B.Keller, and D.W.McLaughlin. The Feynman integral. *Am. Math. Mon. 82*, 5 (1975), 451–465.

[7] M.Freidlin. *Functional Integration and Partial Differential Equations*. Princeton Univ. Press, Princeton, N. J., 1985.

[8] M.Grigoriu. Solution of some elasticity problems by the random walk method. *Acta Mechanica . 125* (1998), 197–209.

[9] M.Grigoriu. *Stochastic Calculus:Applications in Science and Engineering*. Birkhauser, Boston, MA, 2002.

[10] M.Kac. On distribution of certain Wiener functionals. *Trans. Am. Math. Soc. 65*, 1 (1949), 1–13.

[11] M.K.Chati, M.Grigoriu, S.S.Kulkarni, and S.Mukherjee. Random walk method for the two- and three- dimensional Laplace, Poisson and Helmholtz equations. *Int. J. Numer. Methods Eng. 51* (2001), 1133–56.

[12] M.Levy. *Parabolic Equation Methods for Electromagnetic Wave Propagation*. The Institute Of Electrical Engineers, 2000.

[13] N.Wiener. Differential space. *J. Math. Phys. 2* (August 1923), 131–174.

[14] R.Courant, K.Friedrichs, and K.H.Lewy. On the partial difference equations of mathematical physics. *IBM Journal* (March 1967), 215–234.

[15] R.Janaswamy. Solution of BVPs in Electrodynamics by Stochastic Methods. *IEEE Applied Electromagnetic Conference, Kolkata, India* (Dec 2007).

[16] R.P.Feynman. The principle of least action in quantum mechanics. *Ph.D. thesis, Princeton Univ., Princeton, N. J.* (1942).

[17] W.R.Smythe. *Static and Dynamic Electricity.* McGraw Hill Book Company, Newyork, 1950.